PH.D/CP/99 SLO

NOVEL THIOPHENE BASED MACROCYCLES

ZACHARY SCOTT SLOMAN BSc(Hons)

A thesis submitted in partial fulfilment of the requirements of

The Nottingham Trent University for the degree of

Doctor of Philosophy.

May 1999.

ABSTRACT.

A range of macrocyclic complexes was prepared utilising α,ϖ-bis(2-formyl-3-oxythienyl)alkanes. Macrocyclic [1+1] metal ion complexes (metal ion = Ni(II), Co(II)) were prepared via condensation of the α,ϖ-bis(2-formyl-3-oxythienyl)alkane with ethylenediamine (en) and subsequent addition of the metal ion to sequester the macrocyclic ligand. Macrocyclic [2+2] metal ion complexes were prepared via condensation of the α,ϖ-bis(2-formyl-3-oxythienyl)alkane with metal ion-ethylenediamine complexes. Complete condensation only occurred with $[Ni(en)_2Cl_2]$ as the template.

New routes that did not result in macrocyclic products are discussed and the new compounds they produced are presented.

The Mannich reaction was utilised for the preparation of macrocycles from α,ϖ-bis(3-oxythienyl)alkanes, formaldehyde and *N,N'*-dibenzylalkyldiamines. These compounds were obtained in good yields without the need for high dilution or column chromatography. The compounds obtained were crystalline and stable to X-radiation.

The crystal structure determination of two of the compounds was undertaken. The 15-membered ring macrocycle $C_{29}H_{32}N_2O_2S_2$ (M1) crystallises in the monoclinic space group $P2_1/c$ with cell dimensions of $a = 12.5043$ Å, $b = 11.2997$ Å, $c = 19.8022$ Å, $\beta = 113.34°$, α, $\gamma = 90°$. The structure was determined using a STOE Stadi-2-circle diffractometer with data collected from two crystals and refined with $I_{obsd} > 4\sigma(I)$ using unit weights to R = 0.0683. The structure has an unusual non-planar geometry and a non-bonded S...N interaction as well as several probable C-H...O hydrogen bonds.

The 14-membered ring macrocycle $C_{28}H_{30}N_2O_2S_2$ (M2) crystallises in the orthorhombic space group Pca2$_1$ with cell dimensions of $a = 22.733$ Å, $b = 11.397$ Å, $c = 20.115$ Å, α, β, $\gamma = 90°$. There are two macrocycles per asymmetric unit which are related via non-crystallographic symmetry which possibly gives rise to the disorder shown on the X-ray photographs. The structure was determined using a STOE Stadi-2-circle diffractometer and refined with $I_{obsd} > 6\sigma$ (I) using unit weights to R = 0.1347. The asymmetric unit consists of two macrocycles with similar geometries, which are discussed and contrasted with the 15-membered macrocycle.

Unit cell and space group data were obtained for two acyclic ligands incorporating two thiophene rings, one potentially pentadentate with five oxygen atoms and one potentially tetradentate with two oxygen and two nitrogen atoms.

A nickel(II) complex of M1 was molecularly modelled using CHEM-X[‡] and the preferable coordination geometry of the macrocycle is discussed.

[‡]CHEM-X, Chemical Design Ltd, Chipping Norton, UK.

ACKNOWLEDGEMENTS.

CONTENTS.

ABBREVIATIONS.

1° - primary

2° - secondary

aq – aqueous

Ar – aromatic

c or conc. – concentrated

C_2 – $(CH_2)_2$

C_3 – $(CH_2)_3$

C_4 – $(CH_2)_4$

DCE – 1,2-dichloroethane

DCM – dichloromethane

DMF – *N,N'*-dimethylformamide

DMS – dimethylsulphate

DMSO – dimethylsulphoxide

en – ethylenediamine (1,2-diaminoethane)

eq – molar equivalent(s)

esd – estimated standard deviation

Et – ethyl

Ex – exchanges

g.AcOH – glacial acetic acid

h – hour(s)

L – leaving group

Me – methyl

Ph – phenyl

ppt – precipitate

Pr or Pr^n – propyl

py – pyridine

RT – room temperature

S.M – starting material

Th – thienyl

THF – tetrahydrofuran

Ts – *p*-toluenesulfonyl

br – broad

m - medium

s – strong (w.r.t infra red)

sh – shoulder

str – stretch

w – weak

d – doublet

m – multiplet

qu – quintet

s – singlet (w.r.t NMR)

t – triplet

1

AIMS OF THE PROJECT.

Previously a wide range of thiophene based macrocycles containing two thiophene rings, type (A), and four thiophene rings, type (B), as shown below were prepared utilising the Mannich reaction[1].
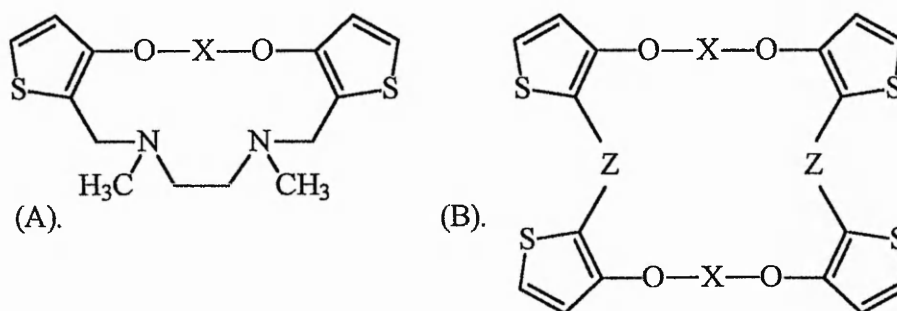
X = alkyl or heteroalkyl, Z = $CH_2N(Pr^n)CH_2$

These compounds were obtained mainly as oils and required column chromatography purification after lengthy synthesis from methyl 3-hydroxythiophene-2-carboxylate.

In order to enable the study of the complexing ability and structure of macrocycles of this type, this work had the aim of obtaining solid, preferably crystalline macrocycles without the need for elaborate purification. This would allow easy handling of the ligands in future complexation studies, with a higher probability of any isolated complexes being crystalline. The aim of obtaining crystalline macrocyclic compounds would also enable the structural geometry of the compounds to be investigated via X-ray crystallography. This was hoped to give valuable structural details that would help facilitate the future selective complexation of metal ions by these compounds. Dispensing with the need for column chromatography would allow the compounds to be

2

prepared easily and therefore be commercially viable should the compounds exhibit desirable properties.

New methods of preparing thiophene based macrocycles from methyl 3-hydroxythiophene-2-carboxylate were also to be investigated with the aim of reducing the number of steps to prepare any macrocycles or macrocyclic complexes.

1. INTRODUCTION.

1.1. Macrocyclic chemistry.

1.1.1. Discovery.

Natural macrocyclic compounds and their biological metal ion transport mechanisms have been known for many years[2]. The area of macrocyclic chemistry gained much of its now appreciable interest through C.J.Pedersen's discovery of 'Crown ethers'. These were discovered accidentally when 'white fibrous crystals' were obtained in 0.4% yield from a reaction between partially protected catechol and bis(2-chloroethyl)ether[3]. The now well known crown ethers produced considerable interest due to their proven ability to form stable complexes with alkali and alkali earth cations. Macrocycles may be defined as cyclic ligands with three or more potential donor atoms in a ring of at least nine atoms. The ligands usually encapsulate the metal ion they are coordinated to.

1.1.2. Properties.

The span and diversity of macrocycles is too vast to cover here, however a brief view of their properties will be illustrated with examples. Macrocycles have been developed to coordinate cations, anions and neutral species, however the discussion here will be limited to the properties affecting the formation of macrocyclic metal ion complexes. The formation of metal-ligand complexes is dependent on a great number of factors. The size of the interacting species must be compatible. For acyclic ligands the formation of metal ion complexes is usually dependent on the number of donors the metal ion can accommodate and the bulk of the ligand(s). The formation of macrocyclic metal ion complexes is mainly dependent on the match between the ionic radius of the cation and the 'hole size' of the ligand. If the sizes match then the expected macrocyclic complex may form. However the consequences of a size mismatch may result in the

complex being unstable or in the formation of unexpected complexes. If the metal ion is too large to 'sit' in the cavity of the ligand then the formation of 'sandwich complexes'[4] may result as shown in figure 1.

Figure 1.

"Sandwich complex".
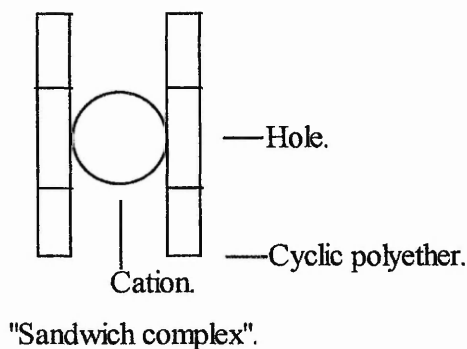
Another consequence of the metal ion being too large for the ligand's cavity may be the ligand adopting an alternative geometry to accommodate the metal ion, an example[5] of which is shown in figure 2.

Figure 2.
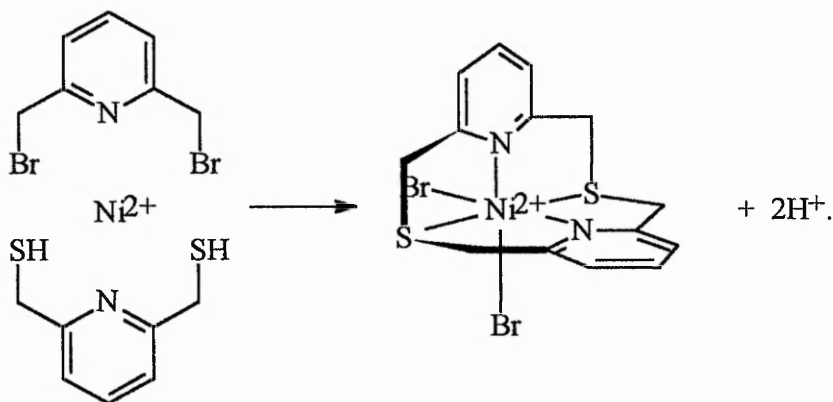
If the metal ion is too small to coordinate effectively with the macrocycle then complex formation may not occur or the metal ion may be labile. However if the macrocycle possesses groups capable of further reaction then the macrocycle may react in order to reduce its cavity size to accommodate the metal ion[6] as shown in figure 3.

The formation of stable complexes is also dependent on the metal ion and the ligand's donor groups being 'compatible'. The categorisation of ligands and metals into hard, soft, and borderline components has been established for many years. The classification is based on a ligand being hard if it is non polarisable as for most first row donor atom ligands, and soft if it has easily polarisable donors such as S or P.

Figure 3.
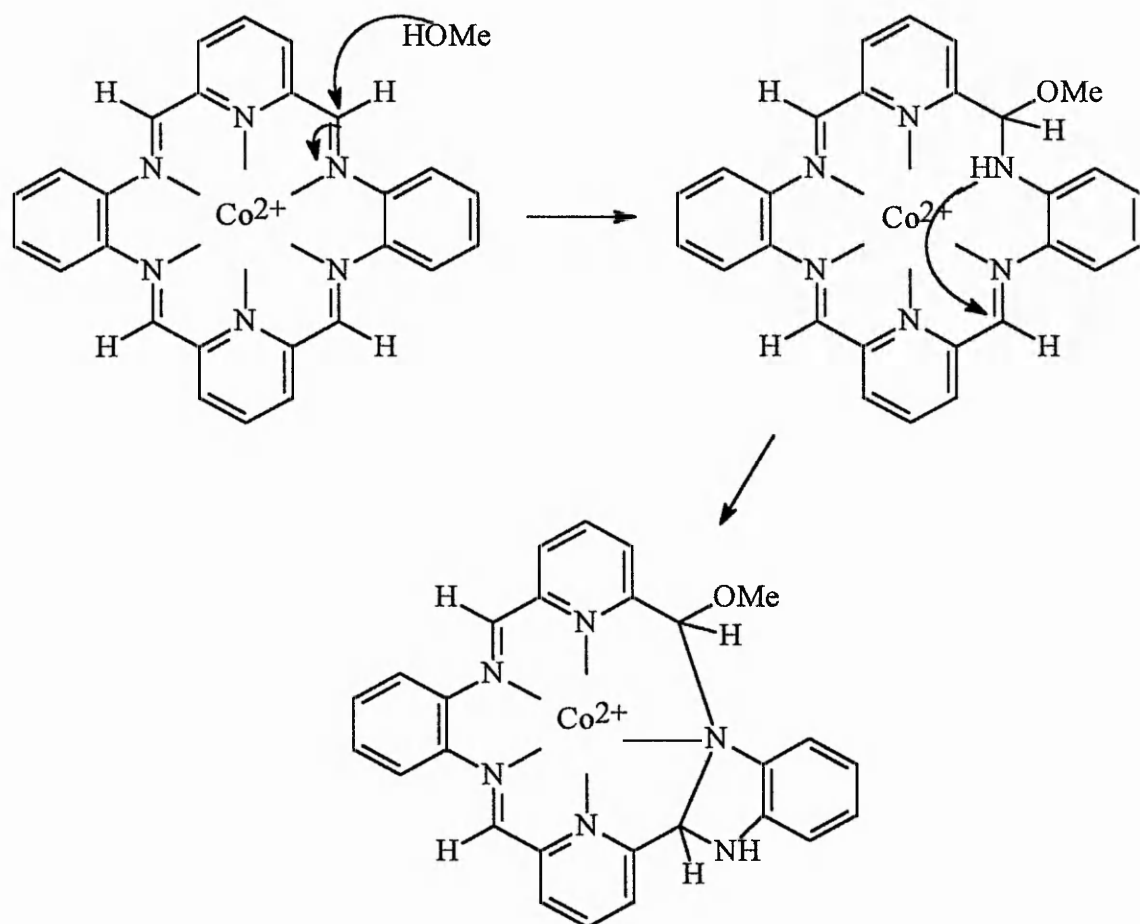
The metal ion is classified as soft if it has easily polarisable electrons, and hard if it has high charge, small size or non-polarisable valence electrons[7]. The stabilisation of metal-ligand complexes is achieved by each substrate coming from the same category. Macrocyclic examples being the hard ligand crown ethers forming stable complexes with the hard 's'-block elements and the stable complexes of soft Cu^+ and Ag^+ ions with

sulfur donor macrocycles. The predictions based on this categorisation are not always achieved however and many features are still subject to controversy.

For macrocyclic ligands the categories may be combined as 'mixed donor' macrocycles can be synthesised. These macrocycles may combine donor types to optimise coordination to metals that often breach categories. Another feature can be the complexation of differing metals by a polynucleating macrocycle, an example is the complexation of two 'soft' (Cu^{II}, Ni^{II}, or Zn^{II}) metal centres and one 'hard' (Ba^{II} or Cs^{I}) metal centre by a trinucleating N,O or N,O and S donor macrocycle[8].

As well as the size and donor type affecting the stability of macrocyclic complexes the underlying thermodynamic and kinetic contributions must be understood. Complexes of macrocyclic ligands are very stable (if the above factors have been optimised) due to the macrocyclic effect. This is similar to the chelate effect where polydentate complexes are thermodynamically more stable than a complex with the corresponding number of monodentate ligands. Macrocyclic complexes are more stable than the corresponding open chain complex containing an equal number of donor atoms[9]. This increased thermodynamic stability can be attributed to many factors. The macrocyclic complex will have a favourable entropy of formation due to the further ordering of the complex (see figure 4). The influence of the entropy factor on formation constants will alter with the number, size, and the arrangement of the chelate rings.

Usually the most important thermodynamic factor is the enthalpy of formation. This varies greatly from case to case and is characteristic of the metal ion and ligand used. The causes of enthalpy effects include the following :-

- Steric and electrostatic repulsion between ligands in the complex.

- Enthalpy effects related to the conformation of the uncoordinated ligand.

Figure 4.

log k = 1.97   log k = 4.30
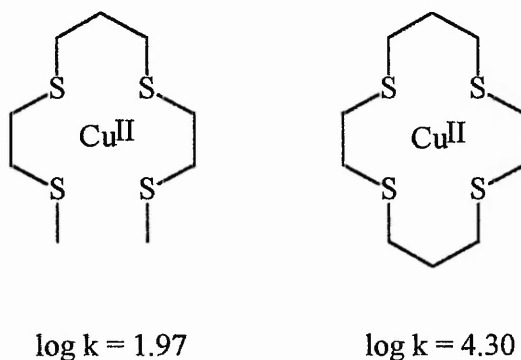
In macrocyclic complexes there is usually only one ligand of any size or consequence so that any steric or electrostatic effects are those within the ligand itself. However the conformation of the ligand is often very different from that of the 'free' ligand and may need to be in a higher energy conformation for coordination to the metal ion. Although the considerations above are justified the exact cause of the increased stability is not fully understood and alters from case to case.

Along with increased thermodynamic stability, macrocyclic complexes also show a marked kinetic inertness to both the formation of the complexes from the ligand and the metal ion and to the extrusion of the metal ion from the ligand. This may be attributed to the metal ion firstly having to enter the cavity in the macrocycle and once entered, having difficulty in leaving such a shielded coordinated environment. For instance once the metal ion is coordinated the flexibility of the coordinate bonds will be less than in an open chain analogue. The mechanism of formation and dissociation will clearly play a role in the kinetics and will vary from case to case, but it is probably the major rearrangement of the ligand required on formation / dissociation which presents the

greatest energy barrier and thus confers the complex's non-lability. A study on the effect of ring size control on kinetic lability is given in reference 10.

There are many other aspects which affect the properties of macrocyclic complexes such as anion and solvation effects but the reader is directed elsewhere[11] for further discussion.

1.1.3. Uses.

Following the considerable advances made in macrocyclic chemistry the major uses of these compounds now include aspects of ion storage and transport, the solvent extraction of metals from leach solutions, the synthesis of chromatography materials for the separation of metal ions and the development of metal ion selective reagents for use in a wide range of analytical, industrial, and other applications[12]. The major aims of future advances suggested in the literature are usually the development of ligands with greater selectivity towards the complexation of chosen substrates and the ease of their formation[13]. The aims (see page 2) of the work described in this thesis formed part of a similar overall strategy.

1.2. Synthetic methods.

1.2.1. Organic reactions.

Macrocyclic ligands can be formed from organic starting materials using a wide variety of organic reactions and synthetic methods. The strategy adopted to effect ring closure over the formation of oligomers and polymers will depend on the characteristics of the individual reaction.

Cyclisations either involve the condensation of the 'head and tail' of a single component or of two or more components. In each case conditions must be optimised so that the species combine in the desired stoichiometry (see figure 5).

Figure 5.

Cyclisation.

Condensation. [1+1]
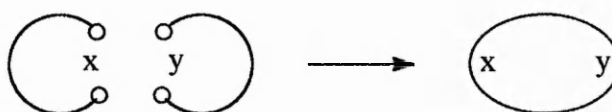
Condensation. [2+2]
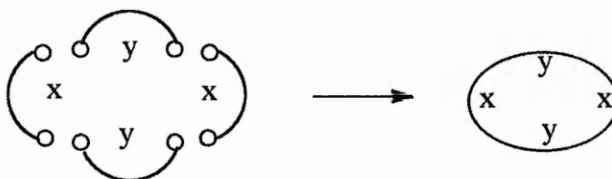
Many factors influence the yields of the desired products e.g. chain length, nature of atoms, functional groups in the system (including rigid groups), reaction type, and experimental technique.

One of the most commonly used methods to reduce the formation of unwanted higher condensates is that of 'high dilution'. The principle involved is that the greater the distribution of the species involved, the greater the prospect of intra- rather than inter-molecular condensation. The intramolecular condensation may be that of the 'head and tail' of a single component or for [1+1] and [2+2] systems the reaction of the 'half condensed' moiety with itself 'head to tail'. The apparatus involved often consists of two motorised syringes containing the precursors being pumped into the reaction vessel

at extremely slow rates. The consequence of this is the concentration of the unreacted reagents in solution at any time is very small. The reaction time is often prolonged but in many cases this is outweighed by the reward of high yields.

Macrocyclisations can be been performed under moderate to low dilutions in reasonable yield[3-5] however often the presence of cations brings into question whether these influence the yield via pre-organisation of the substrates. Nevertheless effective macrocyclisation may be performed occasionally without elaborate techniques (see 'Mannich reactions' presented in this work, section 2.2).

1.2.2. Schiff base condensations.

The formation of imines has resulted in a significant contribution to macrocyclic chemistry[14-28]. The simplicity of the reaction as well as the wide variety of difunctional amines and carbonyl compounds available have influenced the use of this type of condensation. Schiff base condensations involve the condensation between a primary amine or ammonia and an aldehyde or ketone. The reaction is reversible with the elimination of water. The mechanism is outlined in figure 6.

Figure 6.
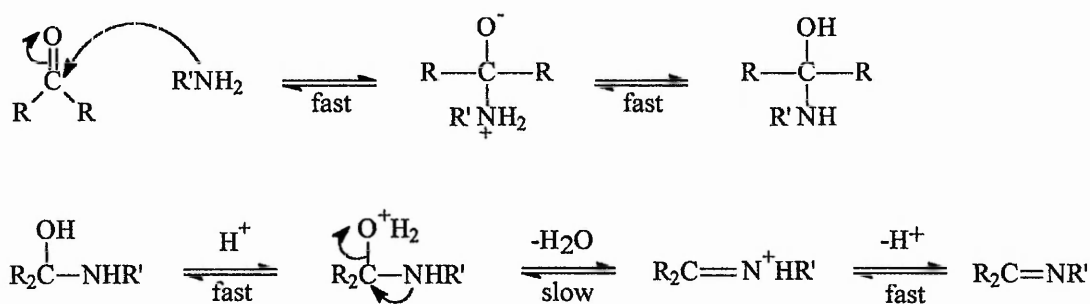
The reaction is pH dependent, i.e. in the first step if the solution is too acidic the amine becomes protonated and non nucleophilic, whereas in step 2 acidic conditions are favourable for the loss of the protonated hydroxyl group as water. A balance must be found between these two steps.

Imines are susceptible to hydrolysis which results in the addition of water to the imine link to yield the original amine and carbonyl compounds. There are examples[14] of macrocyclic imines being isolated without hydrolysis, however often the rigorous exclusion of water is required. A major use of Schiff base condensations is in 'templated' reactions, see below.

1.2.3. Template synthesis.

'Normal' organic reactions used in macrocycle formation can be laborious and often give only poor yields of the desired cyclic ligand. The aim of template synthesis is to orientate the reaction sites so that condensation occurs to yield cyclic systems. The template may be a metal ion or metal complex. The brief discussion here will be limited to the use of templates in Schiff base condensations as the full scope of templated reactions cannot be covered here.

The 'template effect' can be divided into two categories when a metal ion template is involved. The 'thermodynamic template effect' can be described as the metal ion preferentially coordinating one of an equilibrium mixture of products to drive the reaction in favour of this species[15]. The 'kinetic template effect' describes the role of the metal ion as directing the steric course of the reaction such that the formation of the desired product is achieved[15]. The role of the metal ion is easy to conceptualise but in

most real reactions it is difficult to elucidate it and will probably be influential both thermodynamically and kinetically.

An important driving force in the development of templated reactions was Curtis's discovery that metal diamine complexes templated an unusual reaction with acetone and other aliphatic carbonyl compounds[16] (see figure 7).

Figure 7.

en = 1,2-diaminoethane (ethylenediamine)
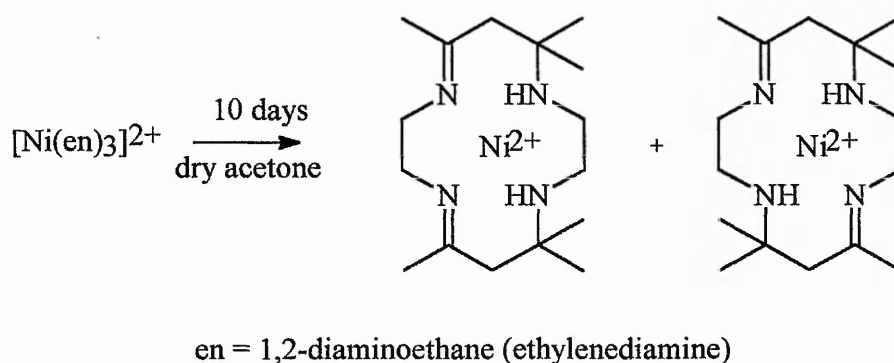
The reaction is initiated via the nucleophilic attack of a labile 1,2-diaminoethane nitrogen on the acetone carbonyl carbon to yield the coordinated imine, and probably proceeds via the nucleophilic attack of an acetonyl carbanion on the imine carbon atom. The reaction is an illustrative example of the ordering power of a metal template.

The effect of metal ion templates in Schiff base condensations can be attributed to many factors[11] but the discussion here will be on the influence the metal ion has on the products formed as this is most relevant to the work described later in this thesis (sections 2.5.1 and 3.5.1).

The *insitu* reactions of Ni(II) salts and the appropriate dialdehyde with en or *o*-phenylenediamine have led to the formation of a series of macrocyclic complexes[14,17,18] of the ligands shown in figure 8.

<u>Figure 8.</u>
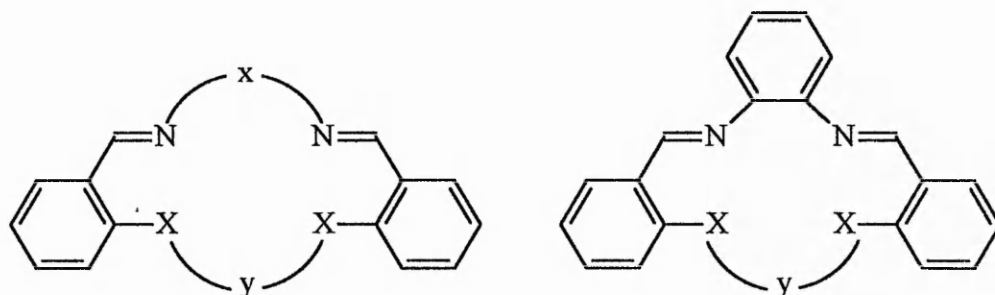
These [1+1] macrocycles are either square planar or octahedral depending on the coordinating nature of the anion. The N,O donor macrocycles may also be prepared directly without the use of a metal template whereas the sulfur containing macrocycles can only be prepared via the template.

When a zinc(II) template was used the 14- or 15- membered macrocyclic N,O donor complexes were isolated[19] however the zinc ion lies outside the cavity of the macrocycle coordinated to the two nitrogen atoms. When a cadmium(II) template was employed the N,O donor macrocyclic complexes were obtained[19] however the cadmium to ligand ratio was found to be 1 : 2.

The $Co(NCS)_2$ complex was prepared directly from the ligand above where X = O, x = $(CH_2)_3$, y = $(CH_2)_2$, however two differing products were recovered. They were both found by various characterisation to be the 1 : 1 complex. When the 'purple' complex's structure was solved by X-ray diffraction the ligand was found to be coordinated in a *β-*

cis-configuration. In the *β-cis*-configuration the ligand's donor atoms occupy both apical positions of the metal ions octahedron and two of the basal positions *cis* to one another. This allows the optimisation (lengthening) of the Co-O 'contacts'[20]. This folded configuration has also been reported for the N_4 'Curtis' type[16] complexes when forced by the introduction of a bidentate ligand which occupies cis basal positions in the octahedral coordination sphere[21].

Another large series of macrocyclic complexes (shown in figure 9) has been prepared by the *insitu* reaction of various metal salts with various diamines and 2,6-diacetylpyridine[22,23,24,25,26].

Figure 9.

(I).

(II).
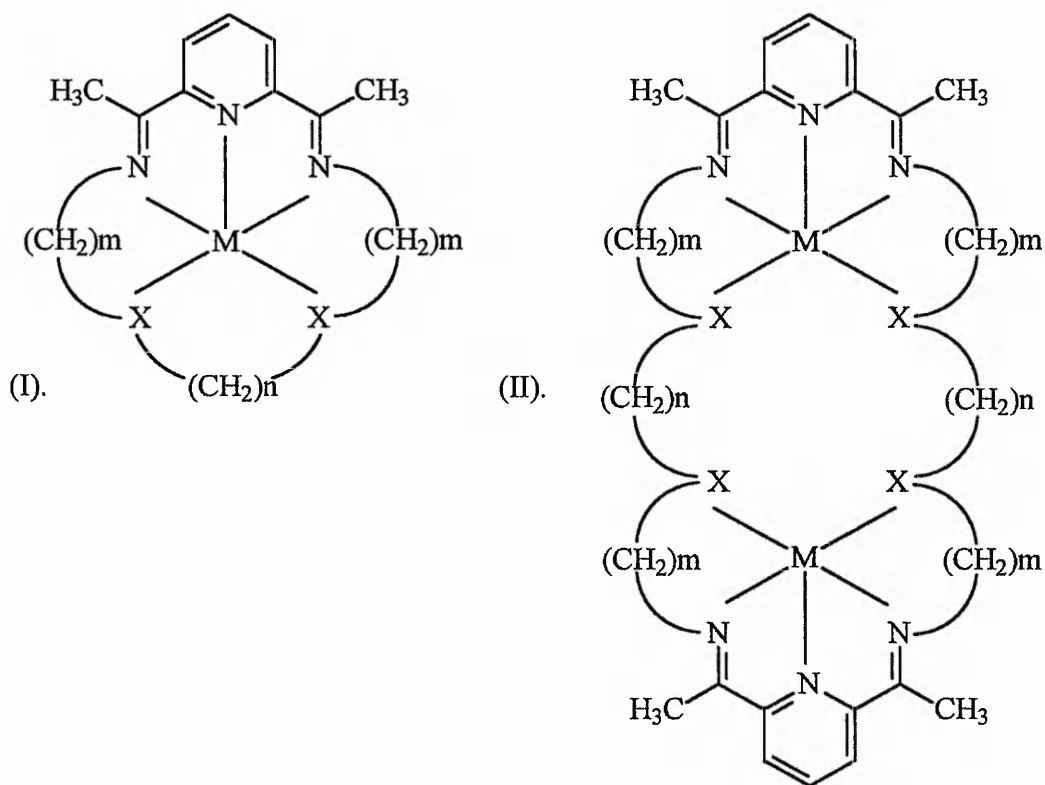
The complexes of type (I) were prepared[22] via template synthesis with the appropriate diamine and metal ion (Mg^{II}, Mn^{II}, Fe^{III}, Zn^{II}, Cd^{II}, Hg^{II} or Ag^{I}). The complex's exhibit

unusual, seven, six, and five coordinate geometries based on (in most cases) an approximately pentagonal conformation of the macrocycle donor atoms.

Lead(II) salts (thiocyanate, perchlorate) may be used to prepare the macrocyclic complexes of type (I) where X = NH, however when the X = O complex was attempted the [2+2] macrocyclic complex of type (II) X = O was obtained[23]. This has been attributed to the ether oxygen having lower affinity for lead than the solvent, methanol. Therefore once one end of the diamine chain has condensed the other end is not brought into close enough proximity to the remaining C=O group of the pyridine moeity and therefore condenses with another 2,6-diacetylpyridine and the [2+2] complex is formed.

Ni(II) salts are ineffective as templates for the formation of the complexes of type (I) however complexes of the ligand type (I) X = NH, m = 3, n = 2 may be prepared via transmetallation of the Ag^I complex[24]. The complex is six coordinate and adopts a new conformation from those of other transition metal complexes prepared via template synthesis. The ligand occupies five sites of the octahedron with the pyridine nitrogen in the apical position. As well as this complex, Ni^{2+} complexes have been isolated with the 16 membered ring macrocycle where solvent (MeOH, EtOH) has added across one of the C=N bonds. The formation of these two types of complex has been attributed to the strong preference of the d^8 ion for an orthogonal arrangement of donor atoms.

When the Pb^{II} dinuclear complex of type (II) X = O is treated with an excess of Fe^{II}, Co^{II}, or Ni^{II} salts the mononuclear complexes from transmetallation are formed. These show only the six nitrogen donors coordinating to the metal ion in a distorted octahedral structure, the four oxygen atoms being uncoordinated[25]. Further Cu^{II} and Zn^{II} complexes

of the ligand type (II), X = O were obtained via transamination of the open chain diimine 2,6-diacetylpyridine complexes[26].

Thiophene analogues of the type (I) and (II) complexes have been prepared from both direct and metal templated reactions involving thiophene-2,5-dicarbaldehyde[27].

These two lines of research demonstrate the powerful role the metal ion can play in directing the course of a reaction to products obtained in good yield which otherwise are impossible or only obtained via lengthy purification in very poor yields[23].

A further mention of Ni[II] chemistry will now be made owing to its use in the research described in this thesis. Ni[II] complexes occur in tetrahedral, square planar and octahedral geometries, however square planar and octahedral geometries are most common for macrocyclic complexes. Four coordinate nickel (II) chemistry has the interesting feature of the interconversion between paramagnetic tetrahedral and diamagnetic square planar geometries. However recently a paramagnetic planar species has been reported[28]. Another feature of square planar Ni[II] complexes is their ability to coordinate extra ligands in solution to set up equilibria between 4, 5 and 6 coordinate complexes. Aggregation of planar units can also occur in both the solid state and in solution to form paramagnetic polymers. Thus [Ni(Me-Salen)$_2$], where Me-Salen = *N*-methylsalicylaldimine, forms dimeric and polymeric oligomers via bridging of the O-donor across planar units[29] (see figure 10).

Figure 10.
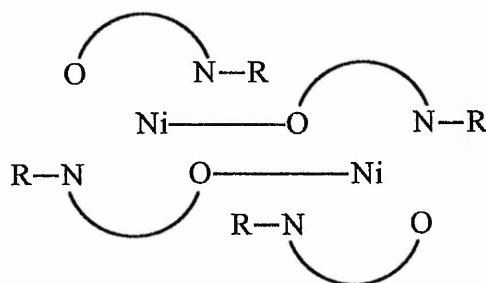
Thus in addition to tetrahedral, square planar, five coordinate and octahedral equilibria, monomer, oligomer and polymer equlibria may also exist for certain Ni^{II} complexes.

1.3. Thiophene chemistry.

Of the 5 membered heterocycles furan and pyrrole based macrocyclic systems are more often reported in the literature than thiophene based systems. This could well be due to the poor donor properties of the sulfur atom. Thiophene does have advantages over furan and pyrrole however as its macrocycles can be readily desulfurised[30]and it is generally more stable.

Interest in the metal bonding properties of thiophenes arose from the industrial process of the hydrodesulfurisation of thiophenes which may involve M-S (thiophene) coordination.

The reports of thiophene-S bonding are usually somewhat vague in their description and with the exception of organometallic complexes (whose modes of coordination will be described) the authors seem unwilling to commit themselves to positively confirming whether or not the sulfur atom is behaving as a donor atom. Thiophenes have been

found to adopt several modes of coordination in organometallic complexes, η^5-, η^4-, η^2-, η^1-S, or η^1-C.

The η^5- mode where all five atoms of the thiophene ring are bonded to the metal centre is the most common and examples are thiophene bound to Rh or Ir[31], tetramethylthiophene bound to Rh[32,33] and 2,5-dimethylthiophene bound to Rh[34].

The η^4- mode where the four carbon atoms of the thiophene ring are bonded to the metal centre occurs most often when the S atom of the ring is bound to another metal centre[33,35,36].

The η^2- mode involves two of the thiophene ring carbon atoms bound to a metal centre as in thiophene bonded via carbons 2 and 3 to Os[37].

The η^1-S mode is the least common of all especially when the rest of the ring is not coordinated as in thiophene bound to Ir[38]. The Ir-S bond distance is 2.452Å. An extremely rare example of the thiophene S atom bound to two Mo atoms and η^4-coordinated to Ir was the first example of a thiophene bound to three metal centres[36].

The η^1-C mode involves one of the thiophene ring carbons bonded to a metal centre[39,40].

Much of the conflict of whether or not the thiophene S atom is genuinely coordinated to a transition metal centre arises from the weak nature of the interaction which reveals itself in the S-metal bond lengths. These are often less than the sum of the van der

Waals radii yet not significantly larger than the sum of the covalent radii (which are however often hard to determine especially for apical positions[41]). The situation is usually best assessed by considering the above coordination possibilities alongside the geometry of the ligand with respect to the usual coordination geometries of the metal centre. For example the Cu(II) complex of 2-(2'-thienyl)pyridine[42] (see figure 11) has an octahedral geometry with the two S atoms coordinated in the apical positions (the basal positions are occupied by the two N donors and two Cl anions) with Cu-S distances of 2.968 and 2.904Å. The ligand in this case is described as "an asymmetrical bidentate N,S-donor".

Figure 11.
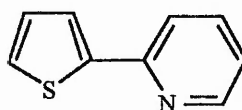
This can be contrasted with the Cu(I) complex of *(R)(S)*-1,2-bis-(5-methyl-thiophene-2-aldimine)cyclohexane[43] (see figure 12).

Figure 12.
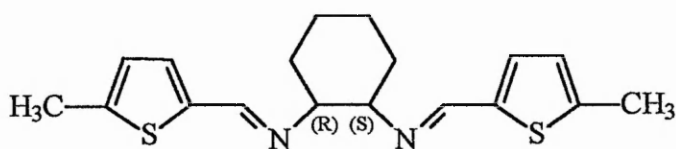
The complex contains two ligands, the complex thus having eight potential donors. The Cu(I) ion is described as being coordinated only by one of the imine N atoms from each ligand in an approximately linear geometry. The distances of the four S atoms from the Cu(I) ion are 2.959, 3.152, 3.735 and 4.055Å. It is obvious that two of the Cu(I)-S distances are far beyond any interaction but it is interesting to note that although the two shorter distances are comparable with the Cu(II) complex bond lengths, due to the

geometry of the ligand (the shorter bond length S atoms are described as "hardly at all directed towards the Cu(I) centre") and "the preference of group 11 +1 oxidation state metal centres for linear coordination"[43] these are not described as bonding distances. The discussion by the authors of the last example can be further contrasted with another of their papers[44] describing a di-Ag(I) complex of practically the same ligand (H replaces Me at the thiophene 5 position), here the two ligands bridge two Ag(I), group 11 centres. In this structure all of the N atoms are coordinating and all of the thiophene S atoms are described as "weakly interacting" with Ag(I)-S distances of 2.961, 2.938, 2.928 and 2.995Å. The "preference of group 11 metals for linear coordination" is not mentioned.

A rare example of a macrocyclic thiophene sulfur-metal interaction[41] occurs for the palladium complex of the thioether shown in figure 13.

Figure 13.
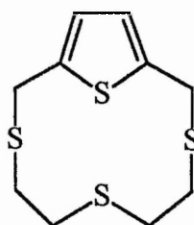
The geometry around the Pd(II) centre is approximately square pyramidal with the basal positions occupied by two of the thioether sulfur atoms (average Pd-S = 2.279Å) and two Br anions. The thiophene S atom is located in the apical position, Pd-S = 3.182Å. The sum of the van der Waals radii for the two atoms is 3.40Å[45].

There are also many examples of thiophene[46-50] containing mixed donor ligands where the thiophene S atoms are directed away from the metal centre or approach the metals apical positions at van der Waals distances.

1.3.1. Mixed donor thiophene based macrocycles.

Macrocycles incorporating thiophene rings can be classified into two groups, those where the sulfur atom is part of the macrocyclic ring (and therefore a potential ring donor atom), and those where the sulfur atom is exocyclic i.e. not part of the macrocyclic ring. An example[46,51] of each type is shown in figure 14.

Figure 14.
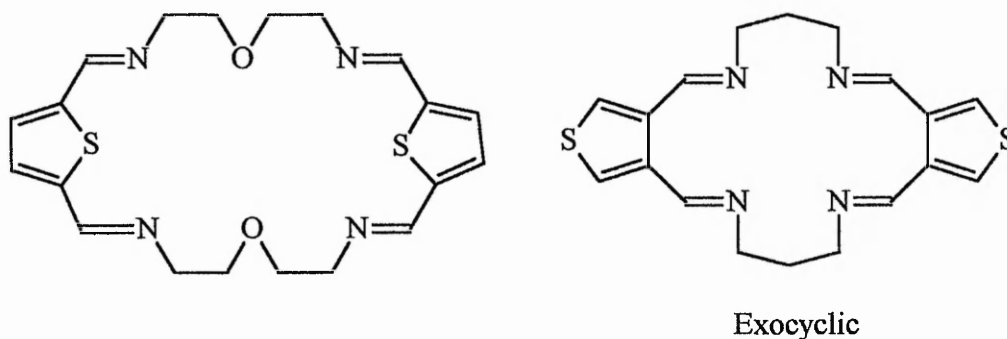
Exocyclic

As can be seen above the exocyclic macrocycle is not of the mixed donor variety (sulfurs considered as non-donor atoms). At present no thiophene based exocyclic mixed donor macrocycles can be found in the literature other than those by Chaffin[1] and those presented in this work.

As for the open chain thiophene ligands discussed previously (page 20), metal ion complexes of mixed donor thiophene containing macrocycles (of the types shown in figure 15) where the sulfur is a potential ring donor atom, also show the metal ions

preference for the O, N or S (thioether) donor atoms. The thiophene sulfur atoms are described as inert spacers[46] or only weakly donating[52].

Figure 15.

$X = O, N$ or S
$(z) = (CH_2)_2$ or $(CH_2)_3$
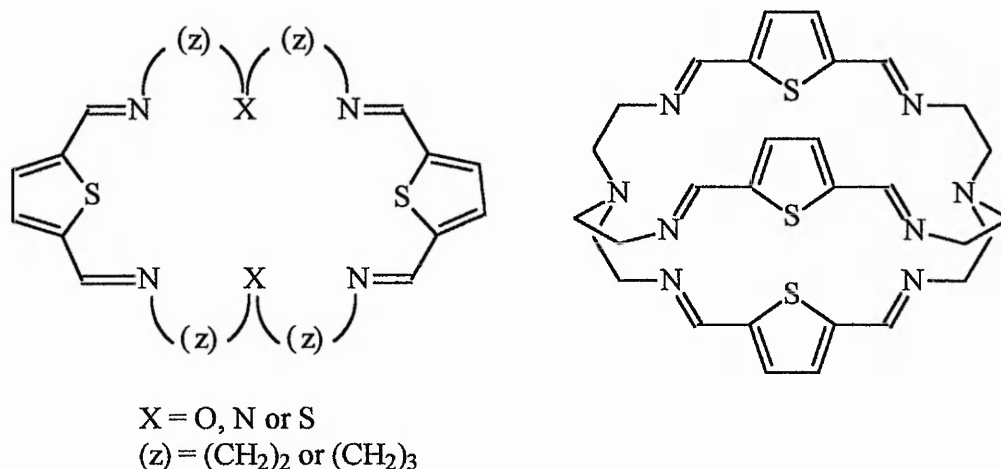
In the macrocycles produced in this work the thiophene sulfur atoms are exocyclic and as can be seen from the discussion above, are unlikely to be involved in the coordination of any metal ions. The main synthetic route to the macrocycles produced in this work involved aminomethylation.

Hartough made an extensive study of the aminomethylation of thiophene and its derivatives in the 1940's[53]. Thiophene possesses α-hydrogens which undergo reaction with the mildly electrophilic condensate of the amine and formaldehyde as shown in figure 16.

Figure 16.

$$RR'NH \ + \ HCHO \ \longrightarrow \ CH_2{=}N^{+}RR'$$

$$ThCH_2NRR' \ + \ H^{+} \ \xleftarrow{\ Th\ } \ {}^{+}CH_2{-}NRR'$$

23
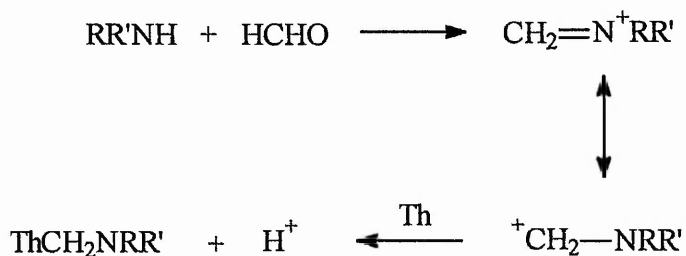
These reactions give products in high yield and demonstrate thiophene's reactivity towards electrophilic substitution.

Barker *et al* formed a number of Mannich bases with secondary amines[54] and recently Chaffin used this reaction to prepare a wide range of thiophene based macrocycles[1] of the type shown in figure 17.

<u>Figure 17.</u>

(A).   (B).
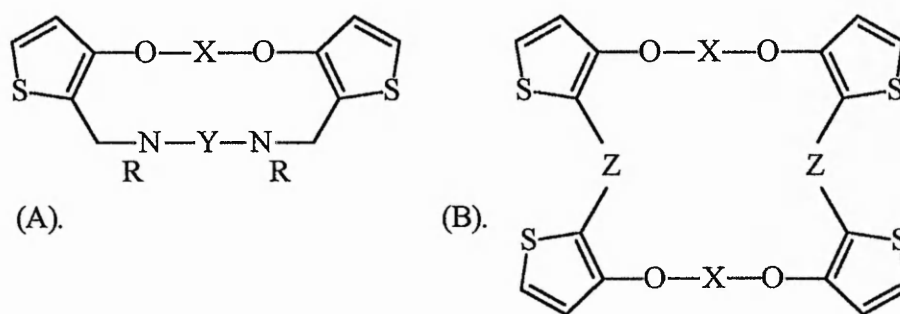
X = alkyl or heteroalkyl, Y = $(CH_2)_2$, R = Me, Z = $CH_2N(Pr'')CH_2$

Recently the Mannich reaction has been employed to synthesise a range of benzene based macrocycles by the *ortho*-substitution of phenolic compounds[55-59]. As in the work by Chaffin[1] these compounds were mainly obtained as oils, required column chromatography purification and were obtained in low to moderate yields. In this work crystalline macrocycles were produced in high yields without the need for column chromatography purification.

For discussion on thiophene macrocyclic chemistry the reader is directed to two reviews by Meth-Cohn[60] and Newkome[61].

1.4. Structure determination.

1.4.1. X-rays.

Since X-rays are the source that leads to X-ray diffraction data which in turn leads to the determination of crystal structure some background information on their production and properties is given below.

X-rays are electromagnetic radiation of short wavelength ($\sim$0.1-100Å; 1Å = 10^{-10}m) and are produced in an X-ray tube as a result of the sudden deceleration of rapidly moving electrons at a target material. The most common type of X-ray tube is a permanently evacuated hot cathode tube. Electrons are emitted from a heated filament (also the cathode) and are accelerated by a potential gradient towards the target anode (made of the material whose wavelength is desired). The anode needs to be water cooled due to the large dissipation of power. When an electron falls through a potential difference of V volts, then it aquires an energy of eV electron volts. If this energy was then converted entirely into a quantum, hv, of X-rays, the wavelength, λ, would be given by :-

$$\lambda = h\,c\,/\,eV$$

h = Planck's constant.

c = velocity of light.

e = charge on an electron.

Numerical substitution gives :-

$$\lambda = 12.4\,/\,V \qquad \text{(units of V = kV.)} \text{————— (A)}$$

The process is very uneconomical however and in most X-ray tubes the majority of the energy is converted into heat and only a few percent is converted into X-rays for crystallographic use.

Equation (A) gives the minimum wavelength for a given accelerating voltage. The actual distribution of X-ray intensities against their wavelength for differing accelerating voltages is shown in figure 18[62].

Figure 18.
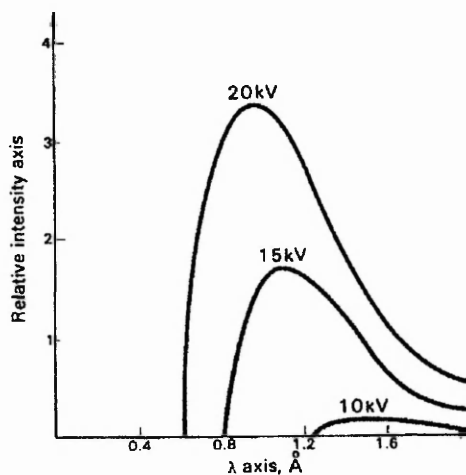
If the accelerating voltage is sufficiently large the electrons striking the target material excite the inner electrons of the target atoms. If these are expelled from the atom then electrons from higher energy levels fall back to replace these inner electrons. These transitions are accompanied by the emission of X-rays whose wavelength is dependent upon the energies of the two levels involved. The white radiation distribution now has sharp lines of very high intensity superimposed upon it.

The principal electronic transitions are from L - K shells (Kα) and M - K shells (Kβ) and because each transition can occur from two possible electronic configurations, of slightly differing energies, the transitions give rise to two (very close) doublets. The 'K' spectrum superimposed on the white radiation continuum gives an intensity distribution as shown in figure 19[63].

Figure 19.
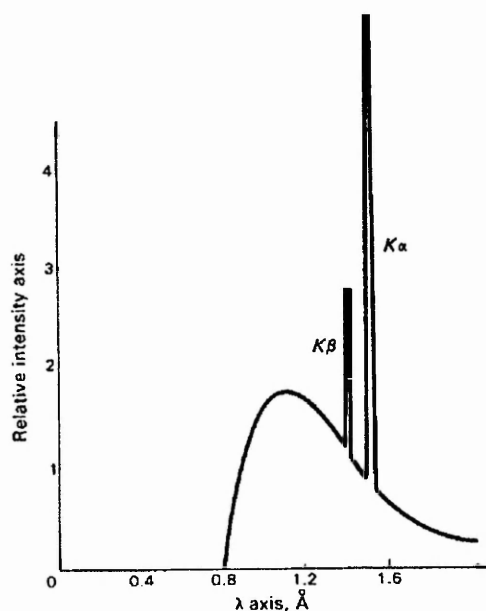
As the wavelength depends on the energy of the K, L and M shells so it depends on the target material. A common target is copper whose characteristic spectrum consists of Kα (λ = 1.542Å) and Kβ (λ = 1.392Å). Kα and Kβ are always produced together and as a monochromatic source is desired a method of filtering out the less intense Kβ wavelengths is required.

1.4.2. Filtering (Absorption of X-rays).

Equation (B) represents the absorption of X-rays by materials.

$$I = I_0 \exp(-\mu t) \underline{\hspace{2cm}} (B)$$

I = transmitted intensity.

I_0 = incident intensity.

μ = linear absorption coefficient.

t = path length through material.

The variation of μ with λ for nickel is shown in figure 20[64].

Figure 20.
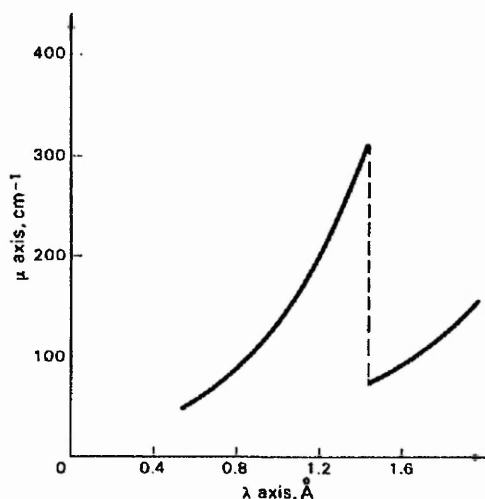
The absorption edge for nickel coincides with the wavelength of Kβ for Cu. Therefore using a thin nickel foil over the X-ray aperture reduces all the wavelengths to a certain extent but almost entirely removes the Kβ wavelength leaving the nearly (Kα₁ and Kα₂) monochromatic Kα X-ray beam.

The desired wavelength can also be selected using a monochromator. This is achieved by reflecting the beam from the surface of a curved graphite crystal.

1.4.3. The direct lattice and unit cell.

Crystals of any given compound are comprised of a compound's molecular arrangement regularly repeated in three dimensions to give a vast array of the repeating unit macroscopically defined by the faces of the crystal. It is the periodic nature of the crystal which causes the diffraction of X-rays under certain conditions.

Diffraction is easily conceptualised in one dimension from a simple grating, however it is less easy to understand from a three dimensional crystal (which Laue[65] described as a

three dimensional grating). In order to better visualise the phenomenon of diffraction from crystals it is convenient to introduce the concept of an imaginary lattice.

The lattice is used as a coordinate grid for the repeating unit. If a point is placed at each corner of a parallelepiped whose volume contains the repeating unit then eight points are produced. If this is then repeated by stacking further parallelepipeds on each face infinitely then an infinite array of lattice points will be produced. Any eight of these may be connected in the original way to give the volume of the repeating unit now described as the unit cell.

As one can imagine any number of unit cells can be constructed by joining points of the lattice. The true unit cell is chosen by convention:- it should be the smallest repeating unit which best represents the symmetry of the lattice.

There are 14 different ways of constructing unique lattices and are therefore 14 different types of unit cell to describe them. This only describes the geometric relationships of the lattices and obviously the lengths e.g. the sides of the unit cell and the angles between them vary but only as allowed by the 14 descriptions.

There are seven basic crystal systems based on the seven main forms of lattice, some of which can be centred to give the total of fourteen lattices. Lattices with points only on the unit cells vertices are called primitive (P), i.e. one point per unit cell (1/8 of each of the 8 points). Other types are face centred i.e. a C face centred cell has lattice points at the centre of the two cell faces that cut the c axis. F means all faces are centred and

body centred (I) implies a single point at the centre of the cell. The conditions relating to the cell lengths and angles are given below.

Triclinic (P) :- $a \neq b \neq c$, $\alpha \neq \beta \neq \gamma \neq 90°$

Monoclinic (P) (C) :- $a \neq b \neq c$, $\alpha = \gamma = 90°$, $\beta \neq 90°$

Orthorhombic (P) (C) (I) (F) :- $a \neq b \neq c$, $\alpha = \beta = \gamma = 90°$

Tetragonal (P) (I) :- $a = b \neq c$, $\alpha = \beta = \gamma = 90°$

Hexagonal (P) :- $a = b = c$, $\alpha = \beta = 90°$, $\gamma = 120°$

Trigonal (R , Rhombohedral) :- $a = b = c$, $\alpha = \beta = \gamma \neq 90°$

Cubic (P) (I) (F) :- $a = b = c$, $\alpha = \beta = \gamma = 90°$

The fourteen lattices are shown in figure 21[66].

Figure 21.
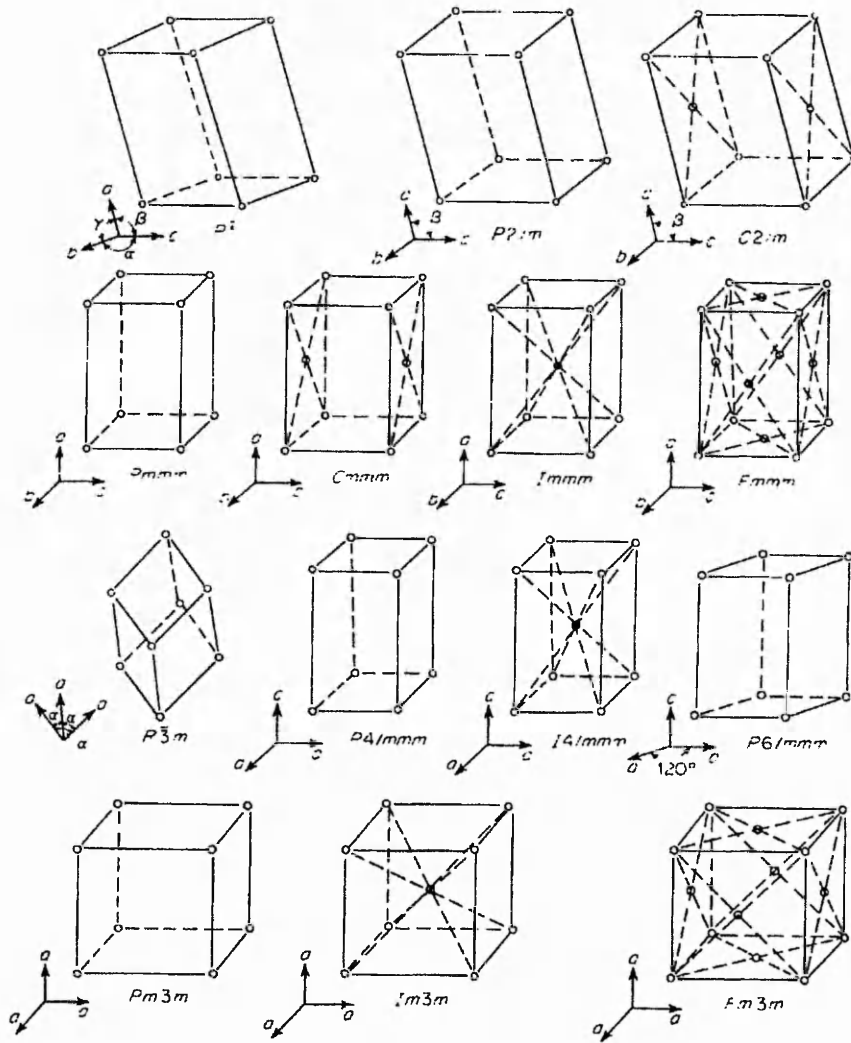
In the lattice it is possible to visualise lattice planes containing regularly arranged sets of points, shown in two dimensions in figure 22.

Figure 22.
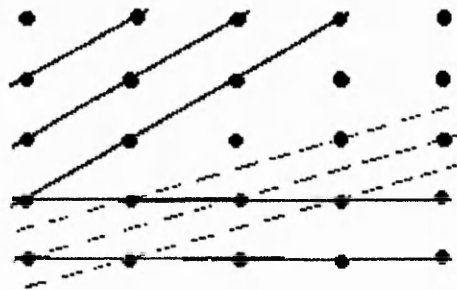
These planes intersect each unit cell side at a set fraction of its length. Therefore each plane can be uniquely described via its intercepts[67]. For example if the sides a, b, and c are intercepted at 1/3, 1/4 and 1/2 of their lengths respectively then the Miller indices of the plane hkl would be 342.

1.4.4. Diffraction of X-rays.

Diffraction may be described as the reinforcement of waves produced from a regular array of points which obstruct an incident wave. However Bragg[68] noted the similarity of diffraction to ordinary reflection and saw that diffraction could therefore be considered in terms of reflection from planes in the imaginary lattice.

Von Laue's attempts to explain his diffraction photographs in terms of a three dimensional diffraction grating were not successful. By seeing the problem in terms of reflection Bragg had reduced a three dimensional problem to a set of one dimensional ones. However the problem was still not easy. Diffraction (reflection) from a single plane would be too weak to give the reflections observed and Bragg therefore concluded that the waves from successive planes in the lattice must be reinforcing to give the strong reflections. Using a narrow beam of fixed wavelength he found that only in certain orientations would the reflections from successive planes reinforce one another. The condition for this reinforcement is known as the Bragg equation and is briefly outlined below.

Figure 23[69].

(a)

(b)
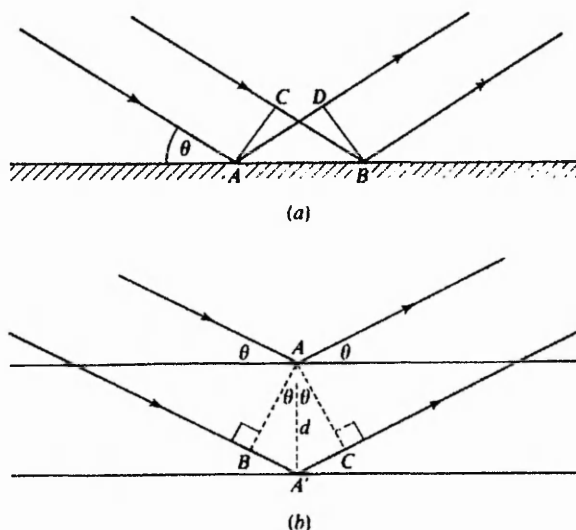
From figure 23 (a) it can be seen that the phase difference for X-rays reflected from points A and B (on the same plane) is CB - AD = 0. However reflection from successive planes occurs only for special angles. If A and A' are separated by the distance d as in Figure 23 (b) the condition for reinforcement is BA' + A'C = nλ, where n is an integer. From figure 23 (b) it can be seen that BA' = A'C = d sin θ, which gives

$$n\lambda = 2d \sin \theta$$

where d is the interplanar distance.

This equation governs the reflection of waves from planes. Having found that diffraction can be explained via the reflection of X-rays from certain planes under the conditions governed by the Bragg equation some explanation of how the observed diffraction relates to the contents of the unit cell is required.

When the electric field associated with X-rays (which are a form of electromagnetic radiation) interacts with an electrically charged electron it causes the electron to vibrate

at the same frequency. The electron therefore becomes a source of X-rays. The energy of the scattered X-rays is identical to that of the incident radiation.

From the Bragg equation we know that electrons associated with any atoms lying on the plane of reflection scatter in phase with each other. Therefore if we have a unit cell with atoms (A, B, C, D) located as in figure 24 then if we consider the 130 reflection from the planes drawn in the figure the strongest possible intensity would be obtained if all the atoms lie on these planes. As they do not then the resultant intensity is reduced by the out of phase X-rays produced from the atoms not lying on these planes. It is by the comparison of the intensities of many reflections that atomic coordinates may be deduced.

Figure 24.
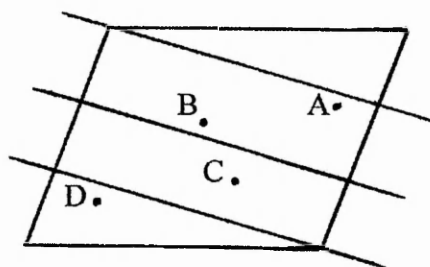
1.4.5. The Reciprocal Lattice.

The first stage of X-ray diffraction data collection involves the determination of the geometry and symmetry of the unit cell. In the case of this work this was done photographically using a Weissenberg camera[70], see section 2.11.3.

To understand how diffraction patterns may be recorded photographically it is necessary to introduce the reciprocal lattice and the sphere of reflection. From the Bragg equation it can be seen that d (the interplanar spacing) has an inverse relationship with sin θ. The interpretation of X-ray diffraction patterns is made easier with a direct relationship, therefore a reciprocal lattice based on λ/d is constructed. In the reciprocal lattice each set of planes hkl in the direct lattice is represented by a point at a distance $\rho = \lambda/d$ from the origin; the direction of the point from the origin indicates the inclination of the set of planes to the normal in the direct lattice. For diffraction to occur at a point in the reciprocal lattice, the point must lie on the surface of the sphere of reflection. This sphere is constructed such that it passes through the origin of the reciprocal lattice, and such that the direction of the beam of incident X-rays (which passes through the origin) forms its diameter. It can be shown that such a sphere will have a radius of one reciprocal lattice unit[71] (see figure 25[71]).

Figure 25.
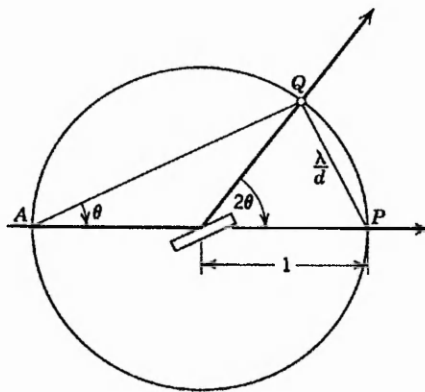
1.4.6. Oscillation and Weissenberg photographs.

When a crystal is rotated with its axis perpendicular to the X-ray beam, layers of the reciprocal lattice intersect the surface of the sphere of reflection in a series of circles, see figure 26[72].

Figure 26.
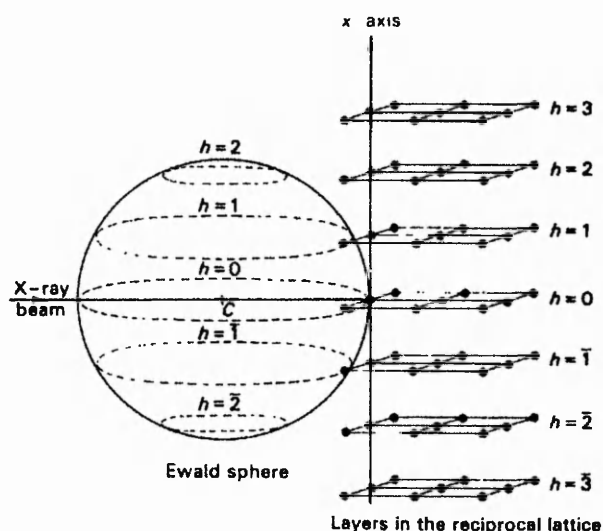
The diffracted X-rays will pass from the centre (C) of the sphere through the circumference of these circles, forming a series of cones. These cones of diffraction intersect the film in the camera and give rise to rotation photographs which contain rows of intensities, each row or layer line representing one layer of the reciprocal lattice. From these layer lines the length of the axis about which the crystal is being rotated may be determined as detailed in the experimental section. Normally the crystal is only oscillated through approximately 40°, not completely rotated, to save time in obtaining the photograph, but this does mean that diffraction is not recorded from all points in the reciprocal lattice. The photograph is then referred to as an oscillation photograph.

The lengths of the other two sides of the unit cell could now be obtained by setting further crystals about these axes and obtaining oscillation photographs. There is however a much more versatile and less laborious method invented by Weissenberg[73]. This involves rotating the crystal as in the previous method, only now screens are fitted

to isolate one 'layer line' whilst the camera moves back and forth past this aperture. The effect of this is to spread the reflection intensities which in the oscillation photograph make up the 'layer line' across the film in the camera. Normally the crystal is oscillated through approximately 240° again saving time. The appearance of Weissenberg photographs consists of rounded 'festoons' of spots separated by two slanted but straight lines of axis spots, see figure 27.

Figure 27.
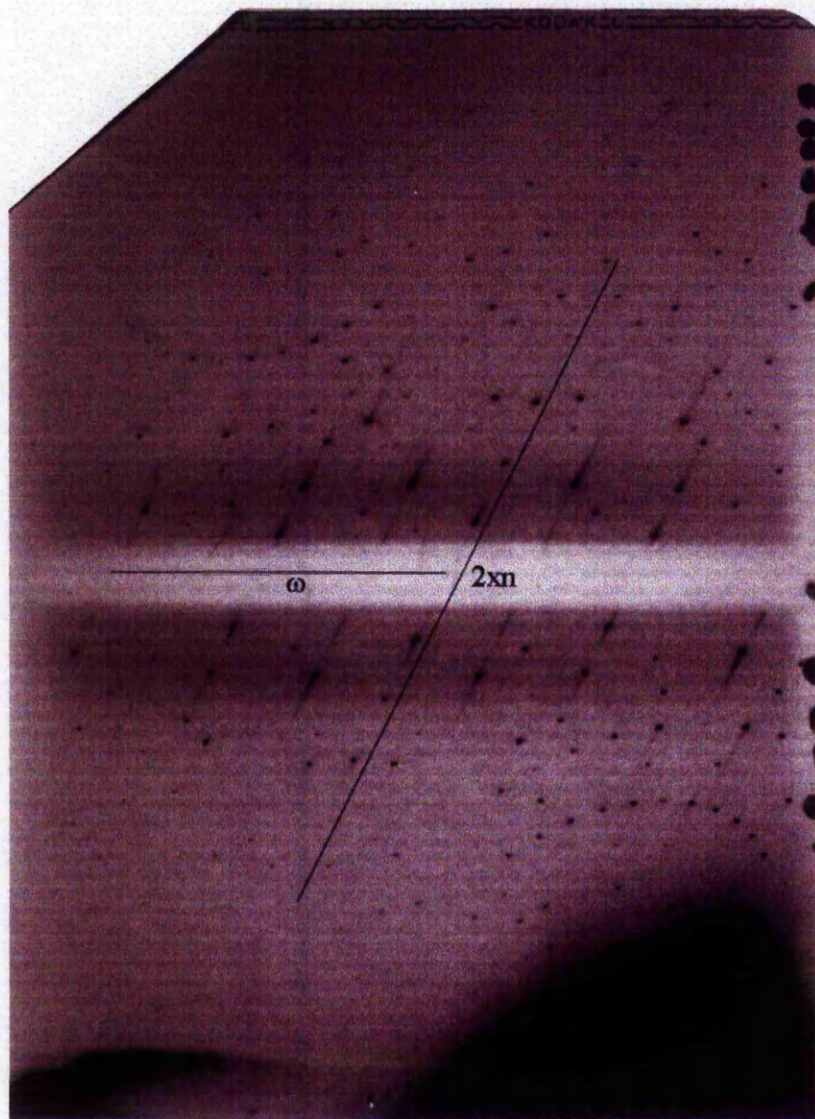
From the measurement of the distance between axis spots of positive and negative index (2xn) the remaining two unit cell lengths may be obtained see section 2.11.3. Using a camera of known radius the angle between the two axes recorded on the Weissenberg photograph may also be calculated from the measurement of the distance (ω) between them. The versatility of Weissenberg photographs comes not only from being able to measure the three axial lengths and one angle from a single crystal setting but also from their use in space group determination. As well as the zero layer Weissenberg photograph, first and second (this is usually sufficient, see Space group determination section 1.4.7.) layer photographs can also be obtained via the equi-inclination Weissenberg method. This involves the movement of the screens to isolate the desired 'layer line' and the movement of the camera through an angle μ (see the experimental section 2.11.3.).

The systematic absence of spots having certain index relationships can often be seen on Weissenberg photographs. These occur due to the unit cell having certain symmetry elements. The determination of these symmetry elements classifies the space group to which the unit cell belongs. Discussion of how Weissenberg photographs reveal these elements is presented in the next section.

1.4.7. Space group determination.

The unit cell often contains symmetry due to the fact that there may be more than one molecule in the unit cell possessing the same geometry but in a symmetry related orientation. Also the molecule itself may possess symmetry. This additional symmetry has consequences for the reflections possible via X-ray diffraction. Therefore from the

systematically absent reflections one should be able to deduce the symmetry elements present, as well as the overall symmetry of the unit cell and classify the structure as belonging to one of the possible 230 space groups. It is now necessary to discuss the symmetry elements and their consequences.

The reason that there are only 230 unique space groups possible arises from the limited number of combinations of the symmetry elements an infinite repeating lattice allows. Three of the possible symmetry elements are a centre of symmetry, an axis of rotation and a plane of reflection. A centre of symmetry (or inversion centre, designated by -1) is a point through which translation will relate one asymmetric unit to another. A plane of reflection (designated by m) is a plane which when present in the unit cell relates one asymmetric unit to another by reflection in the plane. An axis of rotation relates one asymmetric to another by rotation for a fixed number of degrees. A 2 fold axis rotates an asymmetric by unit 180°. Therefore an n fold axis rotates each unit by 360/n°. Due to the necessity for a space filling volume only 2,3,4 and 6 fold rotation axes occur in crystals (designated by number).The combination of rotation with reflection in a point gives the inversion axes –2, -3, -4, -6. The combination of these symmetry elements alone with the seven crystal systems gives rise to the 32 point groups into one of which any crystal can be classified by its morphology. The symmetry elements which describe the 32 point groups only involve rotation and / or reflection. The other two symmetry elements which when combined with those just described give rise to the 230 possible combinations involve translation as well as reflection or rotation and are known as glide planes (designated by letter a, b, c, n or d) and screw axes (designated by a number with a subscript number). The symmetry operations of glide planes and screw axes will be explained in the examples now given.

Consider the space group C2. The symbol tells us that the lattice is C centred which means the crystal system must be monoclinic or higher in symmetry. The 2 fold rotation axis is taken by convention to coincide with the unique b axis in this case. Placing a T to represent an asymmetric unit of structure close to each lattice point gives two units per unit cell as shown in the C face projection below in figure 28.

Figure 28.
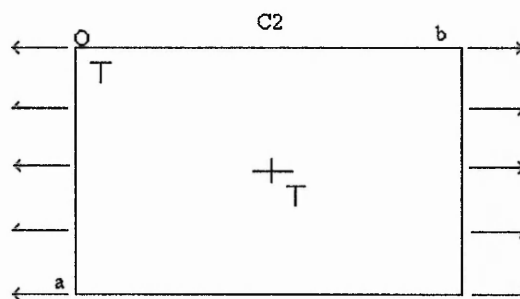
If the T's are rotated 180° about the b axis the distance they were (+) above the paper now becomes (-) below the paper. As can be seen in figure 29 below there are now four units of structure within the unit cell. Each can replace another by rotation in either the 2 fold axis at a = 0, 1 or the accompanying one at a/2 which occurs because of the C centring.

Figure 29.
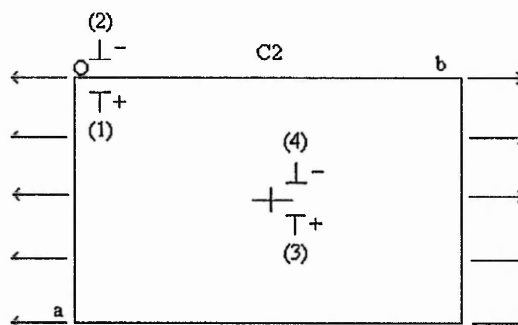
The diagram above shows the 2 fold axes as double sided arrows. Examining the diagram, single sided arrows are also present at a/4 and 3a/4. These represent screw

40

axes (2_1). These symmetry elements although not in the space group symbol occur as a consequence of the C centred lattice. As can be seen T (1) can be transformed into T (4) by reflection through the plane 3a/4 and translating it by the distance b/2 (along the b axis). Thus as well as the 2 fold axis the unit cell possesses two 2_1 screw axes but these are not included in the space group symbols as their action is carried out via the combination of the C centred lattice and the two fold rotation axis.

If the position of T (1) is taken as x, y, z then from the diagram above it can be seen that the positions of (2), (3) and (4) are -x, y, -z; x+1/2, y+1/2, z; -x+1/2, y+1/2, -z. These are known as the *equivalent positions* within the unit cell.

Consider the space group C2/m. Introducing a mirror plane perpendicular to the b axis (coincident with the B faces of the crystal) gives an additional four equivalent positions which arise from reflecting the four positions of C2 through the mirrors at b and b/2 (because of the C centring). The C face projection of C2/m is shown in figure 30.

Figure 30.
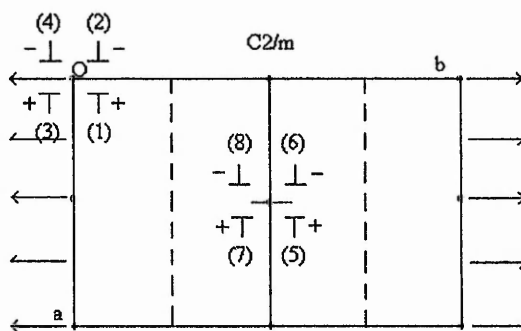
In addition to the mirror planes there can be seen two dashed lines at b/4 and 3b/4. These represent a-glide planes. A glide plane involves reflection through the plane and then translation along the plane. The translation for a, b and c glide planes is half the

axial length (for d glide, half the diagonal length) and for n glide the translation is (a+b)/2, (a+c)/2 or (b+c)/2. Therefore for C2/m it can be seen that T (1) can be converted into T (7) by the a-glide plane. Again the a-glide does not occur in the space group symbol as it occurs as a consequence of the 2 fold axis and the mirror plane.

Having introduced the symmetry elements it is now necessary to discuss the consequences they have on the conditions for X-ray diffraction and therefore how their presence can be elucidated from X-ray diffraction patterns. To do this it is necessary to introduce *structure factor theory*.

1.4.8. Structure factor theory.

X-rays are diffracted from the electron clouds about atoms. It is possible to obtain the amplitude of scattering of the electron distribution in the atom and hence to derive the atomic scattering factor (f). This is the ratio of the scattering by an atom in a particular direction (defined in terms of the angle θ) to the scattering of a single electron.

For zero path difference, the atomic scattering factor equals the atomic number of the atom; from this it can be seen that atoms with a high atomic number will diffract X-rays more intensely than those with low atomic number. As the value of $\sin \theta / \lambda$ increases the value of the atomic scattering factor falls off along a curve which may be calculated[74]. This can be seen on Weissenberg photographs; the intensity of the spots decreases as θ increases (towards the top and bottom of the photograph).

The effects of diffraction from several atoms may be combined together to produce the *structure factor*, F_{hkl}. It has been shown[75] that

$$F_{hkl} = \Sigma_j \; f_j e^{i\phi_j}$$

where ϕ_j, the phase angle $= 2\pi\delta_j \, / \, \lambda$ and δ_j equals the path difference relative to some arbitrary chosen origin.

The phase angle may be expressed as a function of the fractional coordinates of the atoms in the unit cell (x, y, z):

$$\phi_j = 2\pi \; (hx_j + ky_j + lz_j)$$

where h, k and l are the denominators of the fractional axes intercepts.

Hence :-

$$F_{hkl} = \Sigma_j \; f_j e^{i2\pi \; (hx_j + ky_j + lz_j)}$$

Euler's theorem shows that $e^{i\phi} = \cos \phi + i \sin \phi$.

Such that :-

$$F_{hkl} = \Sigma_j \; f_j \; \cos 2\pi \; (hx_j + ky_j + lz_j) + \Sigma_j \; f_j \; i \sin 2\pi (hx_j + ky_j + lz_j)$$

Using the diffractometer the intensity of the diffracted beam (I_{hkl}) is measured rather than its amplitude. The two are related by

$$I_{hkl} = K \, L \, p \, | \, F_{hkl} \, |^2$$

where k is the scale factor and L and p are the Lorentz and polarisation corrections. It is therefore possible to obtain $| \, F_{hkl} \, |$ for each set of planes.

Now having obtained an expression for the structure factor in terms of fractional coordinates of the unit cell, the coordinates of equivalent positions arising from various symmetry elements can be substituted into the structure factor expression. For example if a 2_1 screw axis is parallel to the b axis of the unit cell then the following equivalent

positions arise; x, y, z and -x, y+1/2, -z. When these values are substituted into the structure factor expression, we obtain:

$$F_{hkl} = \cos 2\pi (hx + ky + lz) + \cos 2\pi (-hx + k(y+1/2) - lz)$$

$$= \cos 2\pi (hx + lz) \cos 2\pi (ky) - \sin 2\pi (hx + lz) \sin 2\pi (ky)$$

$$+ \cos 2\pi (hx + lz) \cos 2\pi (k(y+1/2)) + \sin 2\pi (hx + lz) \sin 2\pi (k(y+1/2))$$

For hkl = 0k0, the above expansion reduces to:

$$F_{hkl} = \cos 2\pi (ky) + \cos 2\pi (k(y+1/2))$$

$$= \cos 2\pi (ky) + \cos 2\pi (ky) \cos 2\pi (k/2) - \sin 2\pi (ky) \sin 2\pi (k/2)$$

Since $\sin 2\pi (k/2)$ is always zero:

$$F_{hkl} = \cos 2\pi (ky) + \cos 2\pi (ky) \cos 2\pi (k/2)$$

When k is odd, $\cos 2\pi (k/2) = -1$, so $F_{hkl} = 0$. When k is even, $F_{hkl} = 2 \cos 2\pi (ky)$. Therefore if a 2_1 screw axis is present parallel to the b axis of the unit cell, the line of spots 0k0 on the Weissenberg photograph will only occur when k = 2n.

Following the same argument as above it can be shown how certain symmetry elements lead to systematic absences in the X-ray diffraction pattern. Some space groups of differing symmetry have the same systematic absences, therefore in certain cases a choice of space group must be made using further experimental evidence. However in the next example the space group can be uniquely determined from having made the following observations from the Weissenberg photographs about all three axes of a crystal:-

Three axes of differing lengths, all interaxial angles = 90°.

Conditions governing observed reflections;

hkl : none   0kl : k = 2n   h00 : (h = 2n)

h0l : l = 2n   0k0 : (k = 2n)

hk0 : h = 2n   001 : (l = 2n)

The crystal must belong to the orthorhombic class (noting symmetry).

From hkl having no conditions the unit cell must be primitive.

0kl : k = 2n tells us there is a b-glide perpendicular to the a axis.

h0l : l = 2n tells us there is a c-glide perpendicular to the b axis.

hk0 : h = 2n tells us there is an a-glide perpendicular to the c axis.

The remaining conditions tell us that there are screw axes parallel to each of the unit cell edges. These are however a consequence of the presence of three glide planes at right angles to each other and therefore the space group is uniquely defined as Pbca.

Once the geometry and the symmetry of the unit cell have been assessed the next stage in structure determination is intensity measurement.

1.4.9. Intensity data collection and preliminary treatment of data.

The intensity data was collected using a 2-circle diffractometer (see section 2.11.4.). A diffractometer is simply a mechanical device for measuring the intensity of diffraction from chosen planes (once these have been orientated into a reflecting position) using a quantum counter moved to the computed angular orientation. There are certain factors which affect the diffracted beam during the collection of data from a crystal and these

45

must be accounted for in the method of collection or corrected for later at the data reduction stage.

The most important quantity derived from the intensities is the structure factor modulus (structure amplitude), $|F_{hkl}|$ (section 1.4.8.). The relationship between $|F_{hkl}|$ and I (Intensity) depends on a number of factors, primarily geometric, that are related to the individual reflection and to the apparatus used to measure its intensity. The relationship is given by

$$|F_{hkl}| = (K I_{hkl} / L p)^{1/2}$$

Therefore to arrive at the true value for $|F_{hkl}|$ the Lorentz (L) and polarisation (p) corrections must be applied to the data once the data has been ranged on an overall scale using the factor K.

The polarisation factor is given by

$$p = (1 + \cos^2 2\theta) / 2$$

and is independent of the precise method used to collect the intensities. Its importance is now explained. When an incident beam of unpolarised X-rays is reflected from a crystal plane it becomes partly polarised. Where the electric field vectors associated with the photons are parallel to the reflecting plane, the extent of their reflection depends only upon the amount of electron density in the plane. Where the electric vectors are perpendicular to the plane however, the extent of their reflection depends not only upon the amount of electron density in the plane but also upon $\cos^2 2\theta$ and therefore varies considerably.

The Lorentz factor depends upon the method used for collecting intensities. It arises because the time taken for a reciprocal lattice point to pass through the sphere of reflection is not constant, and depends on its position in the lattice. For the equi-inclination Weissenberg geometry used in the present work:-

$$L = \sin \theta / \sin 2\theta \, (\sin^2 \theta - \sin^2 \mu)^{1/2}$$

where μ is the equi-inclination setting angle.

1.4.9.1. Absorption correction.

The absorption of X-rays by matter is governed by the equation

$$I = I_o \exp(-\mu\tau)$$

where I is the diffracted beam intensity, I_o is the incident beam intensity, μ is the linear absorption coefficient and τ is the thickness of the specimen. Hence the transmission of the X-ray beam through a crystal is given by

$$T = I / I_o = \exp[-\mu(\tau_i + \tau_d)]$$

where τ_i and τ_d are the incident and diffracted beam path lengths. If the shape of the crystal is known exactly, then it is possible to correct for absorption by calculating

$$T = V^{-1} \, (\textstyle\int V) \exp[-\mu(\tau_i + \tau_d)] \, dV$$

where dV is an infinitesimal volume of the crystal[76].

1.4.9.2. Scale factors.

The data measured for this work were scaled using the SHELX-76 program[77] and an Overall Scale Factor (K) and Inter Layer Scale Factors were introduced. The scale factors are deduced by the equation below:-

$$\text{Scale factor} = \Sigma \, | F_c | / \Sigma \, | F_o |$$

Where F_c and F_o are the calculated and observed structure factors respectively. Inter-layer scale factors are required when using 2-circle (equi-inclination Weissenberg) diffractometer geometry as a different standard has to be used for reflections from each layer of the reciprocal lattice and it is necessary to bring each layer to a common scale afterwards.

1.4.10. Solving the structure.

The following section will describe some of the methods often employed to solve a crystal structure once the intensity data has been collected and corrected via data reduction. The process of solving a structure is usually a stepwise procedure where each step builds on the previous one until all the atoms of the structure have been located and their parameters determined. During this procedure a good indicator of how well the model being built up is progressing is known as the *residual* or R-value. This provides a measure of the agreement between the actual structure and the model being proposed.

$$R = \Sigma \, || \, F_o \, | - | \, F_c \, || \, / \, \Sigma \, | \, F_o \, |$$

$| \, F_o \, | = $ modulus of the observed structure factor.

$| \, F_c \, | = $ modulus of the calculated structure factor.

For a perfectly fitting model, R = 0. Wilson[78] has shown that for the correct number and type of atoms placed randomly in the unit cell the R values for centric and non-centric structures would be 0.828 and 0.586 respectively.

1.4.10.1. The phase problem.

From section 1.4.10, to find the fractional coordinates of atoms in the unit cell the *structure factor*, F_{hkl} is required. The relationship between this and the measured

intensities is $I_{hkl} = KLp \mid F_{hkl} \mid^2$. Therefore from the measured intensities only the modulus of the structure factor $\mid F_{hkl} \mid$ can be found. This gives no direct phase information which needs to be determined to locate atomic coordinates. The structure factor theory for atomic coordinates can be extended to consider electron density at any point in the unit cell by using a three-dimensional Fourier series. It can be shown that

$$\rho(x, y, z) = {}^1\!/_V \, \Sigma_h \Sigma_k \Sigma_l \, F_{hkl} e^{-2\pi i \, (hx + ky + lz)}$$

where $\rho(x, y, z)$ is the electron density at some real and positive point x, y, z and V is the volume of the unit cell.

From this expression if the structure factors and phases are known, the electron density distribution of the unit cell can be calculated. The problem of the directly unobtainable phase information would probably be, for a random electron density distribution, unsolvable. The nature of crystalline materials however means that the electron density distribution is far from random. Everywhere it is expected to be real, and positive. Considering chemical theory, the electron density is expected to be located in approximately spherical regions (atoms), and the constraints between these regions should be chemically sensible. This for practical purposes represents a unique solution. Therefore any method of obtaining phase information should, when all the information has been applied to calculating the electron density, give a chemically sensible pattern. Any incorrect models should be easily identified by the considerations above as well as a poor agreement between the observed structure factors ($\mid$ Fo $\mid$'s), and the calculated structure factors ($\mid$ Fc $\mid$'s). This has been presented previously (section 1.4.10) as 'the residual'.

49

Methods of obtaining the structure factor phases i.e. solving the "phase problem" are now discussed.

1.4.10.2. The heavy atom Patterson synthesis.

For structures containing 'heavy' atoms (sulfur is considered a 'medium' weight atom) Patterson[79] elucidated a method of solving the phase problem. The method involves using an equation almost exactly the same as the three-dimensional Fourier series as mentioned above, however Patterson showed that a Fourier calculation on the phaseless $|F_{hkl}|^2$ quantities resulted in a map that gave peaks corresponding to all the interatomic vectors.

The series in three dimensions

$$P(x, y, z) = \frac{1}{V} \Sigma_h \Sigma_k \Sigma_l |F_{hkl}|^2 \cos 2\pi (hx + ky + lz)$$

is derived from the following integral :-

$$P(x, y, z) = V \int_0^1 \int_0^1 \int_0^1 \rho(u, v, w) \rho(u + x, v + y, w + z) \, du \, dv \, dw$$

If $P(x, y, z)$ is large then this represents the maximum of the corresponding vector between two points of high electron density; $\rho(u, v, w)$ and $\rho(u + x, v + y, w + z)$. It is possible to work out the positions of the atoms from the positions of these peaks, and as the magnitude of the peaks is directly related to the product of the atomic numbers of the two atoms concerned, the Patterson peaks for heavy atoms should be large compared to the others present.

1.4.10.3. Direct methods.

These methods are most suitable for molecules of up to 100 atoms and give best results for molecules with less than 50 atoms. They are also most effective on

50

molecules without heavy atoms, since the large electron density associated with a heavy atom distorts the intensity distribution of the data and means that some incorrect phase attributions can have a disproportionate effect.

Attributing the structure factor phases at random, calculating a Fourier synthesis and seeing if anything recognisable is produced would be totally impractical. A lot of these syntheses would produce negative regions of electron density. Thus any method of determining phases can discard any combination of phases which produce negative electron densities. Harker and Kasper[80] found that for certain combinations of phases of some of the *strong* reflections, negative electron densities occurred whatever the phases of the rest of the reflections. These could be discarded and by introducing more strong reflections they could gradually fix the phases of most of them. The process is easiest to describe for a centrosymmetric structure as only cos terms are involved in the equation for F_{hkl}. The procedure involves trial and error. For example take two reflections known to be strong e.g. 100 and 200. For 100 $F_{hkl} = \Sigma_j\, f_j \cos 2\pi\,(x)$ and for 200 $F_{hkl} = \Sigma_j\, f_j \cos 2\pi\,(2x)$. Therefore points where both are strong are 0 (both + phase) and 180° (+ phase for 200 – phase for 100). Hence at points where 200 is strong and 100 is strong the sign of F_{200} is +. Other related reflection phases are then built up by what is known as sign relationships.

A simplification in direct phase-determining formulae results from replacing $|\,F_{hkl}\,|$ by the corresponding *normalised*[81] structure factor $|\,E_{hkl}\,|$ which is given by the equation

$$E_{hkl} = F_{hkl} \,/\, \langle F \rangle$$

where $\langle F \rangle$ is the local average structure factor, taken over a range of similar θ values. This is equivalent to the equation

$$E_{hkl}^2 = | F_{hkl} |^2 / \varepsilon \, \Sigma_j \, f_j^2$$

The appropriate value of ε may be obtained from the International Tables[82].

Once $| E |$'s have been calculated their distribution can give information on the crystal's space group as it is dependent upon the presence or absence of a centre of symmetry. For a centrosymmetric and noncentrosymmetric structure the average $| E^2 \text{-}1 |$ values are 0.968 and 0.736 respectively. Once the phases of one or two $| E |$'s has been assigned many more may be built up using sign relations. Triple product sign relationships have the form

$$S_{hkl} \bullet S_{h'k'l'} \bullet S_{h\text{-}h', \, k\text{-}k', \, l\text{-}l'} \approx +1$$

where S_{hkl} means the sign of hkl.

An electron-density map is generated using the calculated phases and the observed F_{hkl} values. If no reasonable structure or partial structure is obtained from this then a new set of starting phases must be calculated and the process repeated. The direct method of phase determination is based on probabilities rather than certainties and therefore some structures fail to yield to these methods. Direct methods are however by far the most widely used at present.

1.4.11 Least squares refinement.

Once the atomic coordinates for all atoms within the structure have been found the positional and thermal parameters for each atom along with any other structural

52

parameters (scale factors, weighting factors etc) need to be refined. The purpose of the refinement process is to find the best possible agreement between the calculated and observed diffraction pattern. The method of refinement used in this work was that based on the principle of least squares.

The calculations involved in least squares refinement are not complex but are very lengthy and in the case of this work were calculated using the crystallographic program SHELX76[77]. Therefore the discussion here will be limited to basic principles. A two dimensional example will be used to illustrate the method.

The equation of a line in two dimensions is

$$Y = mX + b$$

If there are two pairs of values of X and Y for measurements which are related by this equation, a unique answer for the constants m and b can be found. If however several pairs of values contain random errors, values for m and b which best fit the complete set of observations are required. Often in practical problems the errors in one parameter may be negligible compared with those of another parameter. Under these conditions the best estimates of m and b are m_o and b_o and the error of fit in the ith observation is

$$e_i = m_o X_i + b_o - Y_i$$

The principle of least squares states that the best-fit parameters are those that minimise the sum of the squares of the errors. Therefore

$$\Sigma_i\, e^2{}_i = \Sigma_i\, (m_o X_i + b_o - Y_i)^2 \quad (i = 1, 2, \ldots, N)$$

must be minimised over the number N of observations. This condition corresponds to differentiating partially with respect to m_o and b_o, in turn, and equating the derivatives to zero. Hence,

53

$$m_o \Sigma_i X_i^2 + b_o \Sigma_i X_i = \Sigma_i X_i Y_i$$

$$m_o \Sigma_i X_i + b_o N = \Sigma_i Y_i$$

which constitute a pair of simultaneous equations which can be solved for m_o and b_o.

In crystal structure analysis more observations are being manipulated than there are unknown quantities and the system is therefore overdetermined. The reader is directed elsewhere[83] for details of the application of the method of least squares.

2. EXPERIMENTAL.

2.1. Preparation of starting materials.

The starting materials for this project were prepared via the route shown in scheme I.

Scheme I.

2.1.1. O-Tosylation[1].

$$HO(CH_2)_2O(CH_2)_2OH + 2CH_3C_6H_4SO_2Cl \longrightarrow TsO(CH_2)_2O(CH_2)_2OTs$$
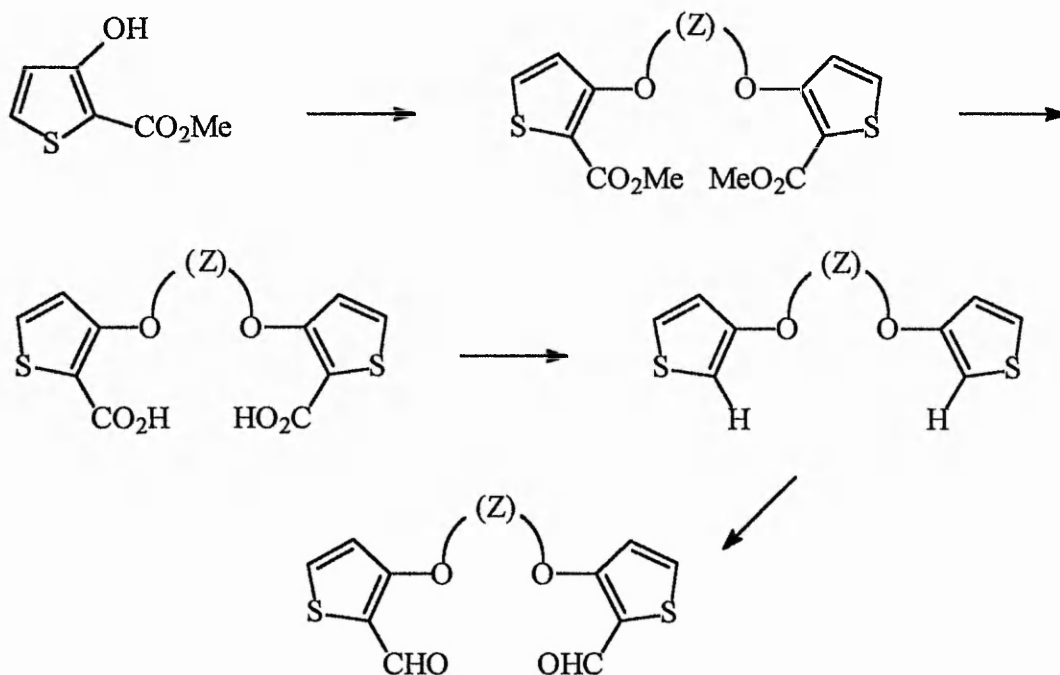
p-Toluenesulfonylchloride (2.2eq) was added portionwise to a stirred cooled [0°C] solution of diethylene glycol (1.1eq) in anhydrous pyridine [10mlg⁻¹ of diol]. The temperature of the solution was not allowed to exceed 10°C. The mixture was stirred with ice cooling for a further 30 minutes and then at RT for 30 minutes. The mixture was then poured into ice acidified with conc. HCl; the resulting white precipitate was then filtered off and washed with and recrystallised from methylated spirits.

The recrystallised solid was obtained in 78% yield, M.P = 87.5-89.8°C.

Literature M.P = 87-89°C[84].

2.1.2 Williamson's ether synthesis[1].
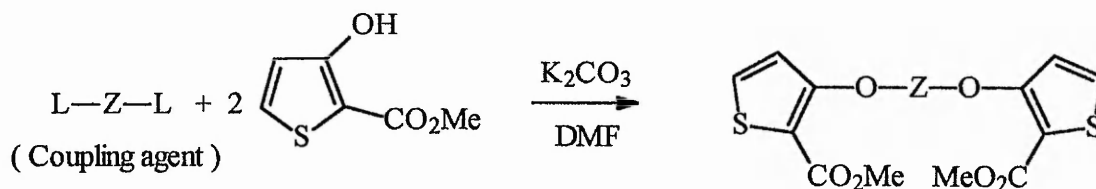
A stirred solution of methyl 3-hydroxythiophene-2-carboxylate (1.0eq), anhydrous potassium carbonate (0.55eq) and the coupling agent (0.55eq) in anhydrous DMF [5mlg^{-1} of thiophene ester] was heated on an oil bath maintained at 95-100°C for 5h. The reaction mixture was then poured into ice and treated in the manner described below.

Alkyl bridged bis esters.

The precipitate obtained on quenching was filtered off, washed with water and digested in hot solvent. The residual solid was then filtered off and washed with the same solvent and dried.

C_2 (L-Z-L = BrCH$_2$CH$_2$Br) Solvent = MeOH.

C_3 (L-Z-L = BrCH$_2$CH$_2$CH$_2$Br) Solvent = Me$_2$CO.

C_4 (L-Z-L = Br(CH$_2$)$_4$Br) Solvent = MeCN.

<u>C$_2$OC$_2$ bridged bis ester.</u> (L-Z-L = TsOCH$_2$CH$_2$OCH$_2$CH$_2$OTs)

The precipitate obtained on quenching was filtered off, washed with water and recrystallised from methanol.

The bis esters were obtained as described below.

Z	YIELD(%)	M.P (°C)
C$_2$	78	188.8-191.0
C$_3$	66	137.8-139.6
C$_4$	69	189.9-192.2
C$_2$OC$_2$	86 -	76.1-77.5

2.1.3. Saponification[1].
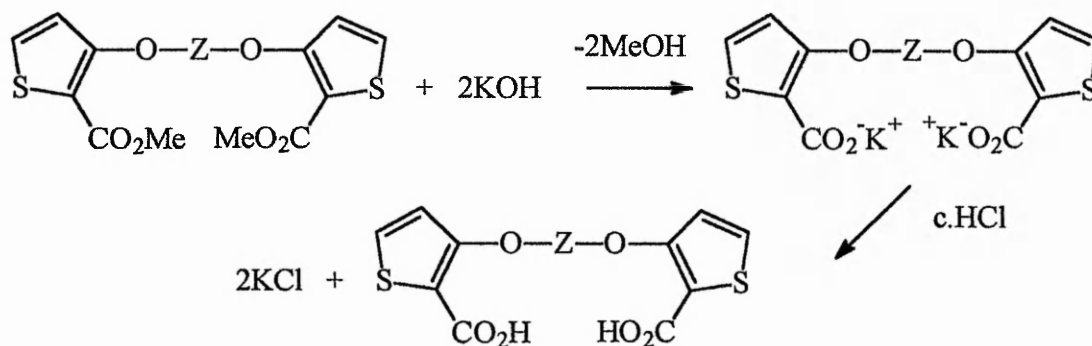
A solution of the α,ϖ-bis(2-methoxycarbonyl-3-oxythienyl)alkane (1.0eq) and potassium hydroxide (4.0eq) in 80% aqueous ethanol [20mlg^{-1} of S.M] was boiled under reflux for 2h. The solution was filtered through glass wool into ice and the resulting solution acidified with conc. HCl. The bis acid was then filtered off, washed with water and dried under vacuum at 60°C for an extended period.

After extensive drying (24-48h) at 60°C under vacuum the bis acids were obtained as described below.

Z	YIELD(%)	M.P (°C)
C_2	93	218.9-219.6
C_3	100*	214.1-214.3
C_4	100*	228.2-229.4
C_2OC_2	100*	188.5-189.3

*The acids were particularly hard to dry probably due to strong hydrogen bonding towards water.

2.1.4. Decarboxylation[1].
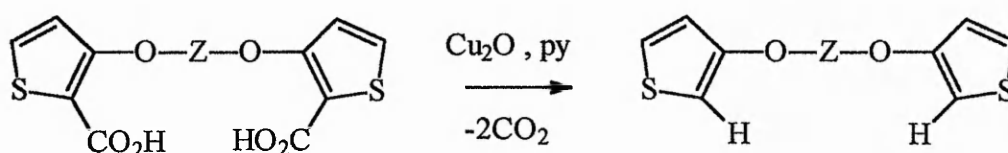
A mixture of the α,ω-bis(2-carboxy-3-oxythienyl)alkane and copper(I) oxide (1.2wt eq) in pyridine [$10mlg^{-1}$ of bis acid] was boiled under reflux for 1h. The solvent was removed under reduced pressure and the residue was extracted repeatedly with DCM.

The combined organic extracts were washed with dilute hydrochloric acid ×2, saturated brine solution ×1, and saturated $NaHCO_3$ solution ×1. The extracts were then dried ($MgSO_4$) and evaporated to give the crude α,ω-bis(3-oxythienyl)alkane.

The crude products were then recrystallised from the following solvents:-

C_2 digested in MeOH.

C_3 recrystallised from EtOH.

C_4 recrystallised from MeOH

C_2OC_2 recrystallised from MeOH.

The α,ω–bis(3-oxythienyl)alkanes were obtained as described below.

Z	YIELD(%)	M.P (°C)
C_2	73	156.2-158.6
C_3	82	64.3-67.2
C_4	86	103.8-105.2
C_2OC_2	89	58.3-59.7

Infra red spectroscopic data.

The absence of any carboxyl group vibrations indicated full decarboxylation. The compounds all exhibited characteristic heteroaromatic C=C absorption bands [1549-1539s cm^{-1}].

^{1}H NMR data.
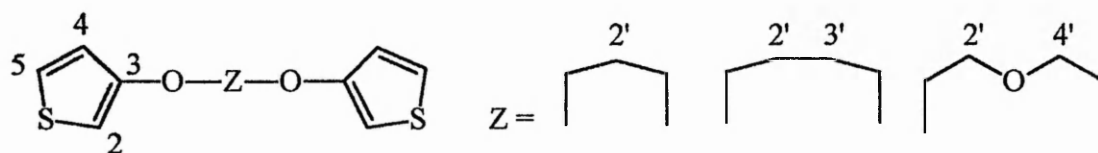
Solvent = CDCl$_3$.

Z	TH H'S			THOCH$_2$	OTHERS
	H5	H4	H2		
C_2	7.21m	6.79m	6.33m	4.30s	
C_3	7.17m	6.75m	6.14m	4.10t	2.23 H2' qu
C_4	7.16m	6.71m	6.21m	4.00m	1.95 H2'+H3' m
C_2OC_2	7.15m	6.75m	6.24m	4.15m	3.87 H2'+H4' m

^{13}C NMR data.

Solvent = $CDCl_3$.

Z	TH C'S				THOCH$_2$	OTHERS
	C3	C5	C4	C2		
C_2	157.16	124.87	119.33	97.72	68.48	
C_3	157.70	124.71	119.44	97.32	66.60	29.25 C2'
C_4	157.86	124.63	119.48	97.11	69.61	25.97 C2'+C3'
C_2OC_2	157.50	124.69	119.55	97.54	69.81	69.54 C2'+C4'

2.1.5. Vilsmeir-Haack formylation[1].
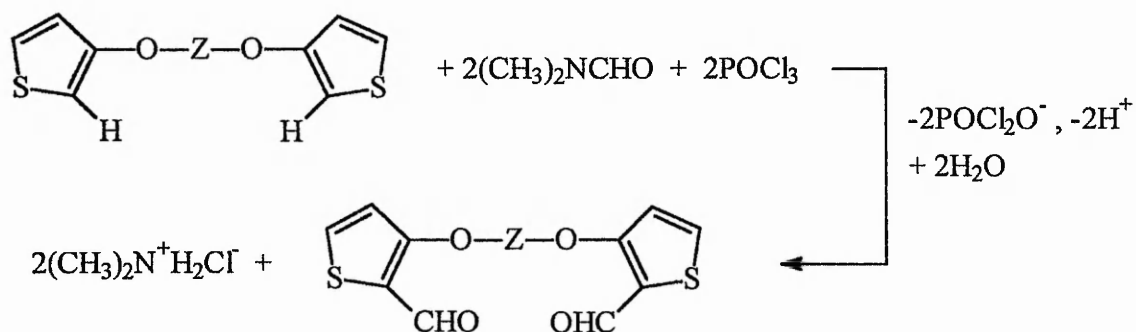
A solution of the α,ϖ-bis(3-oxythienyl)alkane (1.0eq) in dry 1,2-DCE [10mlg^{-1} of bis ether] was added to a stirred solution of anhydrous DMF (2.2eq) and POCl$_3$ (2.2eq) in the same solvent [10mlg^{-1} of bis ether]. The mixture was heated on an oil bath at 95-100°C for 2h and then poured into a 10% aqueous solution of sodium acetate and stirred for a further hour at RT. The aqueous layer was adjusted to pH 7 with 4M NaOH. The two phases were separated and the aqueous layer extracted with DCM. The combined organic extracts were dried (MgSO$_4$) and evaporated to give the crude dialdehyde as a solid. This was then recrystallised from ethanol.

The α,ϖ–bis(2-formyl-3-oxythienyl)alkanes were obtained as described below.

Z	YIELD(%)	M.P (°C)
C$_3$	79	138.3-139.4
C$_2$OC$_2$	95	94.9-95.7

Infra red spectroscopic data.

Z	C=O cm^{-1}	C=C cm^{-1}
C$_3$	1641.4	1535.9
C$_2$OC$_2$	1651.7	1537.9

^{1}H NMR data.

Solvent = CDCl$_3$.

Z	CHO	TH H'S		THOCH$_2$	OTHERS
		H5	H4		
C$_3$	9.96s	7.62d	6.85d	4.37t	2.34 H2' qu
C$_2$OC$_2$	9.98s	7.62d	6.84d	4.35m	3.92 H2'+H4'm

^{13}C NMR data.

Solvent = CDCl$_3$.

Z	CHO	TH C'S				THOCH$_2$	OTHERS
		C3	C5	C2	C4		
C$_3$	180.97	163.88	135.36	121.60	116.21	67.65	29.31 C2'
C$_2$OC$_2$	181.26	164.00	135.09	121.89	116.60	71.32	69.92 C2'+C4'

2.1.6. Preparation of the *N,N'*-dibenzylalkyldiamines.

The compounds prepared as described below were to be coupled with the bis ethers in the Mannich reaction to give varying ring size macrocycles with varying benzyl substituents. The method of preparation employed was the coupling of two equivalents

61

of the appropriately substituted benzaldehyde with one equivalent of the required diamine to form the diimine which was then reduced to give the desired diamine.

$(C_6H_5CH=NCH_2)_2CH_2$.
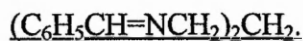
Benzaldehyde (34.8g, 2.1eq) and 50% aqueous 1,3-diaminopropane, (24ml, 1.0eq) were heated for 0.5h at 120°C. The reaction mixture was cooled to room temperature and extracted with diethyl ether (300ml). The combined organic extract was dried (MgSO$_4$) and the solvent was evaporated under reduced pressure to give the crude diimine, 34g as a white solid. The crude diimine was used in the next reaction without further purification.

$(C_6H_5CH_2NHCH_2)_2CH_2$.

The crude diimine (34g, 1.0eq) was added to a stirred solution of sodium borohydride (16g, 3.1eq) in dry ethanol (300ml) over 2h. Water (200ml) was added to the cooled solution and stirred overnight. The mixture was then extracted with ether. The extract was dried (MgSO$_4$), and the solvent was removed *in vacuo*. Ethanol (200ml) was added to the crude residue and the dihydrochloride was then precipitated by the addition of dilute hydrochloric acid. The dihydrochloride was isolated and treated with 30% sodium hydroxide solution (200ml). The resulting free diamine was extracted with ether, dried (MgSO$_4$) and the solvent removed *in vacuo* to give the desired diamine as a colourless oil.

(ClC$_6$H$_4$CH=NCH$_2$)$_2$.

Ethylenediamine (5ml, 1.0eq) was added to a solution of *p*-ClC$_6$H$_4$CHO (16.66g, 1.58 eq) in dry ethanol (50ml). The solution was heated at 120°C on an oil bath for 1 hour. The crude diimine precipitated out upon cooling and was filtered off and air dried. The crude diimine was used in the next reaction without further purification.

(ClC$_6$H$_4$CH$_2$NHCH$_2$)$_2$.

The crude diimine (14.8g, 1.0eq) was added portionwise to a solution of sodium borohydride (8g, 0.55 wt eq), dissolved in dry ethanol (150ml) over 45 minutes with gentle heating (50°C) and stirring and this was maintained for a further 45 minutes. Water (100ml) was added to the cooled solution and stirring continued overnight. The solution was extracted with ether, the extract was evaporated *in vacuo* and ethanol (150ml) was added. The dihydrochloride was precipitated by the addition of 2M HCl. The dihydrochloride was isolated and treated with 30% sodium hydroxide solution (200ml). The resulting free diamine was extracted with ether, dried (MgSO$_4$) and the solvent removed *in vacuo* to give the desired diamine as a colourless oil.

(ClC$_6$H$_4$CH=NCH$_2$)$_2$CH$_2$.
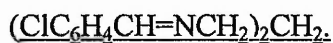
1,3-Diaminopropane (1.0eq, 5ml) was added to a solution of *p*-ClC$_6$H$_4$CHO (1.58eq, 13.35g) dissolved in ethanol (80ml). The solution was heated at 140°C on an oil bath for 1 hour. The solution was cooled and the white precipitate filtered off and air dried. The crude diimine was used in the next reaction without further purification.

(ClC$_6$H$_4$CH$_2$NHCH$_2$)$_2$CH$_2$.

The crude diimine (9.37g, 1.0eq) was added portionwise to a solution of sodium borohydride (5.5g, 0.55 wt eq) in ethanol (120ml) over 45 minutes with gentle heating (50°C) and stirring and this was maintained for a further 45 minutes after the addition

was completed. The solution was cooled and water (150ml) was added and stirred overnight. The solution was extracted with ether, the extract was evaporated *in vacuo* and ethanol (100ml) added. The dihydrochloride was precipitated by the addition of 2M HCl. The dihydrochloride was isolated and treated with 20% sodium hydroxide solution (100ml). The resulting free diamine was extracted with ether, dried (MgSO$_4$) and the solvent removed *in vacuo* to give the desired diamine as a colourless oil.

(O$_2$NC$_6$H$_4$CH=NCH$_2$)$_2$.

Ethylenediamine (1.0eq, 2.79ml) was added to a solution of *p*-O$_2$NC$_6$H$_4$CHO (1.583 eq, 10g) in dry ethanol (70ml) and heated at 120°C on an oil bath for 1 hour. The resulting precipitate was filtered off and washed with a small amount of ethanol and ether. The crude diimine was used in the next reaction without further purification.

(O$_2$NC$_6$H$_4$CH$_2$NHCH$_2$)$_2$.

The attempted NaBH$_4$ reduction in EtOH failed due to solubility problems.

The diimine (1.0eq, 9.50g) was added portionwise over 20 minutes to a solution of NaBH$_4$ (5.5g, 0.55 wt eq) dissolved in dry THF / MeOH (1:1 ratio, 200ml) with stirring and gentle heating (50°C). The solution was then stirred and heated for a further 40 minutes. The solution was evaporated *in vacuo* and water (150ml) was added and left overnight. The solution was extracted with DCM and the DCM phase evaporated *in vacuo* at 65°C. The resulting oil was redissolved in DCM and the dihydrochloride was precipitated by the addition of 2M HCl. The precipitate was filtered, washed with ether and dried. The dihydrochloride was isolated and treated with 20% sodium hydroxide solution (150ml). The resulting free diamine was extracted with DCM, dried (MgSO$_4$) and the solvent removed *in vacuo* to give the desired diamine as a yellow oil.

The *N,N'*-dibenzylalkyldiimines were obtained as described below.

$(RC_6H_4CH=N)_2(CH_2)_n$
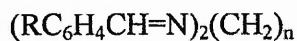
n	R	YIELD (%)	M.P (°C)
3	H	(-)[a]	(-)[a]
2	Cl	82	146-147
3	Cl	62	66.3-68.5
2	NO$_2$	94	201.6-202.5

a = used as crude

Infra red spectroscopic data.

n	R	C=N cm^{-1}	NO$_2$ MODES cm^{-1}
3	H	(-)[a]	
2	Cl	1643	
3	Cl	1645	
2	NO$_2$	1644	1519, 1339

^{1}H NMR data.

Solvent = CDCl$_3$

n	R	CH=N	PH-H'S	CH$_2$
3	H	(-)[a]	(-)[a]	(-)[a]
2	Cl	8.2s	7.6d, 7.35d	3.95s
3	Cl	8.25s	7.65d, 7.35d	3.7t, 2.1qu
2	NO$_2$	8.4s	8.25d, 7.9d	4.05s

The *N,N'*-dibenzylalkyldiamines were obtained as described below.

$(RC_6H_4CH_2NH)_2(CH_2)_n$

n	R	OVERALL YIELD	M.P (°C)
3	H	44	Oil
2	Cl	61	Oil
3	Cl	38	Oil
2	NO$_2$	68	Oil

Infra red spectroscopic data.

n	R	N-H cm^{-1}	NO$_2$ MODES cm^{-1}
3	H	3296	
2	Cl	3308	
3	Cl	3297	
2	NO$_2$	3318	1518, 1344

^{1}H NMR data.

Solvent = CDCl$_3$

n	R	PH-H'S	PHCH$_2$	NHCH$_2$, CH$_2$	NH
3	H	7.15-7.35m	3.75s	2.65t, 1.7qu	1.45s
2	Cl	7.25d, 7.18d	3.7s	2.7s	1.65s
3	Cl	7.26d, 7.21d	3.7s	2.65t, 1.7qu	1.45s
2	NO$_2$	8.15d, 7.45d	3.9s	2.75s	1.7s

^{13}C NMR data.

Solvent = CDCl$_3$.

n	R	PH-C'S	PHCH$_2$	NHCH$_2$	CH$_2$
3	H	140.5, 128.5, 128.3, 126.8	54.1	48.0	30.2
2	Cl	139.0, 132.8, 129.1, 128.2	53.1	48.6	
3	Cl	139.0, 132.5, 129.6, 128.4	53.3	47.9	30.1
2	NO$_2$	148.4, 142.9, 128.6, 123.6	53.5	48.7	

2.1.7. Metal diamine complexes.

The following metal complexes were prepared for use as templates in Mannich and Schiff base condensations.

2.1.7.1. Preparation of Cu[II] and Ni[II] secondary diamine complexes.

[Cu(CH₃NHCH₂CH₂NHCH₃)₂] I₂ [85]

$[Cu(CH_3NHCH_2CH_2NHCH_3)_2] I_2$ [85]

Copper (II) nitrate (1.0eq, 4.23g) was dissolved in water (20ml) and

N,N'-dimethylethylenediamine (2.85eq, 5.32ml) was added. A solution of KI (8.5eq, 24.9g) in water (70ml) was added dropwise to the first solution. The resulting purple solid was collected by filtration and washed with small amounts of cold water, ethanol and ether. The product was then recrystallised from water.

The purple complex was obtained in 73% yield.

The product's infra red spectrum conformed to its expected structure, the only significant absorptions being N-H str at 3212.5m cm^{-1} and 3167.1m cm^{-1}.

[Ni(CH₃NHCH₂CH₂NHCH₃)₂] (NO₃)₂ [86]

$[Ni(CH_3NHCH_2CH_2NHCH_3)_2] (NO_3)_2$ [86]

Nickel (II) nitrate (1.0eq, 7.27g) was dissolved in ethanol (100ml) and added dropwise to a solution of N,N'-dimethylethylenediamine (2.0eq, 5.32ml) in the same solvent (60ml). The product was recrystallised from methanol, washed with cold methanol and dried under vacuum.

The blue complex was obtained in 65% yield.

The product's infra red spectrum conformed to its expected structure and showed two N-H str at 3273.4s cm^{-1} and 3252.5s cm^{-1}.

2.1.7.2. Preparation of Cu^{II} and Ni^{II} primary diamine complexes.

Ni(en)$_3$Cl$_2$.2H$_2$O[87]

A 70% aqueous solution of ethylenediamine (3.2eq, 12.8ml) was added to a solution of NiCl$_2$.6H$_2$O (1.0eq, 10g) in water (150ml). The solution was reduced in volume to 60-70ml on a heating mantle. Two drops of en were added and the solution cooled in an ice bath. The precipitate was filtered off and washed with methanol.

The pink / purple complex was obtained in 78% yield.

The product's infra red spectrum showed N-H str 3167-3325 cm^{-1} and N-H bends 1605 and 1589 cm^{-1}.

Ni(en)$_2$Cl$_2$.xH$_2$O[88]

NiCl$_2$.6H$_2$O (1.0eq, 1.238g) and Ni(en)$_3$Cl$_2$.2H$_2$O (2.0eq, 3g) dissolved in a mixture of 30ml methanol and 2ml of water were gently refluxed for five minutes. Seed crystals were obtained by adding 3-4ml of acetone to 2-3ml of the reflux liquor whilst scratching with a glass rod. The seed crystals were then added to the remaining liquor sporadically while adding 50ml of acetone. The light blue complex which precipitated was filtered off and washed with a small amount of ice cold methanol.

The blue complex was obtained in 68% yield assuming x = 0.

The product's infra red spectrum showed N-H str 3119-3331 cm^{-1} and N-H bends 1597 and 1588 cm^{-1}.

$Cu(en)_2Cl_2.xH_2O$[89]

A 70% aqueous solution of ethylenediamine (10ml) was added with stirring to copper (II) sulphate (1.0eq, 12.5g) dissolved in water (50ml). To the resulting solution barium chloride (1.0eq, 10.4g) dissolved in water (50ml) was added slowly with stirring. The precipitated barium sulphate was filtered off. The solution was evaporated *in vacuo* and redissolved in the minimum hot methanol. The complex precipitated from the cool solution and was filtered off. Acetone was added to the remaining solution and the second batch of complex filtered off. The combined batches were washed with ice cold methanol and dried at 50°C under vacuum.

The purple complex was obtained in 81% yield assuming x = 0.

The product's infra red spectrum showed N-H str 3141-3302 cm^{-1} and N-H bends 1610 and 1584 cm^{-1}.

$Ni(en)_3(ClO_4)_2.xH_2O.$

A 70% aqueous solution of ethylenediamine (7ml) was added to a solution of $Ni(ClO_4)_2.6H_2O$ (1.0eq, 9.14g) dissolved in water (50ml). The resulting purple precipitate was filtered off. The remaining solution was cooled in an ice bath and the precipitate formed filtered off. The combined solids were washed with ethanol and air dried.

The pink / purple complex was obtained in 77% yield assuming x = 0.

The product's infra red spectrum showed N-H str 3172-3323 cm^{-1} and N-H bends 1602 and 1591 cm^{-1}.

<u>Attempted synthesis of Ni(en)₂(ClO₄)₂.xH₂O.</u>

The same method as for Ni(en)₂Cl₂.xH₂O was followed, however on the addition of seed crystals and acetone no precipitation occurred. On volume reduction Ni(en)₃(ClO₄)₂.xH₂O precipitated out leaving a green solution.

This complex was not obtained. The method of obtaining the chloride anion compound is that of a ligand redistribution, adding enough Ni²⁺ to the tris-en complex so that redistribution to the bis-en complex is favoured. However for the perchlorate analogue this may not be favoured due to the non-coordinating nature of the perchlorate anion. The title compound would need to be square planar without anion coordination, whereas the dichloride can be octahedral with the chlorides cis or trans to each other.

<u>2.1.8. 3-Hydroxythiophene-2-carbaldehyde.(Salicylaldehyde analogue.)</u>
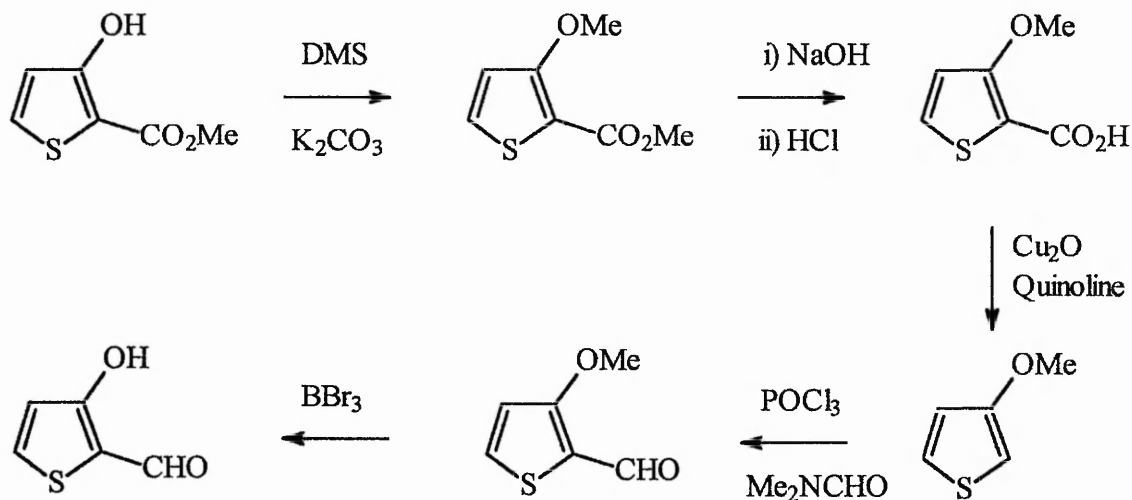
This compound was prepared via the scheme outlined above. The method up to 3-methoxythiophene-2-carbaldehyde was developed earlier by Huddleston[90].

70

2.1.8.1. Demethylation.

3-Methoxythiophene-2-carbaldehyde (1.0eq, 0.426g) dissolved in 20ml of dry DCM was placed in a round bottomed flask fitted with a $CaCl_2$ guard tube and septum and cooled to -78°C. BBr_3 (1.5eq, 4.5ml) was added dropwise to the stirred mixture which was then allowed to warm to room temperature. After two hours the mixture was cooled to -78°C and 3ml of methanol added. The solution was warmed to 0°C and 20ml of 2M HCl added and stirred for ten minutes. The DCM layer was separated and the aqueous layer washed with DCM. The DCM layers were combined and washed with water and brine and dried ($MgSO_4$). The solution was evaporated *in vacuo* to yield 0.25g of the grey / brown crude product. This was subjected to basic extraction (1M NaOH to remove any precursor) to yield the cream / yellow pure solid.

The compound was obtained as described below :-

OVERALL YIELD (%)	M.P (°C)
52	80 – 82

Infra red spectroscopic data.

OH cm^{-1}	C=O cm^{-1}	C=C cm^{-1}
Not detected	1617	1577

^{1}H NMR.

CHO	H5	H4	OH
9.63s	7.60d	6.75d	Not detected.

^{13}C NMR.

C=O	C3	C5	C2	C4
185.69	166.29	136.44	119.66	115.60

2.2. [1+1] Macrocyclic Mannich bases derived from *N,N'*-dibenzylalkyldiamines.
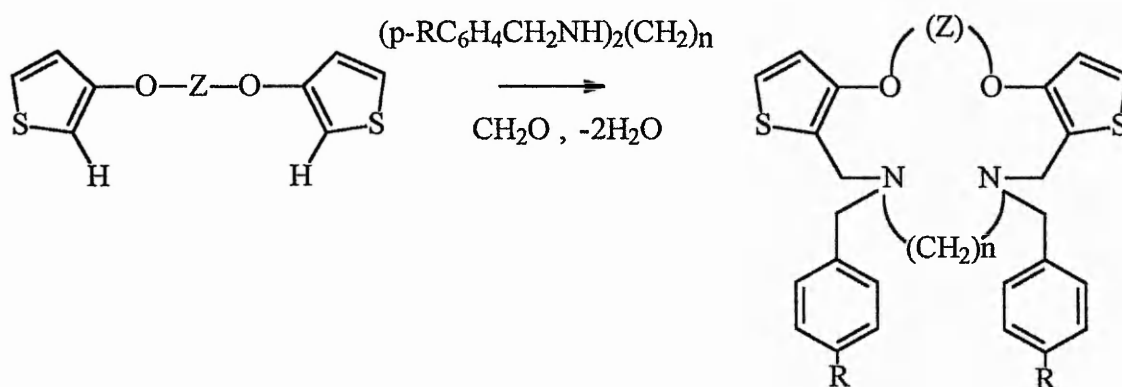
The general procedure developed by Chaffin[1] was used but utilising the new diamines in an attempt to obtain solid / crystalline macrocycles.

General procedure.(Macrocyclisation.)

To a solution of the appropriate *N,N'*-dibenzylalkyldiamine (1.1eq) and formaldehyde (2.2eq) in g.AcOH was added a solution of the α,ϖ-bis(3-oxythienyl)alkane (1.0eq) in g.AcOH. Total volume 100mlg^{-1} bis ether. The mixture was stirred for 24-72h and then basified with 4M NaOH, extracted with DCM, dried (MgSO$_4$) and the solvent evaporated *in vacuo*.

Z = C$_2$, n = 2, R = H

After 72h evaporation yielded an oil which solidified. The longer reaction time was necessary due to the low solubility of the bis ether. The solid product was recrystallised from methanol. At first an oil precipitated out. The hot methanol was decanted off from the oil. On cooling of the methanolic solution the pure macrocycle precipitated out as a light brown solid.

<u>Z = C$_3$, n = 2, R = H</u>
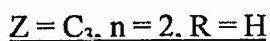
After 24h evaporation yielded an oil which solidified as crystalline needles. These were washed with water and ice cold ether (sparingly).

<u>Z = C$_4$, n = 2, R = H</u>
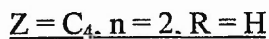
After 20h evaporation yielded an oil. Attempts to get the oil to solidify all failed. An attempt to purify the oil via acidic extraction yielded a precipitate when the ethereal solution contacted 1M hydrochloric acid.

<u>Z = C$_2$OC$_2$, n = 2, R = H</u>
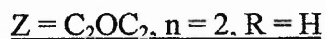
After 48h evaporation yielded an impure oil (as determined via infra-red spectroscopy) which did not solidify.

<u>Z = C$_2$, n = 2, R = Cl</u>
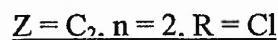
After 72h evaporation yielded an oil with signs of crystal formation therein. The oil was taken up in hot methanol (which upon evaporation yielded the impure product as an oil) and the remaining oily solid dissolved in DCM which upon slow evaporation yields rhombohedral looking crystals of the starting material (bis ether).

<u>Z = C$_3$, n = 2, R = Cl</u>
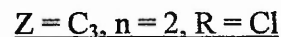
After 24h evaporation yielded an oil. On refridgeration overnight the oil solidified and the waxy solid was put under vacuum to remove any remaining volatiles. The solid was then recrystallised from ethanol to give a white solid. Very fine crystalline needles suitable for X-ray analysis were obtained by redissolving the white solid in 1:1 EtOH / DCM which was slowly allowed to evaporate.

$Z = C_2, n = 2, R = NO_2$

$Z = C_3, n = 2, R = NO_2$

$Z = C_2, n = 3, R = H$

$Z = C_3, n = 3, R = H$

$Z = C_2, n = 3, R = Cl$

$Z = C_3, n = 3, R = Cl$
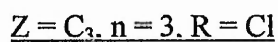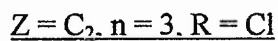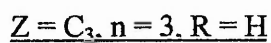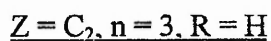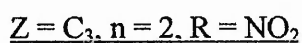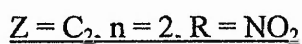
All of the above attempts produced impure oils and all attempts to purify these without resorting to column chromatography failed.

The compounds were obtained as described below.

Z	n	R	APPEARANCE	YIELD (%)	M.P (°C)
C_2	2	H	golden solid	63	84.7-85.6
C_3	2	H	Crystalline	69	128.5-129.9
C_4	2	H	brown oil	72*	Oil
C_2OC_2	2	H	brown oil	75*	Oil
C_2	3	H	Oil	58*	Oil
C_3	3	H	Oil	66*	Oil
C_2	2	Cl	Oil	60*	Oil
C_3	2	Cl	white solid	36	109.0-111.1
C_2	2	Cl	Oil	46*	Oil
C_3	3	Cl	Oil	52*	Oil
C_2	2	NO_2	orange oil	59*	Oil
C_3	2	NO_2	orange oil	64*	Oil

* = crude product.

The crude (*) products were not purified via column chromatography, n = 2 for all of the following.

<u>Infra red spectroscopic data.</u>

Z	R	TH-H cm^{-1}	PH-H cm^{-1}	TH C=C cm^{-1}
C_2	H	3100.4m, 3088.9m	3060.7m, 3023.7m	1565.0s
C_3	H	3106.1m, 3091.5m	3059.9m, 3032.0m	1559.0s
C_4	H	3098.4m, 3088.1m	3057.1m, 3027.5m	1552.6s
C_2OC_2	H	3107.4w, 3083.9w	3060.2m, 3026.5m	1560.0s, 1543.4s
C_3	Cl	3105.9w	Very weak.	1553.8s

The spectra for the compounds listed above also exhibited an increased number of aliphatic C-H str bands. No N-H str or thiophene 2-position C-H str bands were present. The precipitate formed from the acidic extraction of the C_4 oil showed all the bands characteristic of these compounds (single Th C=C str 1552.1 cm^{-1}) plus further bands at 2763.5, 2693.1, 2589.0, and 2422.0 cm^{-1}. However when the hydrochloride was prepared by the addition of a dry ethereal hydrochloric acid solution (from 5-6N propan-2-ol added to dry ether) to a dry ether solution of the C_4 macrocycle the white precipitate formed was hygroscopic and deteriorated to a reddish gum.

The second Th C=C str at 1543.4 cm^{-1} exhibited by the C_2OC_2 oil is probably due to unreacted or incomplete reaction of the bis ether. This occurrence of two bands also occurs in the spectra of the crude compounds (yield denoted with *) omitted (due to their impure nature) from the table above.

^{1}H NMR data.

Solvent = $CDCl_3$.

Z, R	TH H'S	THOCH$_2$	THCH$_2$	PHCH$_2$	NCH$_2$	OTHERS
C$_2$	7.14d, 6.84d	4.32s	3.73s	3.71s	2.72s	7.20-7.40m
C$_3$	7.15d, 6.87d	4.25t	3.75s	3.66s	2.67s	7.20-7.40m, H2' 2.18
C$_4$	N/A					
C$_3$ Cl	7.15d, 6.85d	4.25t	3.70s	3.60s	2.60s	7.25sh, H2' 2.20 qu

^{13}C NMR data.

Solvent = $CDCl_3$.

Z, R	TH C'S				AR C'S			
	C$_3$	C$_5$	C$_2$	C$_4$				
C$_2$	153.85	122.66	118.76	116.42	139.93	128.82	128.19	126.79
C$_3$	154.14	122.64	118.83	117.32	139.69	128.84	128.19	126.83
C$_4$	154.07	122.44	118.51	116.53	139.93	128.75	128.05	126.65
C$_3$ Cl	154.21	122.71	118.51	117.37	138.22	132.45	130.03	128.34

^{13}C NMR data continued.

Z, R	THOCH$_2$	THCH$_2$N	PHCH$_2$	NCH$_2$	OTHERS
C$_2$	70.26	58.76	49.63	46.38	
C$_3$	67.87	58.22	49.36	46.92	C2' 29.87
C$_4$	70.83	58.53	50.44	47.19	C2'+C3' 26.49
C$_3$, Cl	68.03	57.65	49.43	47.17	C2' 29.81

Microanalyses.

$Z = C_2$, $R = H$:-

Calculated (%) - C = 68.5, H = 6.2, N = 5.7.

Obtained   (%) - C = 68.45, H = 6.35, N = 5.84.

$Z = C_3, R = H :-$

Calculated (%) - C = 69.0, H = 6.4, N = 5.6.

Obtained   (%) - C = 68.60, H = 6.46, N = 5.55.

$Z = C_3, R = Cl :-$

Calculated (%) - C = 60.7, H = 5.3, N = 4.8.

Obtained   (%) - C = 60.67, H = 5.31, N = 4.85.

2.3. Templated [1+1] Mannich reactions.

The general procedure (described in section 2.2) was again followed with the addition of metal salts to the reaction mixture and N,N'-dimethylethylenediamine replacing N,N'-dibenzylethylenediamine.

      i) 1.0 eq $Ba(NO_3)_2$ $Z = CH_2CH_2OCH_2CH_2$ 24h.

      ii) 1.0 eq $Pb(OOCCH_3)_2$ $Z = CH_2CH_2OCH_2CH_2$ 24h.

      iii) 1.0 eq $Fe(ClO_4)_2.6H_2O$ $Z = CH_2CH_2OCH_2CH_2$ 60h.

i) $Ba(NO_3)_2$ template.

The reaction yielded an oil whose ^1H and ^{13}C NMR corresponded to the impure N_2O_3, N-methyl substituted macrocycle in no greater yield (taking into account loss on columning) than the untemplated reaction[1].

ii) $Pb(OOCCH_3)_2$ template.

This reaction yielded an oil as in (i) in no greater yield[1].

<u>iii) Fe(ClO$_4$)$_2$.6H$_2$O template.</u>

After sixty hours of stirring (time extended for possible slow coordination kinetics) a brown oil was obtained. This was washed with a coordinating solvent, CH$_3$CN, to give a brown / black precipitate.

The infra red spectrum of the precipitate was inconsistent with any macrocyclic complex the reaction was hoped to yield (see below).
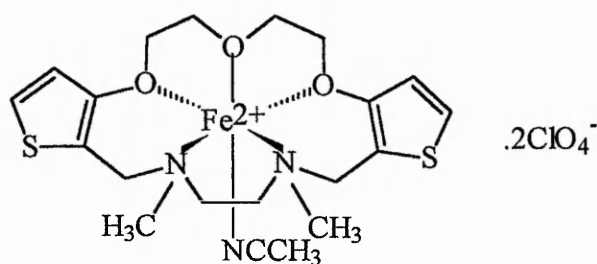
Polymerisation or the oxidising nature of Fe(ClO$_4$)$_2$.6H$_2$O probably thwarted macrocyclic complex formation.

Following the lack of any template effect a ^{1}H NMR study was undertaken.

<u>^{1}H NMR Study.</u>

To acquire further information on the 'O' donor strength of the CH$_2$CH$_2$OCH$_2$CH$_2$ bridged α,ω-bis(3-oxythienyl)alkane a ^{1}H NMR study was undertaken. This involved the partition of Ba(NO$_3$)$_2$ (1.0eq) between equal volumes of water and a solution of the bis ether (2.0eq) in CDCl$_3$. The two phases were thoroughly stirred for 24h. The CDCl$_3$ layer was separated and dried and the NMR performed.

78

If any donor effect was occurring between the C_2OC_2 bridged bis ether and Ba^{2+} this would show up as shifts in the ^1H NMR spectrum of the bis ether. After the partition experiment no shifts in the $CDCl_3$ bis ether layer were apparent.

2.4. Alcohol based templated Mannich reaction attempts.

The NaOH neutralisation work up of the acetic acid based Mannich reactions is unlikely to yield metal complexes of any products formed. Therefore the Mannich reactions described in section 2.3 were performed as for the acetic acid procedures (except for iron (II) perchlorate) but in dry ethanol with 6 drops of conc.HCl.

After stirring for 24h with the exclusion of moisture, the reaction mixtures were filtered. The precipitate obtained was found to be starting material. The solutions were then treated with a dry ethanolic solution of $NaClO_4.H_2O$ (2.0eq) to precipitate any metal complex via metathesis. Even with volume reduction no further precipitation occurred.

2.5. [1+1] Schiff base condensations.

The new 'Schiff base' routes to macrocycles containing two thiophene units involved the condensation of the previously synthesised dialdehydes (I) and (II) with redistilled anhydrous ethylenediamine under a variety of conditions (see figure 31).

Figure 31.

(I)   (II)

79
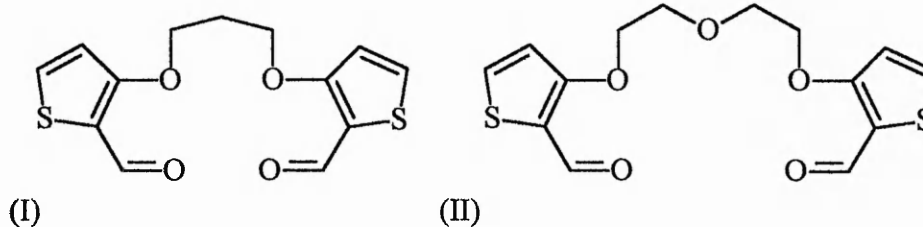
2.5.1. Templated Schiff base condensations.

The use of metal templates in Schiff base condensations has been discussed in the introduction to this report, section 1.2.3. In order to obtain the di-imine macrocycles as their metal complexes '*insitu*', appropriate templates are required. If condensation with ethylenediamine goes successfully the macrocycles from (I) and (II) will have two nitrogen, two oxygen and two nitrogen, three oxygen donors respectively. The metals used as templates, Ni^{2+} and Fe^{2+}, are expected to be able to coordinate in the geometries available to the macrocycle and metal salt combination under the conditions of reaction.

Ni^{2+} templated reactions with compound (I).

i) To a hot dry propan-1-ol solution ($60mlg^{-1}$ dialdehyde) of the dialdehyde (I) (1.0eq) and $Ni(ClO_4)_2.6H_2O$ (1.0eq) was added slowly with stirring a hot dry propan-1-ol solution ($40mlg^{-1}$ of dialdehyde) of ethylenediamine (1.0eq). The solution was stirred and heated at 60-70°C with the exclusion of moisture for 2h and then cooled. The solution was reduced in volume until precipitation commenced. The precipitate was then dried under vacuum over P_2O_5.

A green precipitate was obtained on cooling and solvent volume reduction. No further analysis was performed upon inspection of its infra red spectrum. Only bands attributable to ethylenediamine and perchlorate modes of vibration were present. This coupled with the solution's colour change from green to blue on cooling suggests that on cooling $Ni(en)_2(ClO_4)_2$ is formed, (see ligand redistribution experiment), possibly from hydrolysis of the macrocyclic complex, this then precipitates out as a non stoichiometric $Ni(en)_x(ClO_4)_2$ complex.

The procedure was repeated at RT with a two fold increase in solution volumes.

When the reaction was repeated at ambient temperature with a two fold increase in solution volumes (to ensure dissolution of the dialdehyde) a green precipitate with a comparable infra red spectrum was obtained.

ii) To a hot dry ethanolic solution of dialdehyde (1.0eq) and $NiCl_2.6H_2O$ (1.0eq) was added with stirring a hot dry ethanol solution of en (1.0eq) using the same dilution as above. The solution was stirred and heated as above. Once the solution had cooled it was reduced in volume until precipitation commenced. This was then filtered off and dried as above.

The change in solvent and anion did nothing to stop the eventual formation of a $Ni(en)_xCl_2$ salt.

iii) The incomplete condensation and tendency for the formation of $Ni(en)_xX_2$ complexes displayed by the previous template reactions resulted in a partition experiment to test the coordinating tendency of the the dialdehyde (I) with Ni^{2+}.

A solution of nickel(II) acetate tetrahydrate (1.0eq) dissolved in distilled water (50ml) was added to the dialdehyde, compound (I) dissolved in DCM (50ml). The flask was stoppered and the solution stirred for 24h. After this time the DCM layer was separated and washed four times with 10ml of distilled water. The colour of the DCM layer had not altered. The DCM was then removed under vacuum. The resulting solid's infra-red

81

spectrum showed only the dialdehyde C=O str with no evidence of partitioned acetate ions.

iv) Considering the dialdehyde (I) to be poorly coordinating a 2:1 dialdehyde to nickel(II) ratio was introduced.

A solution of Ni(II) acetate tetrahydrate (1.0eq) and the dialdehyde (2.0eq) dissolved in dry methanol (50ml) were stirred for 0.5h at 50-60°C with the exclusion of moisture. Ethylenediamine (1.0eq) was then pipetted into the reaction mixture. After 0.75h with no apparent colour change one drop of g.AcOH was added. The solution was heated and stirred for a further 60h. The solution was centrifuged, decanted and filtered, the discarded solid being unreacted dialdehyde. To the filtrate was added 2.0eq of $NaClO_4.H_2O$ in dry methanol (20ml). The resulting precipitate was then dried under vacuum.

Following the precipitation of the Ni^{2+} complex via metathesis with sodium perchlorate a light brown solid was obtained as described below:-

YIELD	M.P (°C)
0.26g	159.5 decomposition

Infra red spectroscopic data.

TH-H cm^{-1}	C=O cm^{-1}	C=N cm^{-1}	C=C cm^{-1}	ClO_4^- cm^{-1}
3102.8 m	1646.0s	1636.1s split	1535.1s, 1518.8s	1087sh, 622.4m

^{1}H . ^{13}C NMR data.

No satisfactory spectra were obtained probably owing to the presence of paramagnetic octahedral Ni^{2+} complex formation giving the broadening seen. However the $CDCl_3$ solution spectra corresponded to that of the dialdehyde (I) probably from hydrolysis of the imine complex(s).

Fe^{2+} templated reactions with compound (II).

A dry acetonitrile solution (60ml) of the dialdehyde (II) (1.0eq) and $Fe(ClO_4)_2.6H_2O$ (1.0eq) was heated to reflux with stirring and the exclusion of moisture. To this was slowly added ethylenediamine (1.0eq) in 20ml of dry acetonitrile from a dropping funnel. After 0.5h the addition was complete and the mixture heated for a further 10 minutes and cooled. The red / brown precipitate, 0.13g, was filtered off and dried. On standing pale yellow crystals precipitated from the filtrate, 0.30g. These were filtered off and dried.

Infra red spectroscopic data.

PRODUCT.	N-H cm^{-1}	C=N cm^{-1}	OTHERS cm^{-1}
1st ppt	3258.2sh	1636.1br	C=C 1570.1, 1559.5, 1540.1, 1526.5
2nd ppt	3389.6m *(O-H), 3238.1 split w	1632.1s	C=C 1522.1s, ClO_4^- modes 1121.6, 1085.4, 1054.0, 624.7

^{1}H NMR data.(2nd ppt).

Solvent = DMSO.

CH=N	TH H'S		THOCH$_2$	H2'+H4'	NCH$_2$
	H5	H4			
8.78s	8.43d	7.22d	4.53d	3.84d	4.14s

2.5.2. Non templated Schiff base condensations.

A number of experiments were performed in order to achieve the condensation of en or

o-phenylenediamine with the dialdehydes (I) and (II). The conditions attempted were in

dry solvents, MeOH, EtOH, PrOH, CH$_3$CN with and without heating, alteration of pH

and various isolation methods including kinetic quenching and *in-situ* reductions using

NaBH$_4$. See section 3.5.2.

2.6. Schiff base condensation + metal complexation.

After the difficulties in obtaining the imines without them reverting back to the

carbonyl and amine compounds, an alternative source of isolation was sought. This

involved the condensation between the dialdehyde and diamine at elevated

temperatures as before but then adding the appropriate complexing metal salt and

stirring as the mixture cools and then for an extended period to discourage imine bond

hydrolysis.

i) The dialdehyde (I) (1.0eq) and en (1.0eq) dissolved in dry ethanol (80mlg^{-1} of

dialdehyde) were refluxed for 1h. To the solution was then added NiCl$_2$.6H$_2$O (1.0eq) in

dry ethanol (20 mlg^{-1} of dialdehyde) and stirring continued for a further 60h. The

precipitate was filtered off and dried at 50°C under vacuum.

The light brown precipitate after drying weighed 0.21g (28% $NiC_{15}H_{16}O_2N_2S_2Cl_2$), M.P = 177.8°C (decomposition).

Infra red spectroscopic data.

TH-H cm^{-1}	C=N cm^{-1}	C=C cm^{-1}
3097.9m, 3075.4m	1623.9s	1526.1s

The lack of N-H and C=O str's implies macrocyclisation has occurred as does the C=N band and the lowering of the C=C str frequency due to coordination.

^{1}H, ^{13}C NMR data.

No NMR data could be obtained due to paramagnetic broadening.

Microanalytical data.

Calculated for $NiC_{15}H_{16}O_2N_2S_2Cl_2$; C: 40.03%, H: 3.56%, N: 6.22%.

Found C: 42.67%, H: 4.35%, N: 7.38%.

ii) The procedure above was followed except the metal salt used was $Ni(ClO_4)_2.6H_2O$ and the reaction mixture was stirred for 72h following metal salt addition.

The light green precipitate after drying weighed 0.32g (52% $NiC_{15}H_{16}O_{10}N_2S_2Cl_2$), M.P = 162.7°C decomposition.

Infra red spectroscopic data.

TH-H cm^{-1}	C=N cm^{-1}	C=C cm^{-1}	ClO$_4^-$ IONIC	ClO$_4^-$ UNIDENTATE
3106.2m	1616.6s	1529.9s	1090sh, 623.2m	1121.6m, 1062.5sh, (635.9)

Again the infra red spectrum implies macrocyclisation, however the presence of unidentate and ionic perchlorates suggests either square pyramidal coordination or the presence of both square planar and octahedral complexes (see metal complex equilibria in the introduction).

^{1}H. ^{13}C NMR data.

No NMR spectra could be obtained due to paramagnetic broadening.

Microanalytical data.

Calculated for NiC$_{15}$H$_{16}$O$_{10}$N$_2$S$_2$Cl$_2$; C: 31.16% H: 2.79% N: 4.85%

Found C: 38.10% H: 3.59% N: 5.44%

iii) The dialdehyde (II) (1.0eq) and en (1.0eq) dissolved in dry propan-1-ol (60mlg^{-1} of dialdehyde) were refluxed for 1h. To the solution was then added FeSO$_4$.7H$_2$O (1.0eq) in dry methanol (30mlg^{-1} of dialdehyde) and stirring continued for a further hour. The precipitate formed on the addition of the metal salt was filtered off and dried.

On inspection of the product's infra red spectrum no further investigation was undertaken. This showed significant broadening in the 3300-3000 cm^{-1} region and remaining uncondensed C=O str.

iv) In order to further characterise the product of reaction (ii) it was reduced by addition to a refluxing dry ethanolic solution of NaBH₄ (4.0wt eq). The solvent was then removed under vacuum and the residue washed with water and extracted with DCM. This was dried (MgSO₄) and evaporated to give an oil which was purified via acid extraction.

Infra red spectroscopic data.

TH-H cm⁻¹	N-H cm⁻¹	C=C cm⁻¹
3101.2m, 3083.0m	3311.0	1556.0

¹H NMR data.

Solvent = CDCl₃

TH H'S		THOCH₂	THCH₂N	NCH₂	H2'
H5	H4				
7.05d	6.78d	4.15t	3.80s	2.62s	2.15qu

¹³C NMR data.

Solvent = CDCl₃

TH C'S				THOCH₂	THCH₂N	NCH₂	C2'
C₃	C₅	C₂	C₄				
153.37	122.03	120.30	117.09	68.00	47.08	43.79	29.85

v) The dialdehyde (I) (1.0 eq, 0.5g) and en (1.0 eq, 0.11ml) dissolved in dry ethanol were refluxed for one hour. Cobalt (II) chloride (1.0 eq, 0.2204g) dissolved in the minimum amount of ethanol was added to the hot solution and stirred at RT for 48 hours. The turquoise precipitate formed was then filtered and washed with ether.

The turquoise precipitate after drying weighed 0.58g (76% $CoC_{15}H_{16}O_2N_2S_2Cl_2$), M.P = 189°C decomposition.

Infra red spectroscopic data.

C=N STR cm^{-1}	C=C STR cm^{-1}
1599.7	1527.1

vi) The above method was repeated for the C2 bridged dialdehyde (1.2 eq, 0.6g), ethylenediamine (1.0 eq, 0.106ml) and cobalt(II) chloride (1.0 eq, 0.2302g). The green precipitate obtained was filtered and washed with ether.

The green precipitate after drying weighed 0.42g (84% $CoC_{14}H_{14}O_2N_2S_2Cl_2$), M.P = 198°C decomposition.

Infra red spectroscopic data.

C=N STR cm^{-1}	C=C STR cm^{-1}
1625.2	1546.7

2.7. New route to 2'O', 2'N' donor macrocycles.
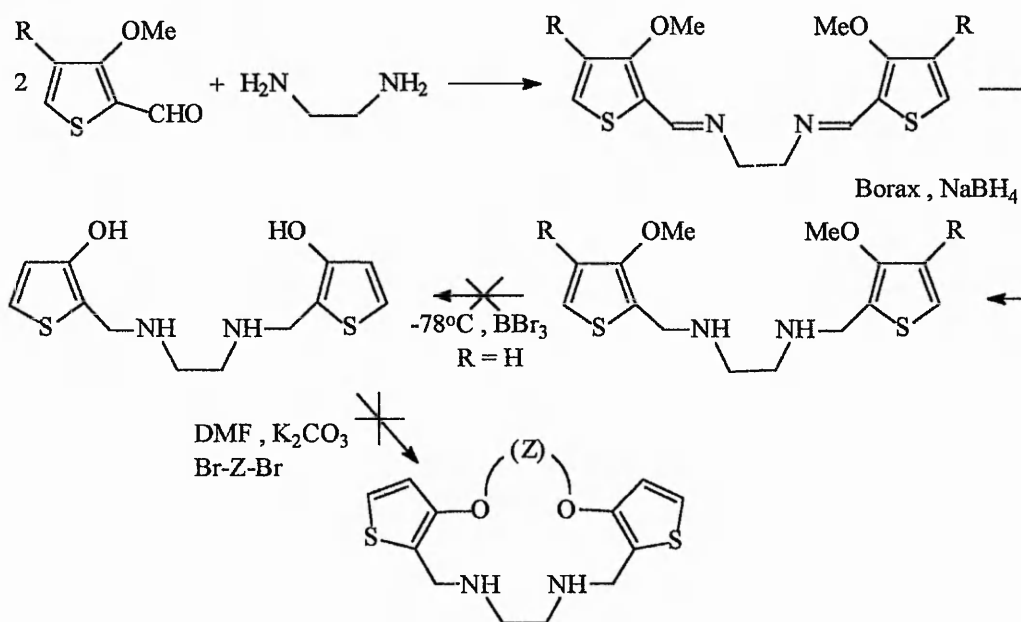
i) *Insitu* reduction.

3,4-Di-methoxythiophene-2-carbaldehyde (2.0eq) and en (1.0eq) were added to dry ethanol (50mlg^{-1} of aldehyde) over anhydrous sodium sulfate, 6 drops of g.AcOH were added and the mixture was stirred for 3h. The yellow solution was filtered quickly and transferred to a dropping funnel with a CaCl$_2$ guard. The solution was added dropwise to a refluxing dry ethanol solution of NaBH$_4$ (4.0eq). Stirring was continued for 0.5h after addition was complete. The ethanol was then removed *in vacuo* and the white residue washed with water and extracted with DCM. The DCM was dried (MgSO$_4$) and removed to leave an oil.

Infra red spectroscopic data.

N-H cm^{-1}	TH-H cm^{-1}	N-H BEND cm^{-1}	C=C cm^{-1}
3289.5w	3114.2w	1578.8w	1504.1s

<u>^{1}H, ^{13}C NMR data.</u>

The spectrum was run three days after the oil was obtained and showed significant decomposition. Demethylation was not attempted.

<u>ii) Imine isolation.</u>

a) 3,4-Dimethoxythiophene-2-carbaldehyde (2.0eq) and en (1.0eq) dissolved in dry ethanol (50 mlg^{-1} of aldehyde) were refluxed with 2 drops of g.AcOH for 10 minutes. The solution was immediately poured into ice and filtered through a sintered glass funnel. The white solid obtained was then dried under vacuum at 60°C.

<u>Infra red spectroscopic data.</u>

TH-H cm^{-1}	C=N cm^{-1}	C=C cm^{-1}
3129.5w	1627.5s	1498.7s

<u>^{1}H NMR data.</u>

Solvent = CD$_3$OD.

CH=N	H5	4 CH$_3$O	3 CH$_3$O	NCH$_2$
8.27s	6.56s	4.87s	3.80s	3.29m

<u>^{13}C NMR data.</u>

Only the carbons with hydrogens attached were detected in the spectrum obtained.

b) 3-Methoxythiophene-2-carbaldehyde (2.0eq) and en (1.0eq) dissolved in dry ethanol (60 mlg^{-1} of aldehyde) were refluxed with 3 drops of AcOH for 10 minutes. The solution was poured into ice and filtered as above. The resulting off white solid was dried as above.

Infra red spectroscopic data.

TH-H cm^{-1}	C=N cm^{-1}	C=C cm^{-1}
3098w, 3077.3m	1621.3s	1544.3s

^{1}H NMR data.

Solvent = CD_3OD.

CH=N	H5	H4	OCH$_3$	NCH$_2$
8.44s	7.26d	6.78d	3.86s	3.82s

^{13}C NMR data.

Solvent = CD_3OD.

CH=N	TH C'S				THOCH$_3$	NCH$_2$
	C$_3$	C$_5$	C$_2$	C$_4$		
153.69	159.12	127.80	119.12	115.14	61.74	58.63

Microanalysis results.

Calculated for $C_{14}H_{16}N_2O_2S_2$:   C = 54.5%   H = 5.2%   N = 9.1%

Found: C = 54.4%   H = 5.2%   N = 8.8%

iii) Reduction.

The isolated '3-methoxy' diimine (1.0eq) was added portionwise to a hot stirred solution of NaBH$_4$ (4.0eq) and borax (0.1eq) dissolved in dry ethanol and heating and stirring continued for 40 minutes. The solution was cooled and evaporated, the residue washed with water and extracted with DCM. The DCM solution was dried (MgSO$_4$) and evaporated *in vacuo* to give an oil. This was then purified via acidic extraction.

Infra red spectroscopic data.

N-H cm⁻¹	TH-H cm⁻¹	C=C cm⁻¹
3307.9m	3101.5m	1560.0s

¹H NMR data.

Solvent = CDCl₃.

TH H'S		OCH₃	THCH₂	NCH₂	N-H
H5	H4				
7.07d	6.80d	3.84s	3.80s	2.75s	1.83s (ex.)

¹³C NMR data.

Solvent = CDCl₃.

TH C'S				THOCH₃	THCH₂N	NCH₂
C₃	C₅	C₂	C₄			
154.27	121.78	119.60	116.19	58.80	48.23	43.97

iv) Demethylation.

In a nitrogen purged flask the '3-methoxy' di-secondary amine (1.0eq) dissolved in DCM was cooled to -78°C and stirred. To this was added BBr₃ (3.0eq) via a syringe and the mixture stirred for 3h. The solution was quenched with 2M hydrochloric acid and extracted with DCM. The extract was dried (MgSO₄) and evaporated *in vacuo*. The oil obtained decomposed within a few hours (found via I.R spectra).

2.8. Templated [2+2] Mannich reactions.

Previously macrocycles of type (B) (see page 24) had been synthesised via a Schiff base condensation with subsequent reduction. The diamine obtained then underwent the Mannich reaction with the appropriate α,ω-bis(3-oxythienyl)alkane. The Mannich

reaction stage was performed in the presence of various metal salts to give similar yields (32-35%) to when the reaction was carried out under high dilution (35%). The one exception being $BaCO_3$ which gave a 43% yield.

In order to test this template effect two metal diamine complexes were synthesised (see section 2.1.7.1). Here the metal coordinates strongly with the diamine ligands and is held at the centre of the complexes, thus testing if in fact it is the directing influence of the metal causing the increased yields.

Metal diamine complex templated Mannich reactions.

The C_2OC_2 bridged α,ϖ–bis(3 oxythienyl)alkane (2.0eq) was added to a solution of $[Cu(CH_3NHCH_2CH_2NHCH_3)_2]I_2$ (1.0eq) and CH_2O (4.4eq) dissolved in g.AcOH (25mlg^{-1} of bis ether). The mixture was stirred for 24h. The solution was neutralised with 2M NaOH and filtered. The solid was extracted into boiling methanol and sodium perchlorate (2.0eq) was added. No precipitation occurred and when the blue / green solution was evaporated the brown solid obtained quickly decomposed. The filtrate was evaporated (cold finger apparatus) and the residue dissolved in dry methanol and filtered. The filtered solid was discarded and the blue solution evaporated to give a green solid, which was not the desired product (indicated via infra red spectroscopy).

Further reactions using the metal diamine complexes in g.AcOH and in dry EtOH / trace hydrochloric acid only yielded the unreacted bis ether and metal salts.

2.9. Templated [2+2] Schiff base condensations.

Following the failure of templated Mannich reactions to yield [2+2] macrocycles of type (B) in one step a similar approach was undertaken using metal primary diamine templates and the dialdehydes (I) and (II) (figure 31) as shown below.
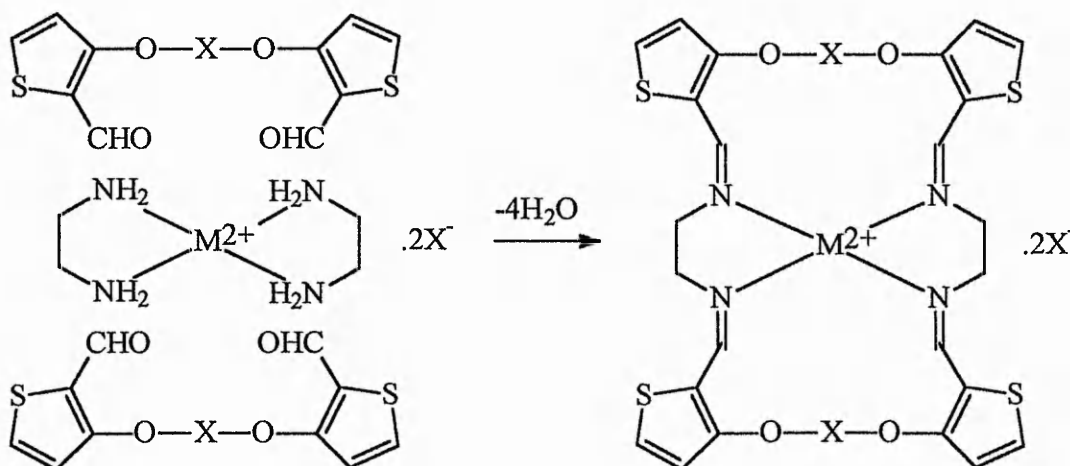
In order to characterise the products from some of the reactions described below a number of the complexes were reduced via the following general method:-

The complex was added to a refluxing dry ethanolic solution of NaBH$_4$ (4.0wt eq) and the mixture heated for 20 minutes. The solvent was removed *in vacuo* and the residue washed with water and extracted with DCM. The extract was dried (MgSO$_4$) and evaporated *in vacuo* to yield an oil in all cases. This was subjected to acidic extraction again to yield an oil. The infra red and NMR spectra were then obtained.

Procedure

i) Cu(en)$_2$Cl$_2$.xH$_2$O (1.0eq) dissolved in the minimum dry methanol was added to a stirred solution of the dialdehyde II (2.0eq) dissolved in dry methanol (50mlg^{-1} of

dialdehyde) and 10 drops of g.AcOH were added. The solution was stirred with the exclusion of moisture for 24h. Sodium perchlorate (2.2eq) dissolved in the minimum dry methanol was added to the solution and the resulting precipitate filtered off and washed sparingly with dry methanol.

Infra red spectroscopic data.

N-H cm^{-1}	C=N cm^{-1}	C=C cm^{-1}	ClO_4^- MODES.
3307.8m, 3219.5m	1607.5s	1518.7s	1116.6sh, 622.9s

^{1}H, ^{13}C NMR data.

When the spectra were obtained from d-DMSO they showed paramagnetic broadening in the ^{1}H spectrum with the ^{13}C spectrum corresponding to the precursor dialdehyde. It can be concluded that the complex is broken down in this harsh solvent.

Microanalysis.

Calculated for $CuC_{18}H_{26}N_4S_2O_{11}Cl_2$

	C%	H%	N%
	32.12	3.87	8.33
Found :-	38.09	4.22	6.82

ii) The same procedure as above was carried out substituting $Ni(en)_3Cl_2.2H_2O$ for $Cu(en)_2Cl_2.xH_2O$.

Infra red spectroscopic data.

N-H cm^{-1}	C=N cm^{-1}	C=C cm^{-1}	ClO_4^-
3340.4w, 3282.1w	1608.4s	1518.1s	1112.0sh, 623.0s

<u>^{1}H. ^{13}C NMR data.</u>

On first inspection the ^{1}H spectrum run in CDCl$_3$ seems to just exhibit the dialdehyde (from complex hydrolysis) but on closer inspection an imine and shifted H4 and H5 thiophene protons are evident as well as shifted C2' and C4' protons and a further singlet at 4.1 ppm. The ^{1}H spectrum in CD$_3$CN shows significant broadening but again two sets of H4, H5; C2', C4' protons and an imine proton at 8.38 ppm are present. The greater broadening seen of the imine proton over the H2', H4' protons is indicative of the nitrogen's greater coordination tendency[91]. The ^{13}C spectrum could not be obtained.

<u>Microanalysis.</u>

	C%	H%	N%
Calculated for Ni C$_{18}$H$_{26}$N$_4$S$_2$O$_{11}$Cl$_2$	32.35	3.89	8.39
Found :-	41.65	4.44	7.20

<u>Complex reduction.</u>

On reduction of the product described above a small amount of a yellow oil was obtained after acidic extraction.

<u>Infra red spectroscopic data.</u>

N-H cm^{-1}	TH-H cm^{-1}	C=C cm^{-1}
3279.3br, 3146.4w	3106.2w, 3096.2w	1557.3s + sh

<u>^{1}H. ^{13}C NMR data.</u>

The oil could not be obtained in great enough yield (due to the small amount of precursor complex) to obtain satisfactory spectra.

iii) The same procedure as above was carried out substituting $Ni(en)_2Cl_2.xH_2O$ for $Ni(en)_3Cl_2.2H_2O$.

Infra red spectroscopic data.

N-H cm^{-1}	C=N cm^{-1}	C=C cm^{-1}	ClO_4^-
3246.4 v.w	1639.9s	1522.2s	1009.5sh, 623.1m

^{1}H. ^{13}C NMR data.

When the ^{1}H spectrum was obtained from a CD_3CN solution the spectrum was broad in nature with two sets of thiophene protons, the more shifted set being almost as pronounced as the lesser shifted set. The coupling of both sets of H4 and H5 protons is different from the dialdehyde's spectrum. The greater broadening of the imine proton over that of the H2', H4' protons is again indicative of the nitrogen's greater coordinating tendency[91]. The ^{13}C spectrum could not be obtained.

Although the ^{1}H spectrum cannot be interpreted fully due to its broad (paramagnetic) nature the presence of complexed and uncomplexed (via hydrolysis in the deuterated solvent) species can be detected by shifts in the thiophene protons.

Microanalysis.

Calculated for $NiC_{32}H_{36}N_4S_4O_{14}Cl_2$.

	C%	H%	N%
	40.10	3.76	5.85
Found :-	38.92	4.07	4.67

For further characterisation the compound was reduced.

<u>Complex reduction.</u>

After acidic extraction a yellow oil was obtained. The infra red and NMR data of the oil corresponds to either the [1+1]* or [2+2] reduced imine macrocycle. *The [1+1] complex cannot be ruled out as it could be produced via en dissociation, reaction and re-complexation.

<u>Infra red spectroscopic data.</u>

N-H cm^{-1}	TH-H cm^{-1}	C=C cm^{-1}
3298.2br	3099.6 w split	1556.0s

<u>^{1}H NMR data.</u>

Solvent = CDCl$_3$.

TH H'S		THOCH$_2$	THCH$_2$N	H2' + H4'	NCH$_2$
H5	H4				
7.05d	6.80d	4.10m	3.85s	3.78m	2.68s

<u>^{13}C NMR data.</u>

Solvent = CDCl$_3$.

TH C'S				THOCH$_2$	C2'+C4'	THCH$_2$N	NCH$_2$
C$_3$	C$_5$	C$_2$	C$_4$				
153.74	122.06	120.11	117.07	70.91	70.00	46.97	43.29

iv) (i), (ii), and (iii) were repeated except the solutions were refluxed for 2h rather than stirring for 24h.

The products obtained were of a polymeric nature (deduced from their infra red spectra).

v) In a transmetallation experiment the product from (i) (1.0eq assuming structure, see results) was dissolved in dry methanol to which was added AgNO$_3$ (4.0eq) dissolved in dry methanol and the solution stirred for 12h. The resulting light brown precipitate was filtered off and dried under vacuum at 60°C.

Infra red spectroscopic data.

TH-H cm^{-1}	C=N cm^{-1}	C=C cm^{-1}	ClO$_4^-$ MODES
3106.2w	1611.1s	1533s	1113.2sh, 622.0m

The lack of N-H str's which were present in the Cu^{II} condensate and the influence of the softer metal ion raising the C=N and C=C str's led to this assumption. No further analysis (via complex reduction and ligand isolation) was carried out due to the small yields involved.

vi) The dialdehyde (I) (2.0eq) in 50ml of dry methanol was heated until the solid dissolved. To the solution was added Ni(en)$_3$(ClO$_4$)$_2$ (1.0eq) in dry methanol and the mixture heated at 50-55°C for 20h with the exclusion of moisture. The mixture was cooled and the resulting red / brown crystalline solid filtered off and washed with ether.

Infra red spectroscopic data.

N-H cm^{-1}	C=N cm^{-1}	C=C cm^{-1}	ClO$_4^-$ MODES
3339.5w, 3284.0w	1616.0s + sh	1517.8s, 1533sh,w	1121.6, 1104.1, 622.8

No satisfactory NMR data could be obtained.

vii) Due to the inability to obtain $Ni(en)_2(ClO_4)_2$ a ligand redistribution and condensation was undertaken.

Basis:- $2 Ni(en)_3(ClO_4)_2 + Ni(ClO_4)_2.6H_2O = 3 Ni(en)_2(ClO_4)_2$

$Ni(en)_3(ClO_4)_2.xH_2O$ (2 eq) and $Ni(ClO_4)_2.6H_2O$ (1 eq) were dissolved in dry methanol ($25mlg^{-1}$ of $Ni(en)_3(ClO_4)_2$) and heated. The purple solution changed to blue after two minutes. The dialdehyde (I) (2.0 eq) dissolved in 1:1 methanol / acetonitrile ($30mlg^{-1}$ of dialdehyde) was added to the first solution and heating (50-55°C) and stirring continued for 54h with the exclusion of water. On cooling an orange / brown powder precipitated out. This was washed with ether and air dried. Due to the small amount of precipitate other attempts were made to isolate further product. Triturating the solution with various solvents all failed. The solvent mixture was removed *in vacuo* to yield a red oil. This was redissolved in dry methanol and excess $NaBPh_4$ added. No further product was obtained.

Infra red spectroscopic data.

C=N cm^{-1}	C=C cm^{-1}	ClO_4^- MODES
1616.4s	1521.8	1121.5, 1111.4, 622.6

No N-H or C=O modes were evident. Assuming the product to be the [2+2] complex the sample was sent for microanalysis. The results were not in agreement with the [2+2] macrocyclic complex.

viii) $Ni(en)_3(ClO_4)_2.xH_2O$ (2 eq) and $Ni(ClO_4)_2.6H_2O$ (1 eq) were dissolved in a 10:1 dry acetonitrile / methanol solution ($150mlg^{-1}$ of starting materials). The dialdehyde (I) (2.0eq) dissolved in the minimum dry acetonitrile was added to the first solution and the

resulting solution heated (50-55°C) and stirred for 24h. KI (2.0eq) in dry methanol was added to the solution followed by AgNO$_3$ (4.0eq) dissolved in dry methanol and the solution stirred for a further 12h. The resulting light brown precipitate was filtered off and air dried.

Infra red spectroscopic data.

C=N cm^{-1}	C=C cm^{-1}	ClO$_4^-$ MODES
1615.8s	1534.0s	1121.8, 622.4

No N-H or C=O str's were evident. The product's spectrum is very similar to that of the silver complex obtained from transmetallation with the product of (i). The only differences are those associated with the differing dialdehydes. The characterisation difficulties incurred with these complexes and the small yield meant that further characterisation was abandoned.

ix) Ni(en)$_3$(ClO$_4$)$_2$.xH$_2$O (2 eq) and Ni(ClO$_4$)$_2$.6H$_2$O (1.0eq) were dissolved in the minimum amount of dry methanol and heated. To the resulting blue solution was added the dialdehyde (I) (2.0eq) dissolved in dry methanol (30mlg^{-1}) and stirring continued for 60h. After this time the precipitate was isolated and its infra red spectrum taken. Discovering incomplete condensation the solid was returned to the filtrate and stirring continued for a further 12h. The precipitate was once again isolated and washed with ether and air dried.

The product of this ligand redistribution / condensation experiment gave exactly the same infra red spectrum as the product obtained by metathesis in experiment (ii) in slightly higher yield: 24%.

x) Procedure (iii) was repeated using anhydrous sodium sulphate as an 'in-situ' drying agent and dry EtOH as the solvent. Upon addition of the ethanolic sodium perchlorate solution a light brown precipitate formed and was filtered off. The filtrate was protected from moisture and left for 48h under refrigeration. Further precipitation occurred and the solid was filtered off and washed with ether.

A portion of the ether washed complex was added to a dry ethanolic solution of NaBH$_4$ (4.0wt eq) and heated at 60°C with heating and exclusion of moisture for 0.75h. The solution was cooled and the solvent removed *in vacuo*. The residue was washed with water and extracted with DCM. The DCM was dried (MgSO$_4$) and evaporated to give an oil. This was then treated to acidic extraction again to yield an oil.

The products gave the same spectroscopic data as (iii)

xi) Ni(en)$_2$Cl$_2$.xH$_2$O (1.0eq) and the dialdehyde (II) (2.0eq) were dissolved in dry methanol (140mlg^{-1} of Ni^{2+} complex), 2 drops of pyridine were added and the pH adjusted to 9 with 2M NaOH. The solution was heated for 2.5h and cooled. The green precipitate was filtered off and washed with ether. The residual solution was evaporated to yield a purple solid and a yellow oil. The purple solid was removed via water solubilisation. The oil was extracted into DCM which was dried (MgSO$_4$) and evaporated *in vacuo* to yield an oil which solidified.

All products corresponded to starting materials.

2.10. Further Approaches.

This section describes various attempted routes to thiophene based macrocycles. None of these resulted in new methods to macrocycles or macrocyclic complexes.

2.10.1. Ni(II) complex of methyl 3-hydroxythiophene-2-carboxylate (Ni[OL]$_2$).

The purpose of making this complex was to increase the electropositivity of the carbonyl carbon for reaction with nucleophiles.
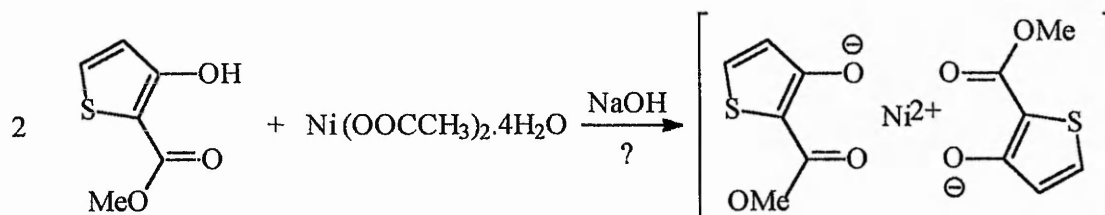
Procedure.

Nickel(II) acetate tetrahydrate (1.0eq, 4g) was dissolved in hot methanol, filtered to remove any nickel oxide and methyl 3-hydroxythiophene-2-carboxylate (2.0eq, 6.66g) dissolved in hot methanol was added to the first solution and the resulting solution stirred. The solution was neutralised by the slow addition of NaOH (2.0eq) dissolved in hot water. The green precipitate obtained was filtered off and washed with ether and dried at 130°C overnight.

Infra-red spectroscopic data.

TH-H cm^{-1}	C=O cm^{-1}	C=C cm^{-1}
3095w	1619s	1503s

NMR data.

The ^{1}H NMR spectrum is paramagnetically broadened however the three broad peaks occur at (H5) 7.25s, (H4) 6.75s and (OMe) 3.90s.

Magnetic measurements.

The compound's magnetic moment was measured. The average of three readings gave $\mu_{eff} = 3.94$ ($\pm$ 0.12) B.M. This falls in the range for octahedral Ni(II).

Solution conductivity.

No precise calculations were involved. A simple comparative measurement of a 0.01M solution of the complex in acetone and a 0.01M solution of the 2:1 electrolyte $Ni(NO_3)_2.6H_2O$ in acetone was undertaken. The conductivities of the two solutions were 2.6μS and 138.0μS respectively. The complex was thus considered non-conducting as expected.

Microanalysis.

The complex was analysed for C, H and ash content. The results are shown below:

C : 35.84% H : 2.69% Ash : 21.99%. (Ni : 17.28%).

The percentage Ni is 17.28% if the ash residue is presumed to be NiO. The analyst Mr Spencer (Nottingham University) quotes the ash content reliability at $\pm$ 5%.

For the 2:1 complex the expected results are :

C : 38.6% H : 2.7% Ni : 15.7%.

For the 1:1 complex with one acetate anion the expected results are :

C : 35.0% H : 2.9% Ni : 21.3%.

2.10.2. Ni(II) complex of 3-hydroxythiophene-2-carbaldehyde.

The procedure above was repeated substituting methyl 3-hydroxythiophene-2-carboxylate for 3-hydroxythiophene-2-carbaldehyde:- nickel(II) acetate tetrahydrate 0.107g, 3-hydroxythiophene-2-carbaldehyde 0.110g and NaOH 0.034g.

Infra-red spectroscopic data.

TH-H cm^{-1}	C=O cm^{-1}	C=C cm^{-1}
3096w	1587s	1483s

2.10.3. Reactions of Ni[OL]$_2$ with various amines.

The nickel complex was reacted with the following amines in solution :-
$CH_2(CH_2)_2NH_2$, $Br(CH_2)_2NH_2$, $Br(CH_2)_3NH_2$.

All reactions failed to give the desired products (see results section 3.10.3).

The nickel complex was reacted with $HO(CH_2)_2NH_2$ as solvent :-

Procedure.

Ni[OL]$_2$ (1.0eq, 0.60g) dissolved in $HO(CH_2)_2NH_2$ (60ml) was heated (40-50°C) for 72 hours, after which time the solution had changed from green to a reddish orange colour. On acidification of the solution with 4M HCl the solution colour went olive green and upon acidity, turned yellow. The solution was extracted with DCM, dried (MgSO$_4$) and evaporated *in vacuo* to give an oil which solidifies, this was washed with ether to give a white solid.

Infra-red spectroscopic data.

OH cm^{-1}	NH cm^{-1}	TH-H cm^{-1}	C=O, NH cm^{-1}	C=C cm^{-1}
3375m	3190m	3096w	1608s, 1578m	1556m

^{1}H NMR data.

TH-OH	NH	TH-H	
11.20s	7.75s	7.25d	6.70d

CH$_2$OH	CH$_2$	CH$_2$	DMSO
4.65s	3.65s	3.25s	3.40m

^{1}H NMR data (after D$_2$O).

TH-H		CH$_2$	CH$_2$
7.25d	6.75d	3.65t	3.50t

^{13}C NMR data.

C=O	TH-C'S				(CH$_2$)$_2$	
163.81	157.93	127.87	119.67	110.49	60.56	41.71

2.10.4. *N*-(3-Bromopropyl)thiophen-2-aldimine.
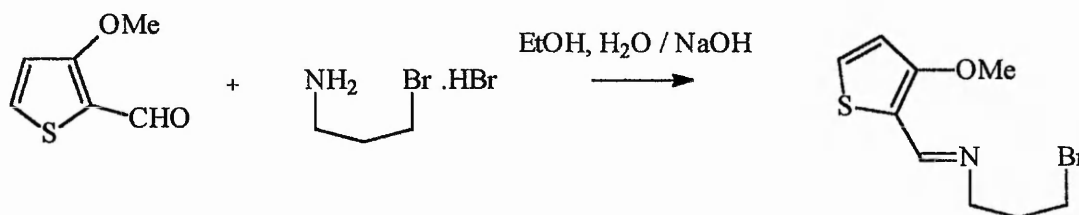
Procedure.

3-Bromopropylamine hydrobromide (1.0eq, 1.09g) dissolved in water (15ml) and NaOH (1.0eq, 0.19g) dissolved in water (5ml) were added to 3-methoxythiophene-2-carbaldehyde (1.0eq, 0.64g) dissolved in ethanol (20ml). The mixture was stirred and

gently heated for 30 minutes after which, water (40ml) was added. The solution was extracted with DCM, dried (MgSO$_4$) and evaporated *in vacuo* to give the product as an oil.

Infra-red spectroscopic data.

TH-H'S cm^{-1}	C=N cm^{-1}	C=C cm^{-1}
3106w	1625s	1545s

^{1}H NMR data.

CH=N	TH-H		OMe	CH$_2$	CH$_2$	-CH$_2$-
8.45s	7.28d	6.80d	3.92s	3.65t	3.45t	2.20qu

^{13}C NMR data.

C=N	Th-C's				OMe	CH$_2$'s		
159.22	153.17	135.12	128.08	118.67	115.76	58.76	33.48	31.82

2.11. Crystallographic methods.

2.11.1. Density measurement.

The flotation method was used for measuring the density of crystals. The crystals were immersed in a solution of two miscible solvents, one of lesser and one of greater density than the crystals. If the crystals floated then more of the less dense solvent was added. If the crystals sank, more of the denser solvent was added. This was carried out until the crystals neither floated nor sank but remained suspended in the solution. The solvent mixture at this point was equal to the density of the crystals. The solvent mixture was then transfered to an accurately weighed density bottle of known volume and the solvent weighed. Using the equation: Density = mass/volume, the density of the crystals may be determined. A $10cm^3$ density bottle was employed and the solvent mixture used was methanol/chloroform. The choice of the solvent mixture must not only be in the correct density range but should also ideally consist of solvents in which the crystals are not soluble. In this case however it was not possible to find such a mixture and the crystals did dissolve slowly during the experiment.

2.11.2. Crystal selection and mounting.

Using a microscope, a crystal of good quality was selected. A 'good quality' crystal should be of a reasonable size, (ideally so that the whole of the crystal is bathed in the X-ray beam) have morphology characteristic of the batch and possess smooth faces free from contamination by other crystal fragments. Once a crystal had been chosen it was then examined under a polarising microscope. Polarised light does not interact with non-cubic crystals in a uniform manner[92] and when a face of a crystal is rotated extinction may occur. If the face of the crystal fully extinguishes then a crystal axis is located in this direction. Once an axis had been located the crystal was mounted to

108

rotate about this axis in preparation for X-ray photographic methods. The crystal was mounted on a set of adjustable arcs (see figure 32[93]) (i.e. a goniometer head) by supergluing a very thin glass fibre along the crystal axis. The other end of the fibre was then either superglued to a stud (which was then held on the top arc via a locating pin) or held on the top arc via SIRA heat sensitive wax.

Figure 32.
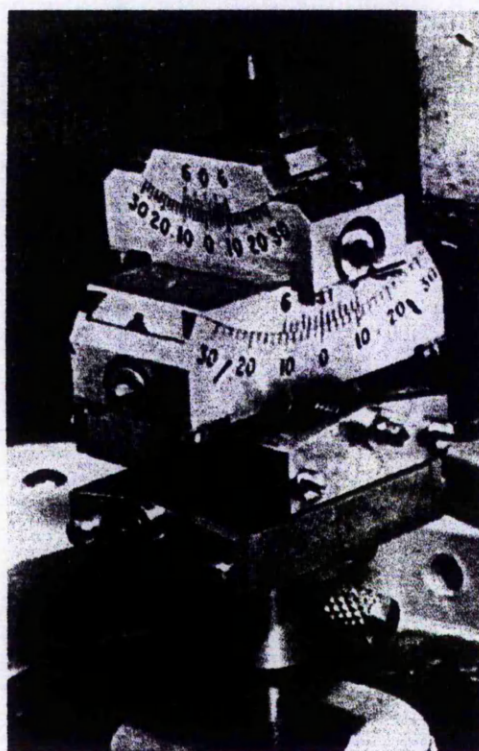
2.11.3. Oscillation, rotation and Weissenberg photographs.

Oscillation photographs are a convenient method of setting a crystal once it has been approximately mounted along an axis. The crystal was set approximately by eye. This usually involved moving the arcs of the goniometer head so that any crystal faces nearly parallel or perpendicular to the crystal axis became exactly aligned. This was done by looking at the crystal down a cross-haired microscope mounted on the instrument. The crystal was then manually rotated so that one arc was parallel to the X-ray beam. A film

was bent around it inside the camera (see figure 33[94]) and the crystal was oscillated approximately 20° about this position and exposed to X-rays (Cu Kα, λ = 1.542Å).

Figure 33.
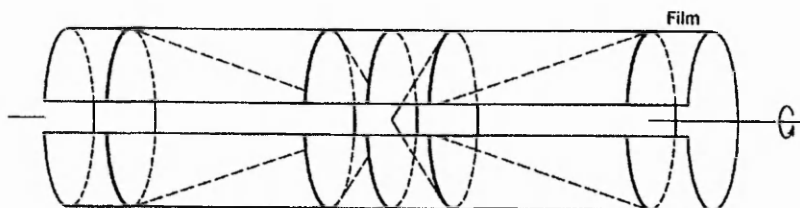
The lines of spots exposed on the film should be perfectly straight for a correctly set crystal. Knowing the diameter of the camera the amount of adjustment of the arcs in degrees required to set the crystal can be calculated from the curve or slant of the rows on the film. When a crystal is set the exposed film will show rows of spots known as layer lines. The distance between the zero and nth layer lines can be related to the length of the unit cell edge along the axis about which the crystal has been rotated by the equation :-

$$r = n\lambda / \sin \tan^{-1} (x_n / R)$$

r = repeat distance along the axis.

λ = wavelength of X-rays.

x_n = distance between the zero and n'th layer line.

R = radius of the camera.

A rotation photograph involved the same procedure only the crystal was rotated through as large an angle as was experimentally practical (a true rotation photograph involves rotation through 360°). The purpose of this was to give a more definite picture of the axis symmetry as not all reflections from a particular layer line are recorded on an oscillation photograph. All photographs were recorded on a Nonius integrating Weissenberg goniometer (Enraf-Nonius, Delft, Holland).

110

Once the length of one of the unit cell's edges had been measured, further crystals could be mounted about the other two axes to determine the remaining unit cell dimensions via the same method. There is however a method of determining these lengths from the crystal already mounted about the oscillation axis. This is the method of Weissenberg[73] (section 1.4.6). The difference between the oscillation and Weissenberg methods is as follows. Firstly screens are fitted (see figure 34[95]) inside the camera to isolate the zero layer line and only allow this to be exposed to the film. (If an oscillation photgraph were now taken only the zero layer line would appear).

Figure 34.
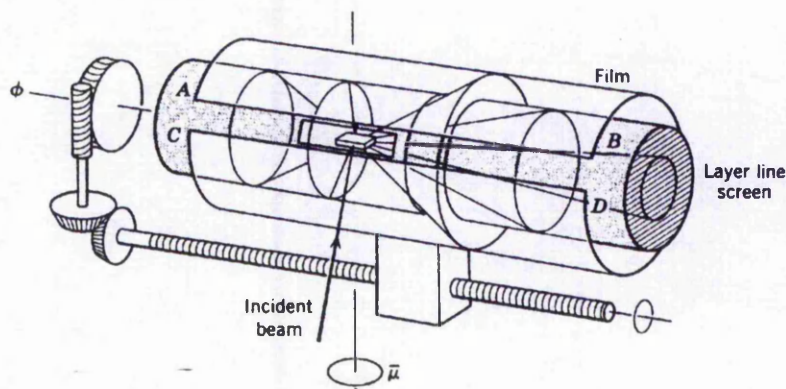
If the camera is now moved backwards and forwards past the slit in the screens whilst the crystal is rotated the spots of the zero layer line (containing spots from the other two dimensions) are spread into two dimensions on the film. This results in "festoons" of spots separated by straight lines of spots from the two axes whose lengths are to be measured. Using the formula :-

$$r = n\lambda / 2 \sin (x_n / R)$$

the two axis repeat distances can be calculated, where x_n = half the vertical distance on the film between two corresponding spots of index n. The angle between the two axes can also be calculated as the radius of the camera is chosen such that the distance

111

(in mm) between spots of equal 2θ is half the angle between the axes. For example if the distance between the axes is 45mm then the angle between them is 90°.

For space group determination the conditions of the indices resulting in diffraction are required. For this it is useful to have Weissenberg photographs of the first and second layers of the reciprocal lattice taken about the oscillation axis. To obtain these the equi-inclination Weissenberg method was used. This method is essentially the same as the zero layer method apart from the fact that the screens must be shifted to capture the relevant layer line and the camera is rotated through and set at an angle μ whose axis is perpendicular to both the crystal axis and the X-ray beam (see figure 34). The equations for calculating the μ angle the camera must be turned through and the distance the screens must be shifted by are given below:-

$$\mu = \sin^{-1} 1/2 \sin \tan^{-1} y_n / R$$

$$\text{screen shift} = r \tan \mu$$

where r = the radius of the screens (= 24.26 mm for the camera used).

Once the unit cell dimensions had been measured as accurately as possible and the space group had been determined via photographic methods then the intensity of the reflections had to be measured. This was done using a STOE Stadi-2 2-circle diffractometer.

2.11.4. Intensity data collection.

2.11.4.1 The 2-circle diffractometer.

The STOE Stadi-2 2-circle diffractometer is based on Weissenberg geometry and its operation for the measurement of the intensities of reflections is detailed below. Mo Kα ($\lambda = 0.7107$Å) X-radiation was used.

The diffractometer differs from the 4-circle in having only the 2θ and ϕ (ω) circles. To measure reflections from layers other than zero, the counter was moved by an equi-inclination angle (μ) to sweep out a different and smaller 2θ circle. The μ angle had to be set by hand for each new layer.

A scintillation counter was used for measuring the intensities of reflections. In this type of counter, the X-rays impinge on a suitable scintillator (a TlI crystal) and fluorescence is produced. This fluorescence is detected by a photomultiplier and converted into an amplified electrical pulse at the photomultiplier output. These pulses may then be fed into electronic circuits for amplification, selection and counting. The X-rays reaching the counter are controlled by two sets of slits (horizontal and vertical) and due to the sharp nature of the reflections observed in the crystals used in this work 1mm slits could be used.

The methods of setting crystals are essentially the same as for the 4-circle diffractometer; for a unique axis the 2θ circle is set at zero and a strong spot on this axis is selected and found by moving the counter through the calculated angle μ. The arcs are adjusted until maximum intensity is obtained at $\omega = 0°$, $90°$, $180°$ and $270°$. For a

non-unique axis, two strong reflections at fairly high θ values are chosen so that for each reflection one of the arcs is approximately parallel to the reflecting plane of the crystal; the one perpendicular to this is then adjusted until maximum intensity is obtained. After each adjustment the crystal is re-centred.

2.11.4.2. Scanning using the 2-circle diffractometer.

The diffractometer used was controlled by a PDP 8F Digital Equipment 4K computer, linked to a BBC Master series microcomputer, which would calculate the required 2θ and ω angles for any reflection and drive the circles to these positions. To do this the computer had to be supplied with the unit cell parameters, λ, and the axis about which the crystal was rotating. It also checked that the shafts of both circles executed a rotation angle equivalent to the number of degrees indicated by the computer register. Information from the counting chain was supplied to floppy disk via the two linked computers.

The type of scan used was variable ω scan. This method has the advantage of allowing for the fact that many reflections at low θ cover a large ω range, while those further out are generally smaller.

$$\Delta\omega = A + B \sin \mu / \tan \theta$$

A and B are constants put in at the start of the data collection and based on trial scans through a number of low-angle reflections. A is the minimum ω angle required to completely scan through high angle peaks and B the factor required to increase the scan width sufficiently to include the widest low angle peak. As θ gets smaller, $\Delta\omega$ clearly becomes larger.

The amount of time to be used for measuring the background intensity and the intensity at each step through the reflection, and the width in degrees of each step, were also inserted using a console command, before the continuous automatic operation was started. With the variable ω scan the total time used to scan a particular reflection was kept approximately constant by automatically reducing the step time for wider reflections.

2.11.5. Data manipulation.

Once the intensity data had been collected on 5¼ inch floppy discs the next stage was to convert the data from DFS to ADFS format. This was done using a BBC utilities program[96]. The ADFS data was then converted to IBM format using the BEEBDOS[97] program. Once the data was in IBM format it was transferred from 3½ inch floppy discs to the VAX mainframe computer using File Transfer Protocol. The data was then formatted for the data reduction program DATR[98]. The input file to DATR consisted of the intensity data headed by various factors pertaining to the specifics of the diffractometer and the console commands used during data collection. The output of the data reduction program (I and $\sigma(I)$ corrected for Lorentz and polarisation factors and placed on a common scale) was copied to the input file for SHELX76[77]. The SHELX76 program also requires an instruction file, the contents varying with the task being performed. The reflection data input file for the direct methods program MULTAN87[99] was obtained as follows:-

The SHELX program was run with the command LIST 3 to produce data corrected for absorption. The output file was used to run the local program MULTFORM to produce

the MULTAN data input file in which $F < 4(\sigma F)$ are flagged. MULTAN also requires an instruction file and this varied for each macrocycle. MULTAN consists of three separate programs and these were run in the sequence NOFI87a, LAST87, MAPS87.

The program DATR[98] (see section 1.4.9) is a data reduction program which applies Lorentz and polarisation factors to the data and places it on a common scale.

MULTAN87[99] is a direct methods structure solution program which applies the type of methodology discussed in section 1.4.10.3.

SHELX76[77] is an automatic structure solution program which combines all of the computational elements required to solve a crystal structure given a set of post data reduction intensity data. The elements include absorption correction, an (early) direct methods routine, least squares refinement and various Fourier syntheses.

CHEM-X[100] is a molecular modelling package which allows the refinement of structures (either built using the program or via imported atomic coordinates) against internal molecular mechanics parameters using a variety of routines.

3. RESULTS AND DISCUSSION.

3.1. Starting materials.

The starting materials outlined in the experimental section 2.1 were prepared in order to facilitate the synthesis of new thiophene based macrocycles.

3.2. [1+1] Macrocyclic Mannich bases derived from *N,N'*-dibenzylalkyldiamines.
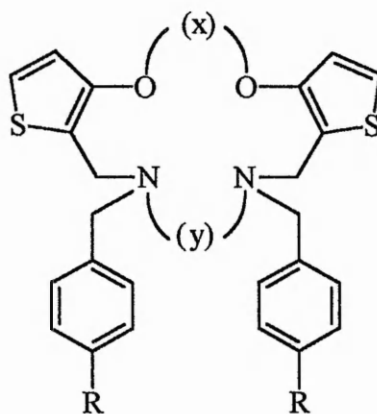
The term '[1+1] macrocyclic compound' refers to the macrocycle being formed from one 'unit' of each substrate. Previously[1], macrocycles prepared using the general method yielded oils when X = C_2, C_3, C_4, and C_2OC_2 and the diamine =

N,N'-dimethylethylenediamine and required column chromatography purification.

The general method was used but it was hoped introducing benzyl substituents would introduce crystallinity and avoid the need for column chromatography.

The introduction of benzylic substituents on the ring nitrogens had the desired effect for three of the macrocycles prepared. The compounds could be easily purified in reasonable yield and crystals obtained either directly or by dissolution in solvent mixtures. The failure of all of the three carbon bridged diamines to couple cleanly with

the bis ethers as well as the impurity of the C_4 and C_2OC_2 macrocycles derived from *N,N'*-dibenzylethylenediamine seems to suggest that the size of the bridges between the thiophene rings needs to be evenly matched for the reaction to proceed cleanly. As mentioned in section 2.2, the infra red spectra of the crude compounds indicate that the desired product is present via the shift in the C=C stretching frequency. However these macrocycles were not isolated via column chromatography as in the previous work by Chaffin[1] as the aims of this work were to eliminate the need for elaborate purification.

The structure of the C_2 and C_3 bridged macrocycles derived from *N,N'*-dibenzylethylenediamine were investigated via X-ray crystallography, see sections 3.11.2 and 3.11.1 respectively.

3.3. Templated [1+1] Mannich reactions.

In order to test the possibility of a metal template effect for the [1+1] macrocycles suitable metal salts were added to the reaction mixtures. Ba^{2+} was chosen as this was believed to increase the yield for the [2+2] reactions[1], Pb^{2+} as it has been shown[22,23] to act as a template for O_3N_2, O_6N_4 donor macrocycles via Schiff base condensations, and Fe^{2+} as it has been shown[101] to act as a template for a S_2N_3 quinquedentate macrocyclic complex.

i) Ba(NO$_3$)$_2$ template.

The reaction yielded an oil whose ^{1}H and ^{13}C NMR corresponded to the impure N_2O_3, N-methyl substituted macrocycle in no greater yield (taking into account loss on columning)[1] than the untemplated reaction.

ii) Pb(OOCCH$_3$)$_2$ template.

This reaction yielded an oil as in (i) in no greater yield.

iii) Fe(ClO$_4$)$_2$.6H$_2$O template.

The oil obtained was washed with acetonitrile to give a brown / black precipitate. The infra red spectrum of this was inconsistent with any macrocyclic complex the reaction was hoped to yield (see figure 35).

Figure 35.
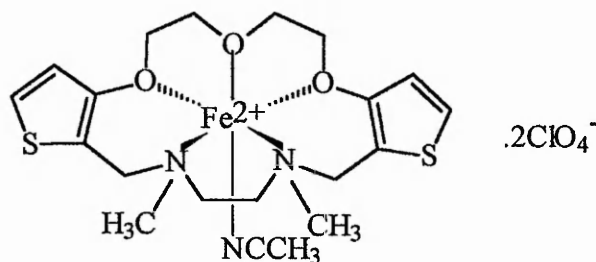
Polymerisation or the oxidising nature of Fe(ClO$_4$)$_2$.6H$_2$O probably thwarted macrocyclic complex formation.

Following the lack of any template effect a ^{1}H NMR study was undertaken.

^{1}H NMR study.

If any donor effect was occurring between the C$_2$OC$_2$ bridged bis ether and Ba^{2+} this would show up as shifts in the ^{1}H NMR spectrum of the bis ether. After the partition experiment no shifts in the CDCl$_3$ bis ether layer were apparent.

After the failure of the templated Mannich reactions to give any increased yield the 'metal ion' template effect was brought into question. This will be discussed later under 'Templated [2+2] Mannich reactions'.

3.4. Attempted alcohol based templated Mannich reactions.

As mentioned in the experimental section the NaOH neutralisation work up of the templated [1+1] reactions may not promote the isolation of the macrocycles as their metal complexes. Previously the Mannich reaction has been performed in acidic ethanolic solutions[102]. The isolation of any macrocyclic complexes would be far easier from ethanolic solutions via metathesis precipitation. Therefore in order to test that the work up wasn't responsible for the lack of a template effect attempts in ethanolic solution were made.

All attempts to promote the Mannich reaction under these conditions failed, yielding only starting materials.

3.5. [1+1] Schiff base condensations.

It was hoped that a new route to the [1+1] macrocycles incorporating two thiophene units could be via a Schiff base condensation between dicarbonyl compounds and ethylenediamine. The mechanism and characteristics of Schiff base condensations having been discussed previously in the introduction of this thesis. Two routes investigated were metal complex formation via templated reactions and condensation with subsequent reduction, see scheme II and III respectively.

Scheme II.

various conditions
$-2H_2O$

H_2N NH_2 $.nX^-$

$.nX^-$

Scheme III.

various conditions
$-2H_2O$

H_2N NH_2

reduction

—NH   NH—
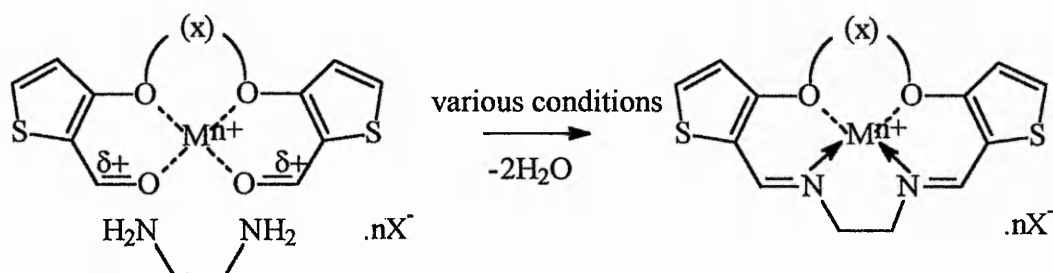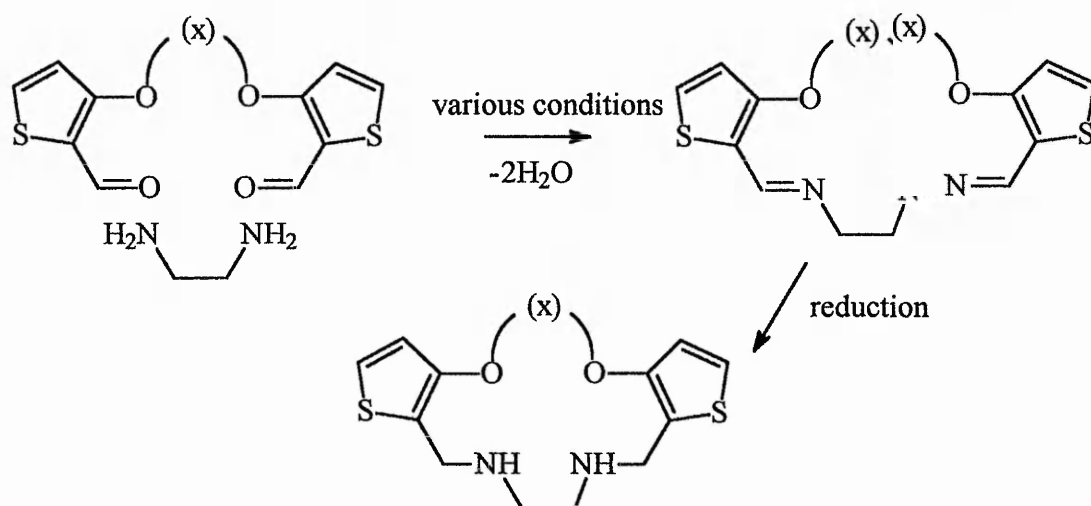
For the metal templated reactions the chosen metal salt should influence the geometry of the dialdehyde and the condensation product so that reaction with ethylenediamine yields macrocyclic products. The chosen metal may then induce a slight electrostatic interaction between itself and the carbonyl oxygen increasing the $C^{\delta+}=O^{\delta-}$ dipole therefore increasing the dialdehyde's susceptibility to nucleophilic attack by ethylenediamine.

3.5.1 Templated Schiff base condensations.

For condensations involving the dialdehyde (I), Ni^{2+} salts were chosen as templates as these have been shown (see introduction section 1.2.3) to be effective templates for the isolation of analogous benzene based diimine macrocycles.

i) A green precipitate was obtained on cooling and solvent volume reduction. No further analysis was performed upon inspection of its infra red spectrum. Only bands attributable to ethylenediamine and perchlorate modes of vibration were present. This coupled with the solution's colour change from green to blue on cooling suggests that on cooling $Ni(en)_2(ClO_4)_2$ is formed, (see ligand redistribution experiment), possibly from hydrolysis of the macrocyclic complex, this precipitates out as a non stoichiometric $Ni(en)_x(ClO_4)_2$ complex. When the reaction was repeated at ambient temperature with a two fold increase in solution volumes (to ensure dissolution of the dialdehyde) a green precipitate with a comparable infra red spectrum was obtained.

ii) The change in solvent and anion did nothing to stop the eventual formation of a $Ni(en)_xCl_2$ salt.

iii) The partition experiment showed that no $Ni(OOCCH_3)_2$ had been transferred to the dialdehyde containing DCM layer.

iv) In this experiment a 2:1 dialdehyde to diamine / metal ion ratio was used. This was hoped to ensure complete condensation and avoid the formation of metal diamine complexes. However the extended reaction time and presence of an acid catalyst seems to have yielded a mixture of products. The metathesis isolation procedure will only

precipitate ionic complexes. From the infra red spectrum instead of simply forming the [1+1] macrocycle leaving the excess dialdehyde in solution (as hoped), the excess dialdehyde has promoted the formation of two complexes.

The lack of N-H str's in the spectrum indicates full condensation of ethylenediamine but the presence of a carbonyl stretching mode as well as the two imine stretching modes suggests the presence of the [2+1] and [1+1] complexes (see figure 36)

Figure 36.

a)   b)
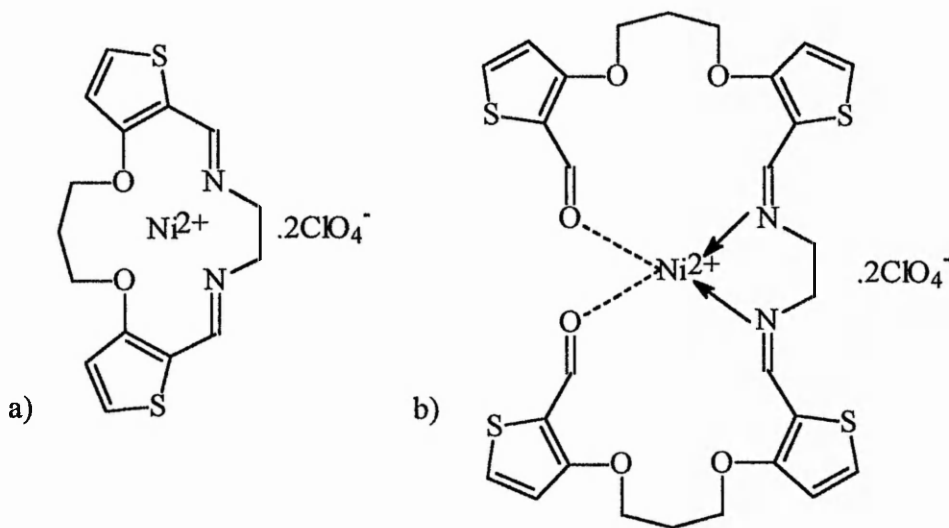
The formation of two complexes is also hinted at by the presence of two C=C str modes (1535.1 and 1518.8 cm^{-1}). The weak coordinating properties of the ClO_4^- anion are also shown in the spectrum. The γ_3 and γ_4 perchlorate modes show as single absorptions at 1087 sh and 622.4 m cm^{-1} typical of complexes containing ionic perchlorates[103].

The presence of a mixture hinted at by the product's infra red spectrum, which would be difficult to separate, meant that no further investigation was made.

Fe²⁺ templated reaction with the dialdehyde (II).

As perchlorate ions are only weakly coordinating the reaction was carried out in the solvent acetonitrile which can act as a monodentate ligand. From 0.556g (1.0eq) of iron (II) perchlorate hydrate a red / brown precipitate was obtained in 0.13g yield. On standing the filtrate gave yellow crystals in 0.30g yield.

From the infra red spectrum of the first red / brown precipitate it is obvious that although the addition of ethylenediamine was slow considerable polymerisation has occurred. No further analysis was carried out. When the experiment was repeated with slower addition of the en solution (ca. 0.33ml min⁻¹) polymerisation was still evident.

The second precipitate obtained on the filtrate standing showed a 'clean', sharp infra red spectrum. The spectrum shows one strong C=N str and a single C=C str however the presence of two N-H str's brought into doubt the macrocyclic nature of the complex.

The infra-red and ¹H NMR data corresponds to the desired macrocyclic complex (see figure 37) however there are lesser peaks corresponding to carbonyl, carboxylic (iron (II) perchlorate is oxidising) and hydroxyl protons (br). From the peak integrals the macrocyclic complex is present in ca.70% with the other 30% probably consisting of the open chain condensates and the macrocyclic aminol (hydrolysis intermediate). This accounts for the two peaks in the infra red spectrum initially assigned as two N-H str's but which can now be assigned as a O-H and N-Hstr's. The presence of unidentate and ionic perchlorate modes is also indicative of this complex formation (one perchlorate ion coordinating in the remaining axial site of the metal ion's octahedron). The complex could not be purified any further via recrystallisation.

Figure 37.
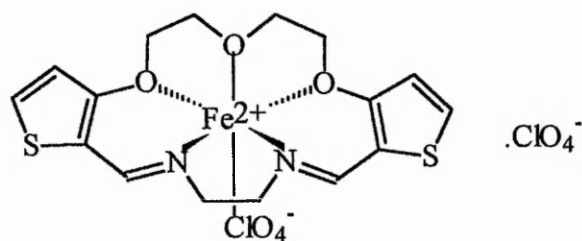
3.5.2. Non templated Schiff base condensations.

The many attempts made at condensation in the absence of a template gave at best mixtures of the macrocyclic imine and 2° amine (from condensation / in-situ reduction reactions) obtained as oils as the macrocyclic diimines could not be isolated without hydrolysis occurring.

3.6. Schiff base condensation + metal complexation.

For these reactions it was hoped that the hydrolysis of any macrocyclic diimine ligands might be prevented by the addition of a suitable metal salt to coordinate the macrocyclic ligand.
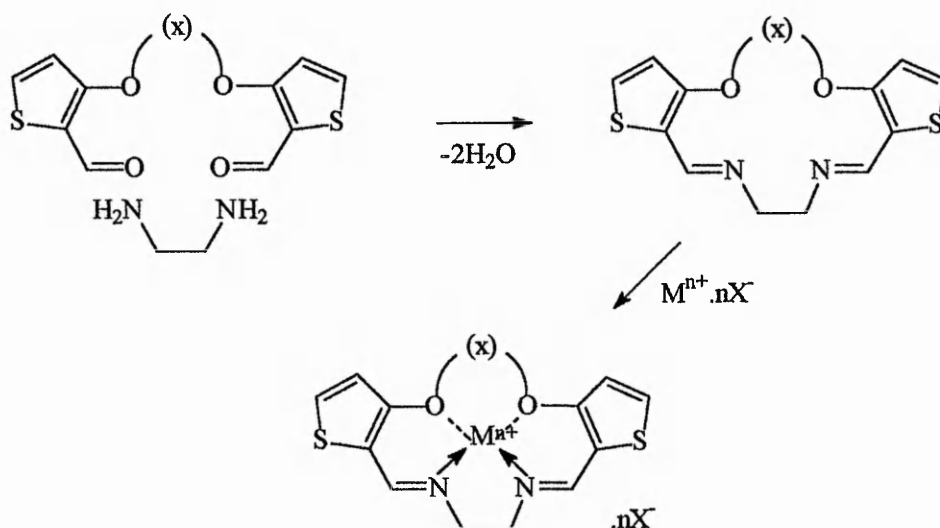
i) The light brown precipitate after drying weighed 0.21g (28% $NiC_{15}H_{16}O_2N_2S_2Cl_2$), M.P = 177.8°C (decomposition).

ii) The light green precipitate after drying weighed 0.32g (52% $NiC_{15}H_{16}O_{10}N_2S_2Cl_2$), M.p = 162.7°C decomposition.

After the promising appearance of the infra red spectra of the two products the microanalytical results came somewhat as a surprise.

Trying to explain the unexpected results the purity of the starting materials was investigated. The ethylenediamine used had been redistilled and the Ni^{2+} salts were fresh from the manufacturer. On re-inspection of the infra red spectra of the C_3 and C_2OC_2 bridged dialdehydes a rogue peak was found at 3252 and 3271 cm^{-1} respectively. These were of weak intensity and are undoubtedly N-H str peaks as a N-H bend is also present as a very slight shoulder on the right of the carbonyl peak in both spectra.

In the formylation reaction dimethylamine is formed and although both the dialdehydes were recrystallised, dimethylamine seems to be present either as its salt or hydrogen bonded between the two aldehyde groups. This interaction must be strong if dimethylamine is present in its free form owing to the high volatility of dimethylamine. The presence of this amine in one form or another has probably contaminated the metal complexes either via coordination (however only in very small amounts as no N-H str are present in the products spectra) or by reaction with the dialdehyde in the presence of

counter ions to produce the iminium salt (as in figure 38). This cannot react further to the enamine due to the lack of a hydrogen on the thiophene C_2 carbon.

Figure 38.
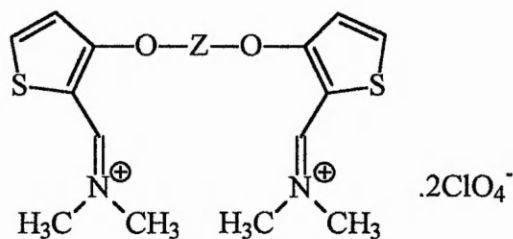
iii) On inspection of the product's infra red spectrum no further investigation was undertaken. This showed significant broadening in the 3300-3000 cm^{-1} region and remaining uncondensed C=O str.

iv) Reduction procedures.

Following the characterisation problems encountered above the ClO_4^- countered complex (ii) above was reduced and the reduced ligand isolated. The product's infra red and NMR spectra confirm the presence of the expected diimine ligand in the pre-reduced Ni^{2+} complex by the confirmation of the reduced ligand's structure:-
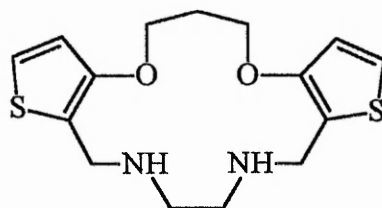
The oils infra red spectrum confirms imine reduction by the presence of a N-H str at 3311cm^{-1} and a shift in the C=C str to 1556cm^{-1}. The NMR data was also in agreement with the proposed structure above.

Although the metal '2N,2O' donor diimine complex is contaminated the reduction and isolation of the ligand gives indirect evidence of the reaction's success. The success of these reactions over the Ni(II) templated Schiff base condensations seems to indicate that the metal ion is sequestering the pre-condensed diimine macrocycle and is therefore acting as a thermodynamic rather than a kinetic template. The small yields involved meant that no further action was taken.

v) The turquoise precipitate after drying weighed 0.58g (76% $CoC_{15}H_{16}O_2N_2S_2Cl_2$), M.P = 189°C decomposition.

vi) The green precipitate after drying weighed 0.42g (84% $CoC_{14}H_{14}O_2N_2S_2Cl_2$), M.P = 198°C decomposition.

The two cobalt complexes described above were not investigated further due to the probable contamination of the preceeding dialdehydes.

3.7. New route to 2'O', 2'N' donor macrocycles.

In order to obtain macrocycles via Schiff base condensations a new route was sought which didn't put such strain or conformational constraints on the imine bond formation. This involved reacting 3-methoxythiophene-2-carbaldehyde or 3,4-dimethoxythiophene-2-carbaldehyde with en in a 2:1 ratio. An alternative method of isolation was introduced to reduce imine hydrolysis. This involved kinetic quenching rather than leaving the reaction mixtures to cool and hydrolyse. The diimine compounds obtained would then undergo reduction and attempted demethylation to obtain the

acyclic dihydroxy compounds. If obtained these would then be cyclised via Williamsons ether synthesis.

i) *In-situ* reduction.

This reaction prompted the following series of reactions. The resulting oil following condensation and reduction was obtained in 52% yield.

The infra red data clearly showed complete reduction of the diimine. The number of aliphatic C-H str's had also increased compared with the original aldehyde as expected.

^{1}H. ^{13}C NMR data.

The spectrum was run three days after the oil was obtained and showed significant decomposition. Demethylation was not attempted.

ii) Imine isolation.
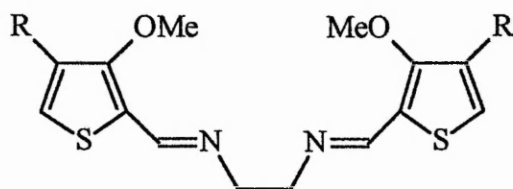
a) The resulting *N,N'*-ethylenebis(3,4-dimethoxythiophene-2-aldimine), R = OMe, was obtained as a white solid in 52% yield after drying. M.P (°C) = 134.9-135.8.

b) The resulting *N,N'*-ethylenebis(3-methoxythiophene-2-aldimine), R = H, was obtained as an off white solid in 70% yield after drying. M.P (°C) = 173.6-174.8.

Crystals suitable for X-ray analysis (section 3.11.3) were obtained and their infra-red spectrum and microanalyses confirmed the crystals were of the intact diimine.

iii) <u>Reduction.</u>
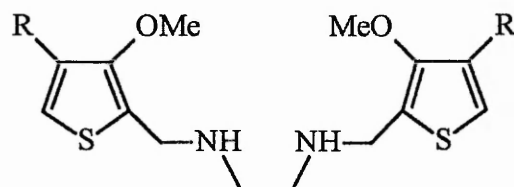
Having successfully isolated the acyclic diimines the reduction of the 3-methoxy compound was undertaken, R = H. After acidic extraction purification the product was obtained as an oil in 65% yield.

iv) <u>Demethylation.</u>

After the successful isolation of the di-2°-amine demethylation was attempted immediately after isolation. The oil obtained decomposed.

The instability of the oil obtained from the *in-situ* condensation and reduction experiment has been mentioned. This with the known instability of 3-hydroxy thiophenes halted any further investigation.

However although it wasn't investigated, it should be mentioned that possibly the demethylated compound could be stabilised by coordination via reaction with Ni^{2+} under basic conditions as shown in figure 39.

Figure 39.
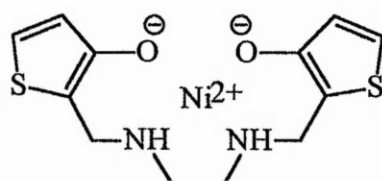
3.8. Templated [2+2] Mannich reactions.

In the numerous reactions involving the complexes, formaldehyde and the C_2OC_2 bridged bis ether nothing but starting materials were obtained. This coupled with the failure of the attempted [1+1] templated Mannich reactions brings into question whether it is in fact the presence of the metal which is templating and increasing the yield in the formation of the macrocycles shown in scheme V[1].

The yield of (X) when the reaction was carried out in the presence of acetate salts of Na^+, Ni^{2+}, Pb^2, and $AgNO_3$ was between 32 and 35% similiar to that of high dilution[1]. When $BaCO_3$ was used the yield increased to 43%.

Scheme V.

(X).
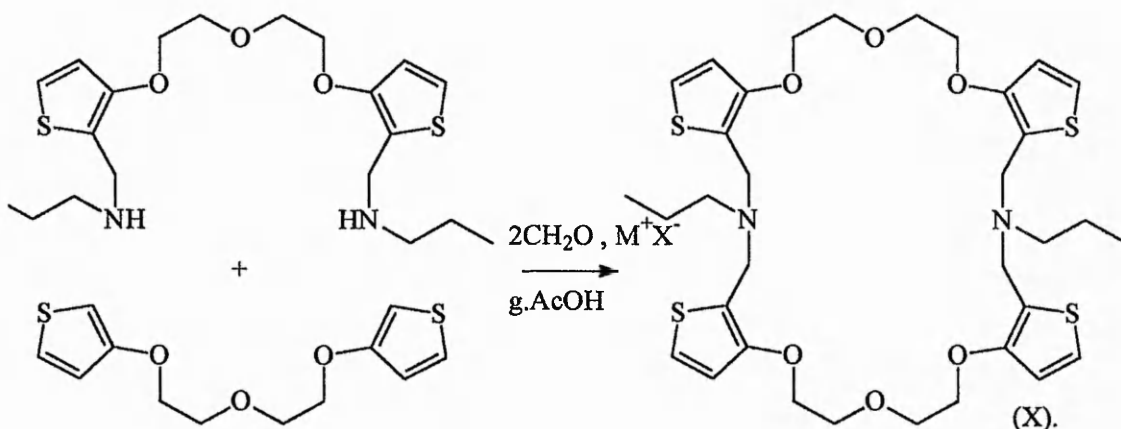
It is suggested that the increased yields are due to anion association with the $R_2N^+{=}CH_2$ moiety rather than any metal ion effect. The vastly differing sizes and properties of the metal ions means that if the effect is due to the cation acting as an internal template the yields would be expected to vary greatly too. The idea that the metal ion is acting as a template is fundamentally flawed for these reactions as the cation will repel or discourage the formation of the intermediate $R_2N^+{=}CH_2$ ion.

Concluding that the anion is responsible for the increased yield, then the greatest yield from the carbonate salt is not surprising as this may bridge the two nitro positive groups arranging them in the correct geometry for further reaction as shown in Figure 40.

<u>Figure 40.</u>
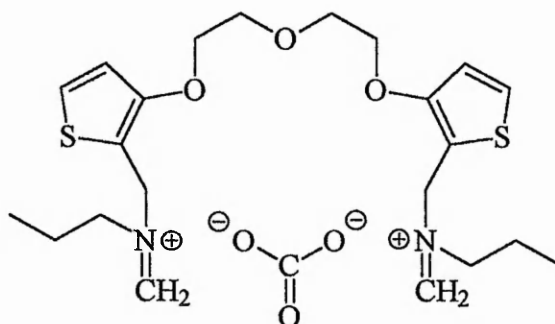
The carbonate ion is shown in one of its canonical forms.

The author suggests using smaller metal carbonates may increase the yield further.

3.9. Templated [2+2] Schiff base condensations.

Metal diamine complexes have been used as templates for the formation of a wide variety of macrocyclic metal complexes via Schiff base condensations[16,104]. It was hoped that the reaction of the dialdehydes (I) and (II) with labile metal diamine

complexes would proceed stoichiometrically to yield the [2+2] macrocycles as shown in scheme VI.

Scheme VI.
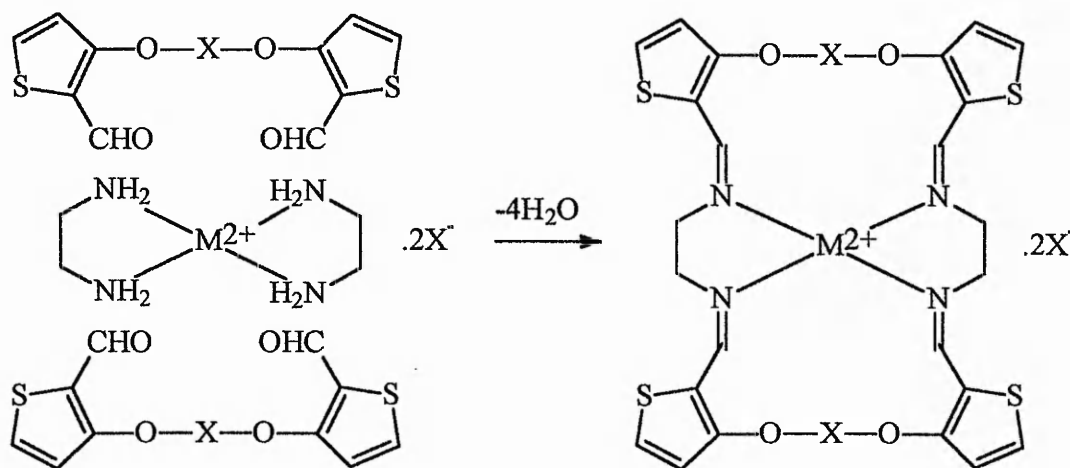
i) On metathesis with sodium perchlorate an olive green powder was obtained.

Yield = 44% *. M.P = 148°C.

*based on en / dialdehyde, 2:1 condensation.

The characterisation results seem to indicate non-stoichiometric condensation and when further studies were attempted in solution hydrolysis of the complex occurred.

ii) On metathesis with sodium perchlorate an orange powder was obtained.

Yield = 19% *. M.P = 158°C decomposition.

* based on en / dialdehyde , 2:1 condensation.

From the characterisation results and as discussed earlier the contamination shown in the dialdehyde's infra red spectrum has probably contaminated the metal complex.

133

The infra red spectrum of the oil obtained from the reduction of the complex shows that a thiophene containing amine compound (from reduction of the imine) has been prepared but the presence of two (well separated) N-H str and the shoulder on the thiophene C=C str suggest a mixture of products and therefore probably the non-stoichiometry of the preceding complex.

iii) On metathesis with sodium perchlorate a red powder was obtained.

Yield = 35% *, M.p = 154 °C decomposition.

*based on en / dialdehyde, 2:2 condensation.

Although the metal complex could not be fully characterised the isolation of the reduced macrocyclic ligand ([1+1] or)‡ [2+2] as an oil is indirect evidence of the formation of the imine macrocyclic complex and suggests it is contamination of the metal complex which gives the unexpected microanalytical results.

‡Cannot be ruled out see experimental page 96.

iv) When the three reactions above were refluxed for two hours rather than stirring for 24h the products obtained on metathesis with sodium perchlorate were of a polymeric nature (deduced from their infra red spectra).

v) In this transmetallation experiment with $AgNO_3$ and the product from (i) a light brown precipitate was obtained. Only the product's infra red spectrum was obtained but this suggests that the silver ion has sequestered a macrocyclic product from the (previously mentioned) non-stoichiometric copper(II) condensate (i).

The lack of N-H str's which were present in the Cu^{II} condensate and the influence of the softer metal ion raising the C=N and C=C str's led to this assumption. No further analysis (via complex reduction and ligand isolation) was carried out due to the small yields involved.

vi) On cooling a red / brown crystalline solid was obtained.

Yield = 65% *, M.P = 169°C decomposition.

* based on en / dialdehyde, 2:1 condensation.

The above complex was also obtained when the experiment was repeated with 3.2eq of the dialdehyde. From the products infra red spectrum there seems to be a mixture of products or a single open chain condensate (two thiophene modes and N-H str's).

vii) The inability to prepare Ni(en)$_2$(ClO$_4$)$_2$ led to a ligand redistribution, condensation experiment. On cooling a very small amount of an orange / brown powder deposited. Attempts to isolate further product all failed (see experimental).

Assuming the product to be the [2+2] complex from consideration of the infra red data the sample was sent for microanalysis. The results were not in agreement with the [2+2] macrocyclic complex.

viii) The ligand redistribution / condensation experiment failed to yield any precipitate. On transmetallation with an excess of AgNO$_3$ a light brown precipitate was obtained.

The characterisation difficulties incurred with these complexes and the small yield meant that further characterisation was abandoned.

ix) The product of this ligand redistribution / condensation experiment gave exactly the same infra red spectrum as the product obtained by metathesis in experiment (ii) in slightly higher yield: 24%.

x) The change of solvent and addition of Na_2SO_4 as a drying agent in this repeat of procedure (iii) yielded an oil in no greater yield, which when characterised by NMR corresponded to the same [1+1] or [2+2] 2°-amine macrocycle.

xi) The pH adjustment to 9 failed to influence the formation of the [2+2] macrocycle. The green precipitate's infra red spectrum showed N-H and C=O str's from incomplete condensation. The only other products isolated were $Ni(en)_3Cl_2$ and the dialdehyde (I).

The infra red spectra of the metal complexes obtained from these attempts (i,ii,iii,v,vi,vii,viii,ix,x) to yield the [2+2] macrocyclic complexes are all very similar and highly characteristic. The bands associated with the condensed dialdehydes are easily detected.

The main problem associated with these reactions was the characterisation of the complexes as they either hydrolyse in the solvents used for NMR analysis or the spectra are too broad for interpretation due to paramagnetism.

Although the microanalysis results do not conform to the predicted structures no ash analyses were performed which is often required when samples contain metals. Another likelihood is that the metal complexes were contaminated with / or by reaction with dimethylamine or its acetate salt which was found as slight contamination in the precursor dialdehydes.

The reader may question the validity of attempting to coordinate such large ring systems around such relatively small Cu(II) and Ni(II) centres but these attempts are not without precedence as a similar Ni^{2+} N_4,O_4 macrocyclic complex[105] has been prepared and its structure determined by X-ray diffraction, showing the coordination of only the N-donors.

The isolation of the reduced macrocycles from experiments (iii) and (x) and the previously discussed [1+1] condensations are evidence that the macrocyclic imine is present in these metal complexes, however the oily nature of the macrocycle defeated the aim of obtaining crystalline macrocycles for further work.

3.10. Further approaches.

3.10.1. Ni(II) complex of methyl 3-hydroxythiophene-2-carboxylate. (Ni [O.L]$_2$).
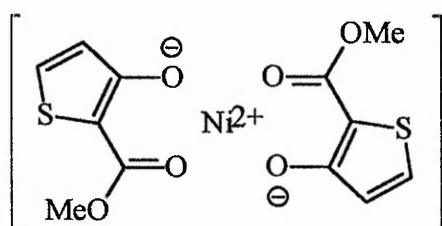
In order to reduce the number of steps required to produce macrocycles from methyl 3-hydroxythiophene-2-carboxylate, a number of reactions were attempted coupling two

equivalents of this compound with one of 1,3-diaminopropane. Reactions in DMF, ethyleneglycol or diethyleneglycol all failed to produce any of the desired diamide or gave only decomposition products. In order to increase the reactivity of the carbonyl carbon via a greater dipole between the carbon and oxygen atoms the Ni(II) complex was prepared.

The complex was obtained as a green solid in 90 – 99% yield after drying. M.P = > 250°C.

The C=O and C=C bands in the infra red spectrum can be contrasted with those of the free ligand (cm^{-1}); C=O = 1670, C=C = 1548. The OH stretching frequency of the free ligand is also absent in the spectrum of the complex. It should be noted that *before* drying at 130°C a sloping shoulder 3300-3100cm^{-1} and a sharper shoulder on the C=O str at $\approx$ 1600cm^{-1} occur in the products infra-red spectrum. These probably arise from associated water molecules.

During the preparation it was noted that on the addition of the methanolic methyl 3-hydroxythiophene-2-carboxylate solution to the solution of nickel(II) acetate a precipitate started to form before the addition of the NaOH solution. Although the addition of NaOH was gradual and the solution was stirred throughout, the microanalysis results seem to indicate that the product is non-stoichiometric and possibly contains both the 1:1 and 2:1 products. The compound was not characterised further as the purpose of increasing the electropositivity of the carbonyl carbon is fulfilled in either case. Also the experiments for which the compound was prepared for

138

would involve the decomplexation of any ligands after reaction, therefore the fact that there may be one or two complexed to the metal centre becomes irrelevant. The probable octahedral coordination sphere of the Ni(II) ion from the magnetic moment measurements may seem unexplainable in the light of the absence of solvent molecules (from the infra-red and microanalysis results), however as was mentioned in the introduction (section 1.2.3) Ni(II) complexes with bidentate O⁻ ligands have been shown[29] to stack giving the Ni(II) ion an octahedral coordination sphere.

3.10.2. Ni(II) complex of 3-hydroxythiophene-2-carbaldehyde.

This complex was prepared in the same way as the one described above. Only the compound's infra-red spectrum was obtained for analysis due to the small amount of material available. The complex was not used in any further experiments.

Yield = 0.062g (46%).

3.10.3. Reactions of Ni[O.L.]$_2$ with various amines.

These experiments were intended to produce amides with terminal functionalities which could then be self condensed to produce the trans-amide macrocycles as in figure 41.

Figure 41.
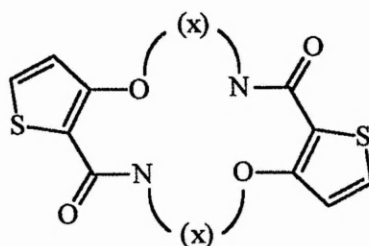
In a series of reactions the following amines were reacted with the Ni[O.L.]$_2$ complex under a variety of conditions with various solvents: $CH_3(CH_2)_2NH_2$, $Br(CH_2)_2NH_2$, $Br(CH_2)_3NH_2$.

The reaction of n-propylamine with the Ni(II) complex in acetone gave a green resinous solid upon work up. This test experiment showing signs of reaction led to the employment of more useful terminally functional amines. The reaction of the bromo functionalised ethyl- and propyl- amines did not lead to the desired amide compounds, however the results of one experiment were of some interest:-

In one experiment, 2-bromoethylamine was reacted with the nickel complex in DCM. After two hours a light green precipitate was filtered from the solution. (The green filtrate was later evaporated). From the precipitate's I.R spectrum which resembled the original complex with additional N-H modes at 3312, 3221(split), 3150 and 1596(bend) cm^{-1}, ether coupling between the O$^-$ and Br atoms was assumed. To test this assumption the precipitate was dissolved in methanol and three equivalents of NaSCN were added and the mixture heated. The assumption was that if the ether had been formed, the ligand(s) would be neutral and the charge of the Ni(II) ion countered by the two displaced Br anions. These would then be displaced via metathesis with the SCN$^-$ anions which would be detectable via infra red spectroscopy. When the precipitate was recovered from the SCN$^-$ containing solution no modes from these anions were evident. The precipitated complex was therefore assumed to be the original complex with the bromoalkylamine coordinated to the metal ion, not having reacted with the ligand. To check the assumption the remaining filtrate was evaporated to give a small amount of a slightly darker green complex. This was digested in hot 4M HCl, the residual precipitate

discarded, and the solution neutralised, extracted and evaporated to give a very small amount of a brown precipitate. If the precipitate from the filtrate were the bromoalkylamine adduct as assumed for the original precipitate the compound obtained after the digestion procedure should be the ligand from the starting complex, (O.L); methyl 3-hydroxythiophene-2-carboxylate. Although only the compound's infra-red spectrum was obtained (due to the small amount of material) this was significantly different from that of methyl 3-hydroxythiophene-2-carboxylate. The major peaks were N-H stretches at 3276 and 3176 cm^{-1} and a C=O str at 1642 cm^{-1}. The lack of an OH str and the uniqueness of the spectrum could lead one to presume that this is the ether bridged compound (which was as desired as the amide the reaction was hoped to produce). Without further evidence however this is only conjecture and the small yield meant that further methods had to be investigated.

The nickel complex Ni[O.L.]$_2$ was reacted with ethanolamine as solvent. After acidification, neutralisation and extraction of the reaction mixture the desired amide was obtained in 5% yield:
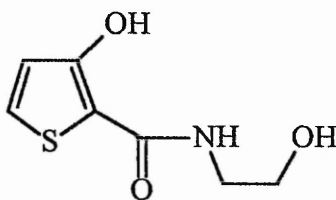
The ^{1}H NMR data prior to D$_2$O presented in section 2.10.3. requires some explanation. The Th-OH peak occurs at such a high δ due to hydrogen bonding. The peak from deuterated DMSO occurs at δ 3.40 whereas this usually occurs at δ 2.49. This shift is probably due to 'hydrogen' bonding[106] and this probably accounts for the methylene

protons occurring as singlets too. These effects are removed upon the addition of D_2O and the spectrum in this solvent is as expected with the OH and NH groups being deuterated.

Due to the low yield, long reaction time and the excess of reagent required to produce the amide above this approach was discontinued.

3.10.4. *N*-(3-bromopropyl)thiophen-2-aldimine.
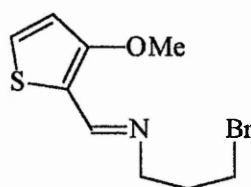
The compound was obtained in 72% yield as an oil.

Due to time constraints this compound was not reduced to the 2° amine, demethylated and self condensed as intended.

3.11. X-Ray Crystallography.

3.11.1.   13,16-dibenzyl-2,6-dioxa-10,19-dithia-13,16-diazatricyclo[16.3.0^{7,11}]heneicosa-1^{18},20,7^{11},8-tetraene. (M1).

3.11.1.1. Crystal morphology.

Good quality crystals were obtained directly from the reaction work up and no recrystallisation was necessary. The crystals have a needle type habit and photographs taken using a polarising microscope plus a computer drawn representation of their morphology[107] are shown in figure 42.

Figure 42.
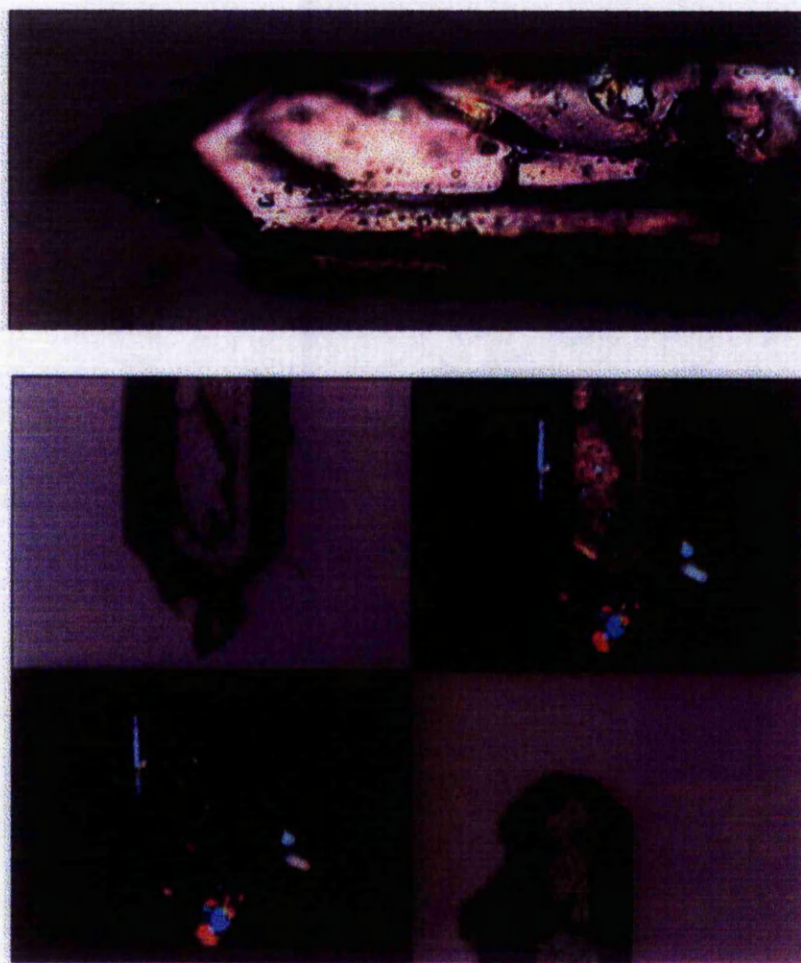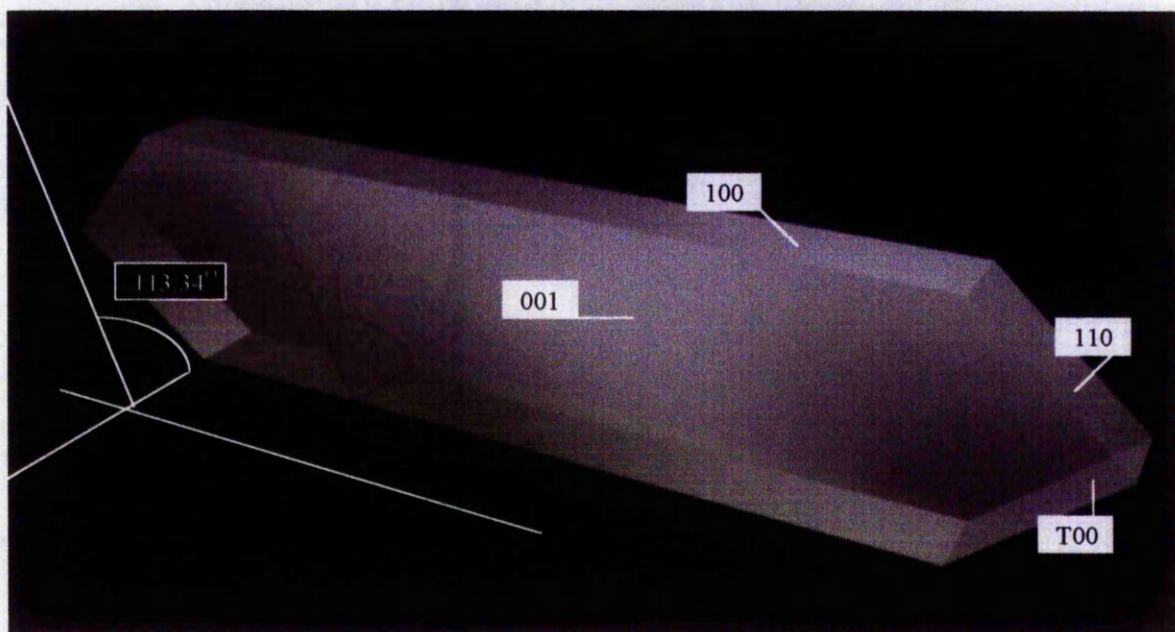
Using the polarising microscope, extinctions were observed on the 001 and 00T faces every 90° parallel and perpendicular to the longest crystal edge, see one of these before and during extinction in figure 42. After obtaining X-ray photographs the crystal axes and faces were assigned. As can been seen from the diagram above the unique b-axis runs parallel to the length of the crystal needle. The angle β, which was later measured at 113.34° can be seen from the photograph looking on to the 110 and T10 faces and measurement from this gives reasonable agreement. The crystal habit points to a monoclinic space group and this was later confirmed via X-ray photographs.

After studying a greater number of crystals it became apparent that there were two distinct types. As well as crystals possessing the morphology described above, a second type having similar needle type habit were observed. These crystal's habit is essentially the same as those above, the difference being that the 100 and 001 faces are interchanged. The crystals viewed as in the computer generated drawing above thus appear broader than they are deep. The interchanging of the a and c axes was confirmed via X-ray photographs. Crystals of this type were not used for intensity data collection.

3.11.1.2. X-ray photographs.

After examination of the crystals under the polarising microscope a crystal was mounted on a glass fibre along the length of the crystal needle to coincide with the observed extinctions. The crystal was then mounted on a set of arcs and oscillation and Weissenberg photographs taken as detailed in the experimental section.

Approximate cell dimensions were obtained.

The systematic absences observed on the zero layer Weissenberg photograph about the b axis conform to the condition h0l for l = 2n-1, i.e only spots of l = 2n occur on the photograph. This showed as the 1st and 2nd layer photographs having twice as many festoons of spots about the c axis. The condition above limits the choice of space groups to Pc, P2/c and P2$_1$/c. The Weissenberg photograph about the c-axis although of poor quality showed a further limiting condition 0k0 for k = 2n. This was later confirmed during intensity data collection and unambiguously defines the crystals as belonging to the space group P2$_1$/c.

145

3.11.1.3. Density measurement.

The density was measured using the method described in section 2.11.1. The solvents used were methanol and chloroform. Density = 1.30 g/cm^3.

3.11.1.4. Intensity data collection.

A good quality crystal having the morphology shown in section 3.11.1.1 was chosen and mounted on a set of arcs along its b axis. The crystal was approximately set via an oscillation photograph and then transferred to the 2-circle diffractometer. The crystal was then centred and set using the diffractometer. The cell dimensions were adjusted to give the centring, i.e. maximum intensity of some chosen reflections and the cell dimensions used for data collection were :-

a = 12.5043(1)Å, b = 11.2994(1)Å, c = 19.8022(2)Å, β = 113.34(2)°.

Intensity data was collected for five layer lines but due to very hot weather the temperature in the laboratory got so high after this that the wax with which the glass fibre was mounted on the arcs, softened so much that the crystal became misaligned. The crystal was removed from the arcs and the fibre 'super-glued' to a stud, the stud attached to a set of arcs, and the crystal reset. Intensity data was recollected up to the seventh layer line. At this point the crystal showed signs of deterioration due to the amount of X-radiation the crystal had been exposed to. Another crystal possessing the same morphology was chosen and mounted, adjusted and set as before. Intensity data for the 8th, 9th and 10th layers was collected from this crystal.

Both crystals gave extremely sharp reflections (occurring within < 0.1° (ω)) which meant that 1mm slits could be employed for the counter and the unit cell dimensions could be refined to a high degree. A standard was measured every 10 reflections (different standard for each layer line).

3.11.1.5. Data manipulation.

Once the intensity data had been collected it was transferred to the VAX mainframe computer as described in section 2.11.5. The data reduction program DATR[98] corrected the data for Lorentz and polarisation factors and placed data from each layer line onto a common scale by reference to the intensities of the standard reflections.

This file was then used as the input file for the structure solution program SHELX76[77] as described in section 2.11.5. Section 2.11.5. also describes the manipulation of this file via SHELX76 and MULTFORM to provide the respective input file for the direct methods program MULTAN87[99].

3.11.1.6. Structure solution.

The structure was solved using the SHELX76 and MULTAN87 programs. Patterson methods were attempted first to try and locate the two sulfur atoms. Interpretation of the Patterson maps proved difficult and no obvious molecular fragments were obtained from the SHELX76 direct methods routines hence the decision to use the direct methods program MULTAN87 was made. Interpretation of the Patterson synthesis was undertaken after the structure had been solved and will be discussed in section 3.11.1.6.4.

3.11.1.6.1. Direct methods.

MULTAN87 was run using the MULTAN.CDR command file which contained the cell data, centrosymmetric nature of the space group, symmetry operators, cell contents (atom types and numbers), and the format of the input file. Maps of the three best solutions (as designated by MULTAN) were plotted. The solutions have RESID(ual) values which are similar in nature to the R factor explained in section 1.4.12. The three solutions had RESID values of 29%, 27% and 16%. The map of the solution with the 16% residual showed peaks which when appropriately connected resembled part of the macrocycle (one thiophene ring and one benzene ring with connecting atoms). The MULTAN87 program also described this as the 'true solution' via the programs protocol (figures of merit *psi (zero)* and *residual* below 1.25 and 20.0 respectively). The next stage was to enter these atomic positions into the SHELX76 program to see how they refined via least squares.

3.11.1.6.2. Atom finding.

The program SHELX76 was used for refining the structure via least squares and for atom finding via Fourier difference maps. The program was also used to apply an absorption correction (μ) to the data. For this the crystal dimensions are required and at this stage of the refinement measurements from the first crystal used in the intensity data measurement were used since there is no provision in the program for using more than one set of dimensions. Later the average (0.7 and 0.3 contribution from the respective crystals) crystal dimensions from both crystals were used. The program requires the measurements in terms of the distance's from the centre of the crystal to particular faces. For this the crystal(s) was approximated to be a parallelepiped with major faces (100), (010) and (001) and dimensions $0.62 \times 1.42 \times 0.23$ mm.

SHELX was run for four cycles of least squares using atomic coordinates taken from the MULTAN run and omitting any data where $F_{obs} < 3\sigma(F_{obs})$.

One sulfur atom (S1), seven carbon atoms (C1...C7), one nitrogen atom (N1) and one oxygen (O1) atom were included at this stage, all with isotropic temperature factors fixed at 0.05. Overall Scale = 1.94904 (from MERG command). $\mu = 1.93$ cm^{-1}. The least squares refinement of the positional and isotropic temperature factors used 3241 reflections and the R value reduced from 0.7040 to 0.5622 after four cycles of least squares refinement. For the next run the coordinates of the highest peak off the difference map were assigned as the second sulfur atom (S2), the coordinates agreed with the highest peak not so far included from the MULTAN run. As before the temperature factor was fixed at 0.05. The coordinates of the other atoms were left as in the first run i.e. the values after refinement were not substituted. The R value dropped from 0.6190 to 0.4988 after four cycles of least squares. The resulting difference map was plotted and the four carbons of the second thiophene ring (C8, C9, C10, C11) were located. Their coordinates were added to the input file (all temperature factors = 0.05) along with the new coordinates of the other atoms obtained from the last cycle of least squares refinement (temperature factors all fixed at 0.05). The R value fell from 0.5947 to 0.4779 after four cycles. The difference map was plotted and the remaining five carbon atoms of the first benzene ring (C12, C13, C14, C15, C16) were located and their coordinates were added to the last instruction file without any of the previous atom coordinates being updated. All temperature factors were initiated at 0.05. The R value fell from 0.5627 to 0.4420. The R value was rather disappointing considering the number of atoms (20) now included but the refinement was continued as meaningful

structural fragments were being located, also the structure contains 32 hydrogen atoms. The difference map was plotted and the second benzene ring was located (C17, C18, C19, C20, C21, C22). The coordinates were added to the input file in the same manner as the last run. The R value dropped from 0.5256 to 0.3912. The difference map was plotted and the two carbon atoms between the nitrogen atoms (C23, C24), the second nitrogen atom (N2) and the second benzylic carbon (C25) were located. The coordinates were added as before. The R value fell from 0.4921 to 0.3307. At this point it became apparent that the second thiophene ring was symmetry related (x, 0.5 -y, 0.5+z) to the rest of the molecule and its coordinates were adjusted accordingly which placed it in a sensible position with respect to the rest of the molecule. Also at this stage the coordinates of some other atoms were given their negative equivalents (i.e. 0.765 becomes –0.235) so that all positive coordinates belonged to atoms in the same unit cell. These adjusted coordinates were run as above and the refinement proceeded exactly as before resulting in the same R value proving no errors had been made. The difference map was plotted and the methylene carbon (C26) between (N2) and the second thiophene ring, the second oxygen atom (O2) and the methylene carbon (C27) attached to it were located. The remaining two methylene carbons (C28, C29) of the ether bridge did not appear on the difference map and were found via the remaining peak list from the original MULTAN run. The coordinates were added to the input file in the same manner as before. The R value fell from 0.4354 to 0.2367 after four cycles of full matrix least squares refinement. All the non hydrogen atoms had now been located.

3.11.1.6.3. Structure refinement.

Before the next run a print out of the observed structure factors (F_o) and calculated structure factors (F_c) was obtained. There were ten reflections of low indices whose F_o was much less than its F_c. These reflections were removed from the data set under the rationale that these reflections were effected by the beam stop, the beam stop blocking some of the reflections intensity reaching the counter thus the F_o being lower than F_c. The reflections removed were 102, 111, 120, 12-1, 13-1, 200, 20-2, 202, 300, 302.

From this point onwards the edited reflection data file was used i.e. with the 10 beam stop affected reflections removed. All subsequent runs used OMIT 3, i.e. reflections with $F_o < 3\sigma(F_o)$ were suppressed. Next FVAR was refined (from 1.0). The coordinates of the 35 non-hydrogen with isotropic temperatures fixed at 0.05 were refined and the R value finished at 0.1647 after four cycles of full matrix least squares. The ILSF factors were introduced and refined (from 1.0) to give R = 0.1553. The positional parameters were once again refined to give R = 0.1546. FVAR was refined to give R = 0.1537. The ILSF's refined to give R = 0.1534. The positional and isotropic temperature factors were refined to give R = 0.1356. After FVAR and ILSF were refined separately R = 0.1350. Anisotropic temperature factors were introduced using ANIS 35 with one cycle of least squares refinement (only one cycle as the positional parameters could not be refined simultaneously). The R value dropped from 0.1350 to 0.1148. FVAR and ILSF were refined as above to give R = 0.1135. The positional and temperature factors were then refined by block least squares. The atoms in the list were arranged so that the individual rigid thiophene and benzene groups were not split between blocks. The atoms were split into four blocks and two of the blocks refined in each cycle. The cycles were rotated so that each block refined with each of the other three twice.

151

Twelve cycles of least squares were used hence each block refined for six cycles. The R value dropped from 0.1135 to 0.1120. FVAR and ILSF were refined as before to give R = 0.1116. At this stage a Fourier difference map was produced. The maximum peak height corresponded to 0.69 electrons per cubic Angstrom. This confirmed that all the non hydrogen atoms had been found and therefore the unit cell contains no solvent molecules. The hydrogen atoms were introduced (with fixed isotropic temperatures of 0.05) in calculated positions riding on the carbon they are attached to (if the carbons position is altered the hydrogens position is recalculated) with block refinement of the positional and temperature parameters as before. The R value decreased from 0.1116 to 0.0906. FVAR and ILSF were refined as before to give R = 0.0902. The hydrogen temperature factors were unfixed and refined with all the other positional (AFIX cards still in place) and temperature parameters via block least squares as before to give R = 0.0818. FVAR and ILSF were refined ro give R = 0.0814. All the positional (hydrogens riding on carbons) and temperature parameters were refined as before to give the final (convergence) R value of 0.0814. In total 358 parameters were refined using 3227 reflections giving a reflection to parameter ratio of 9.0 : 1. The higher this ratio is the more confidence can be placed in the results as each factor is overdetermined (ideally by a factor of 10), in this case by a factor of 9. The last three steps (FVAR, ILSF and bloc position / temperature's) were repeated using OMIT 4 to give an R value of 0.0683. This result is overdetermined by a factor of 7.9.

3.11.1.6.4. Patterson interpretation.

The Patterson map was interpreted after the structure was solved to see if the positions of the two sulfur atoms could be deduced and whether their positions agreed with those from the direct methods structure solution. The asymmetric unit contains two sulfur

atoms whose positions this heavy atom method should locate, however sulfur has an atomic number of only 16 and peaks from the sulfur-sulfur vectors at relative height $16 \times 16 = 256$ may be difficult to separate from sulfur-oxygen vectors at $16 \times 8 = 128$.

Due to the c-glide plane the b-axis projected cell has two equivalent parts so that the simpler cell with $a' = a$ and $c' = 0.5c$ can be considered. This simple cell of two dimensional space group p2 will contain two molecules related by the twofold axis. There should be four S atoms in the simple cell with coordinates $\pm (x_1, z_1)$ and $\pm (x_2, z_2)$ therefore the double weight peaks are expected at $\pm (x_1-x_2, z_1-z_2)$ and $\pm (x_1+x_2, z_1+z_2)$, where the y vector $= 0.5$ from the addition / subtraction of the equivalent positions of the screw related atoms. The two peaks from the Patterson map assumed to be double-weight S-S peaks were 0.717, 0.5, 0.660 and 0.385, 0.5, 0.758 related to the simple cell which gives:

$$x_1-x_2 = 0.717, \ z_1-z_2 = 0.660$$

$$x_1+x_2 = 0.385, z_1+z_2 = 0.758$$

so that

$$(x_1, z_1) = (0.551, 0.709)$$

$$(x_2, z_2) = (-0.166, 0.049)$$

which related to the whole unit cell become

$$(x_1, z_1) = (0.551, 0.3545)$$

$$(x_2, z_2) = (-0.166, 0.0245)$$

Similarly using the peaks 0, 0.824, 0.5 and 0, 0.318, 0.5 ($x = 0$ and $z = 0.5$ from addition / subtraction of the equivalent positions of the glide related atoms):

$$y_1-y_2 = 0.176$$

$$y_1 + y_2 = 0.318$$

so that

$$y_1 = 0.247 \text{ and } y_2 = 0.071$$

the calculated sulfur positions (x, y, z) are therefore:

0.551, 0.247, -0.3545 and -0.166, 0.071, 0.0245

which when translated by the symmetry operators 0.5-x, -y, 0.5+z and 0.5+x, y, 0.5+z

respectively gives the following coordinates:

-0.051, 0.253, 0.1455 and 0.334, 0.071, 0.5245

which can be compared with the sulfur positions after refinement:

-0.085, 0.266, 0.1657 and 0.310, 0.163, 0.5650

As can be seen the positions calculated from the Patterson synthesis do not completely agree with the positions after refinement, but are in fairly close agreement. The coordinates 0.334, 0.071, 0.5245 correspond approximately with the centre of the S1 thiophene ring. It is possible to obtain a Patterson peak from ring-ring vectors and because of the low atomic number of sulfur these may have been more dominant in the calculated Patterson map than S-S vectors.

3.11.1.7. Discussion of the structure.

The following discussion will be of the $F_o > 4\sigma(F_o)$, R = 0.0683 result. Given below is a summary of the crystal, data collection and refinement data.

Empirical Formula	C29 H32 N2 O2 S2
Formula Weight	504.72
Crystal System	Monoclinic
Space group	P2$_1$/c (No. 14)

a, b, c [Å]	12.5043 11.2994 19.8022
α, β, γ	90° 113.34(2)° 90°
V [Å^3]	2568.92
Z	4
D(obs), D(calc) [g/cm^3]	1.31, 1.305
F(000) [Electrons]	1072
μ (MoKα) [/cm]	1.93
Crystal Size(s) [mm]	0.62 × 1.42 × 0.23 and 0.46 × 1.54 × 0.23
Temperature [°C]	25-40 over period of data collection
Radiation [Å]	MoKα 0.7107
Theta Min-Max	3.0°, 60.0°
Scan Type	variable ω scan
Hor. and vert. aperture [mm]	1.00 1.00
Standard	measured every 10 reflections
	(different for each layer line)
Dataset ± h : ± k: ± l	0:16 ; 0:10 ; -25:25
Tot., Uniq. Data, R(int)	6549, 5944, 0.0416
Min./Max. Transmission Factors	0.88, 0.96
Observed data [I > 4.0 sigma(I)]	2828
Nref, Npar	2828, 358
R, S	0.0683, 1.60

3.11.1.7.1. Derived structural data.

Estimated standard deviations are given in brackets.

FRACTIONAL ATOMIC COORDINATES.			
ATOM	X	Y	Z
S1	0.30962(10)	0.1635(2)	0.56499(10)
S2	-0.08513(10)	0.2660(2)	0.16567(10)
O1	0.3637(3)	0.1049(4)	0.3905(2)
O2	0.1802(3)	0.0629(4)	0.2150(2)
N1	0.2052(3)	0.3676(4)	0.4333(2)
N2	-0.0430(3)	0.1713(4)	0.3218(2)
C1	0.3319(4)	0.1993(5)	0.4871(3)
C2	0.3454(4)	0.0988(5)	0.4543(3)
C3	0.3359(5)	-0.0047(6)	0.4895(3)
C4	0.3159(5)	0.0182(6)	0.5519(4)
C5	0.3251(5)	0.3203(5)	0.4615(3)
C6	0.2056(5)	0.4915(5)	0.4190(3)
C7	0.2565(4)	0.5623(5)	0.4885(3)
C8	-0.0214(6)	0.2810(7)	0.1040(4)
C9	0.0730(6)	0.2095(6)	0.1207(3)
C10	0.0916(5)	0.1453(5)	0.1851(3)
C11	0.0145(4)	0.1644(5)	0.2167(3)
C12	0.3469(4)	0.6377(5)	0.5001(3)
C13	0.3868(5)	0.7079(5)	0.5621(3)
C14	0.3372(5)	0.7024(5)	0.6123(3)
C15	0.2466(5)	0.6277(6)	0.6010(3)
C16	0.2068(5)	0.5568(5)	0.5400(3)
C17	-0.2360(4)	0.0787(5)	0.2813(3)
C18	-0.2819(5)	-0.0305(6)	0.2694(3)
C19	-0.3906(5)	-0.0532(6)	0.2136(3)
C20	-0.4512(5)	0.0377(7)	0.1699(3)
C21	-0.4063(5)	0.1465(6)	0.1802(3)
C22	-0.2972(5)	0.1675(6)	0.2362(3)
C23	0.1267(5)	0.3036(5)	0.3665(3)
C24	0.0506(4)	0.2218(5)	0.3874(3)
C25	-0.1215(4)	0.1041(5)	0.3455(3)
C26	0.0026(4)	0.0998(5)	0.2780(3)
C27	0.2947(5)	0.1117(6)	0.2342(3)
C28	0.3817(5)	0.0268(6)	0.2851(3)
C29	0.3608(5)	-0.0022(5)	0.3536(3)
H1	0.34344	-0.09251	0.47026
H2	0.3055	-0.04904	0.58753
H3	0.37983	0.37499	0.50669
H4	0.35637	0.32334	0.41788
H5	0.25659	0.50671	0.38671

H6	0.11712	0.52021	0.38833
H7	-0.05252	0.3401	0.05731
H8	0.12607	0.20293	0.08903
H9	0.38722	0.64244	0.46095
H10	0.45827	0.76802	0.57111
H11	0.37	0.7574	0.66084
H12	0.20614	0.62442	0.64007
H13	0.13617	0.49588	0.5319
H14	-0.23344	-0.10256	0.3038
H15	-0.42639	-0.14159	0.20502
H16	-0.53582	0.02159	0.12681
H17	-0.45428	0.21819	0.14532
H18	-0.26101	0.25571	0.24392
H19	0.07323	0.36643	0.32611
H20	0.17789	0.25318	0.3437
H21	0.01201	0.27036	0.41904
H22	0.1033	0.15061	0.4204
H23	-0.08059	0.02123	0.36906
H24	-0.13868	0.15444	0.38646
H25	0.08751	0.06725	0.31362
H26	-0.05554	0.02599	0.2555
H27	0.31138	0.12385	0.18517
H28	0.30098	0.19584	0.26136
H29	0.37792	-0.05442	0.25551
H30	0.46733	0.0654	0.30176
H31	0.42804	-0.06091	0.38858
H32	0.2768	-0.04394	0.33853

** Note the hydrogen positions are to five decimal places with terminal zero's omitted.

The hydrogen coordinates have no esd's as their positions were not refined.

The esd's for the atomic coordinates are generally reasonable, but for S1 and S2 their esd's are not substantially lower than for the other atoms, although these are the heaviest atoms. This could be due to the fact that the thiophene rings are on the outer edges of the molecule and the rings could be moving (wagging) with thermal motion.

ANISOTROPIC TEMPERATURE FACTORS.					
ATOM	U11	U22	U33	U23	U13	U12
S1	0.0494(9)	0.0594(11)	0.0391(8)	0.0010(8)	0.0187(7)	0.0086(8)
S2	0.0457(9)	0.0547(11)	0.0528(9)	-0.0020(8)	0.0110(7)	-0.0028(8)
O1	0.058(3)	0.041(3)	0.049(2)	-0.008(2)	0.028(2)	-0.005(2)
O2	0.042(2)	0.055(3)	0.068(3)	-0.014(2)	0.031(2)	-0.011(2)
N1	0.028(2)	0.034(3)	0.033(2)	-0.006(2)	0.0006(18)	-0.0013(19)
N2	0.026(2)	0.037(3)	0.034(2)	-0.010(2)	0.0075(18)	-0.0039(19)
C1	0.028(3)	0.039(4)	0.030(3)	-0.003(2)	0.010(2)	0.002(2)
C2	0.033(3)	0.044(4)	0.035(3)	-0.001(3)	0.013(2)	-0.004(3)
C3	0.048(4)	0.045(4)	0.057(4)	0.004(3)	0.022(3)	0.006(3)
C4	0.050(4)	0.052(4)	0.059(4)	0.018(3)	0.022(3)	0.008(3)
C5	0.033(3)	0.041(4)	0.041(3)	-0.007(3)	0.011(2)	0.000(3)
C6	0.044(3)	0.030(4)	0.035(3)	0.001(3)	0.007(3)	0.002(3)
C7	0.037(3)	0.028(3)	0.029(3)	0.001(2)	0.007(2)	0.005(2)
C8	0.072(5)	0.071(5)	0.048(4)	0.001(4)	0.012(4)	-0.020(4)
C9	0.060(4)	0.069(5)	0.048(4)	-0.004(3)	0.025(3)	-0.019(4)
C10	0.043(3)	0.042(4)	0.042(3)	-0.012(3)	0.017(3)	-0.011(3)
C11	0.032(3)	0.039(3)	0.031(3)	-0.010(3)	0.005(2)	-0.005(3)
C12	0.032(3)	0.035(3)	0.039(3)	-0.001(3)	0.012(2)	-0.001(2)
C13	0.035(3)	0.036(4)	0.047(3)	-0.004(3)	0.005(3)	0.000(3)
C14	0.046(3)	0.038(4)	0.044(3)	-0.006(3)	0.011(3)	0.012(3)
C15	0.050(4)	0.054(4)	0.040(3)	0.003(3)	0.019(3)	0.011(3)
C16	0.037(3)	0.042(4)	0.046(3)	0.006(3)	0.012(3)	0.001(3)
C17	0.029(3)	0.040(4)	0.032(3)	-0.002(3)	0.012(2)	-0.003(2)
C18	0.037(3)	0.054(4)	0.037(3)	0.000(3)	0.014(3)	-0.002(3)
C19	0.041(3)	0.057(5)	0.052(4)	-0.010(3)	0.015(3)	-0.020(3)
C20	0.027(3)	0.075(5)	0.045(3)	-0.009(3)	0.008(3)	-0.010(3)
C21	0.029(3)	0.063(5)	0.043(3)	-0.002(3)	0.010(3)	0.006(3)
C22	0.040(3)	0.043(4)	0.047(3)	-0.014(3)	0.019(3)	-0.004(3)
C23	0.037(3)	0.036(4)	0.039(3)	-0.009(3)	0.009(2)	-0.015(3)
C24	0.028(3)	0.052(4)	0.034(3)	-0.013(3)	0.002(2)	-0.003(3)
C25	0.025(3)	0.051(4)	0.034(3)	0.002(3)	0.005(2)	-0.008(3)
C26	0.033(3)	0.034(3)	0.043(3)	-0.008(3)	0.016(3)	-0.005(2)
C27	0.040(3)	0.063(5)	0.053(4)	-0.011(3)	0.023(3)	-0.019(3)
C28	0.039(3)	0.064(5)	0.057(4)	-0.019(3)	0.025(3)	-0.001(3)
C29	0.046(3)	0.041(4)	0.050(3)	-0.014(3)	0.020(3)	0.002(3)

ISOTROPIC TEMPERATURE FACTORS.			
ATOM	TEMP.	ATOM	TEMP.
H1	0.06(2)	H17	0.07(2)
H2	0.05(2)	H18	0.05(2)
H3	0.06(2)	H19	0.03(1)
H4	0.05(2)	H20	0.04(1)
H5	0.08(2)	H21	0.06(2)
H6	0.06(2)	H22	0.04(1)
H7	0.07(2)	H23	0.03(1)
H8	0.07(2)	H24	0.06(2)
H9	0.05(2)	H25	0.04(2)
H10	0.04(2)	H26	0.04(2)
H11	0.08(2)	H27	0.08(2)
H12	0.08(2)	H28	0.04(1)
H13	0.04(1)	H29	0.07(2)
H14	0.04(2)	H30	0.07(2)
H15	0.07(2)	H31	0.06(2)
H16	0.10(3)	H32	0.07(2)

The esd's for the temperature factors are reasonable but again are not as low as expected for the two sulfur atoms. The positions and temperature factors of the atoms in macrocycle are best visualised in the 'ortep style' drawing[108] below.

159
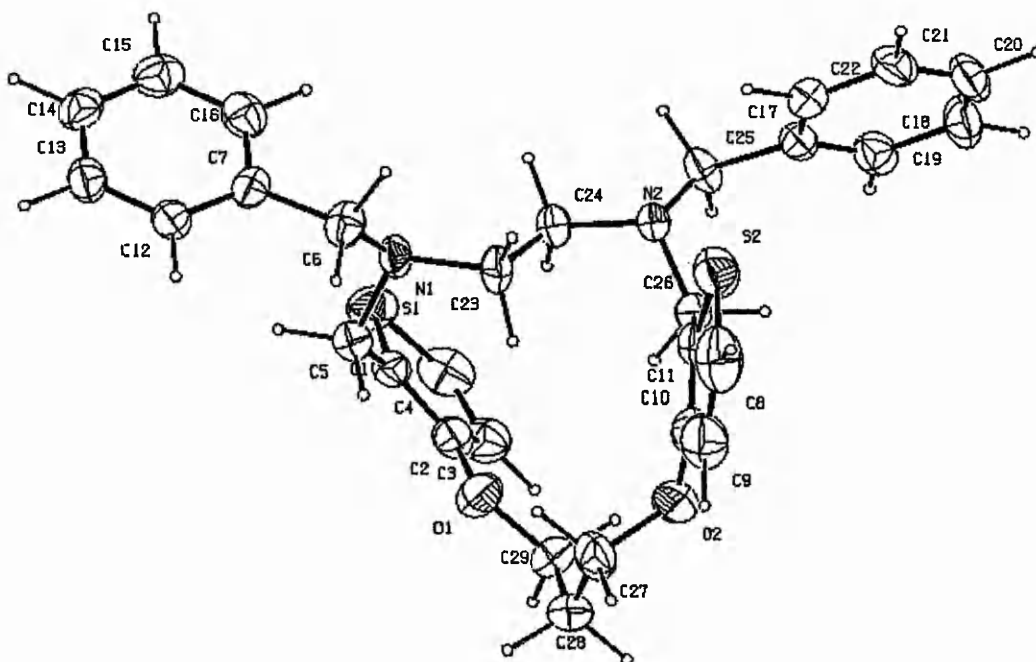
In the previous diagram only the anisotropic temperature factors are plotted (at the 50% probability level), the isotropic hydrogen temperature factors are not shown.

The greatest thermal motion occurs at the extremities of the molecule. In the diagram the distance between C13 and C20 is 12.7656Å and between C4 and C8 is 8.6963Å. The two benzene rings and especially the two thiophene rings have greater thermal motion in their outermost carbon atoms. This is also reflected in the high isotropic temperature factors for the hydrogens attached to these atoms (greatest for H16 (0.10(3)) attached to C20). Greater thermal motion is expected for atoms at the outer regions of the molecule. In contrast to this the more tightly bound (i.e. attached to more carbon atoms) an atom is, the lower its degree of thermal motion is expected to be. This is shown in the two nitrogen atoms (bonded to three carbons) having the smallest degree of thermal motion in the molecule (also note C1, C2, C7, C10, C11, and C17). The greater the mass of an element the lower its thermal motion is expected to be. The two sulfur atoms do not have particularly low temperature factors (due to being at the outer regions of the molecule) but they are significantly lower than those of the two sp^2 carbons bonded to hydrogen of each thiophene ring.

BOND LENGTHS.			
BOND	LENGTH(Å)	BOND	LENGTH(Å)
S1 -C1	1.721(6)	C3 -H1	1.0803
S1 -C4	1.669(7)	C4 -H2	1.0792
S2 -C8	1.711(8)	C5 -H3	1.0797
S2 -C11	1.701(6)	C5 -H4	1.0806
O1 -C2	1.372(7)	C6 -H5	1.0807
O1 -C29	1.407(7)	C6 -H6	1.0797
O2 -C10	1.387(7)	C8 -H7	1.0803
O2 -C27	1.438(8)	C9 -H8	1.0812
N1 -C5	1.477(8)	C12 -H9	1.0806
N1 -C6	1.429(7)	C13 -H10	1.0796
N1 -C23	1.486(7)	C14 -H11	1.0798
N2 -C24	1.476(7)	C15 -H12	1.0798

N2	-C25	1.458(7)	C16	-H13	1.0804
N2	-C26	1.457(7)	C18	-H14	1.0803
C1	-C2	1.352(8)	C19	-H15	1.08
C1	-C5	1.449(8)	C20	-H16	1.0795
C2	-C3	1.390(9)	C21	-H17	1.0793
C3	-C4	1.379(9)	C22	-H18	1.0802
C6	-C7	1.498(8)	C23	-H19	1.0803
C7	-C12	1.360(8)	C23	-H20	1.0803
C7	-C16	1.390(8)	C24	-H21	1.0798
C8	-C9	1.359(11)	C24	-H22	1.0803
C9	-C10	1.404(8)	C25	-H23	1.0803
C10	-C11	1.359(8)	C25	-H24	1.0796
C11	-C26	1.474(8)	C26	-H25	1.0801
C12	-C13	1.378(8)	C26	-H26	1.0798
C13	-C14	1.366(9)	C27	-H27	1.0796
C14	-C15	1.358(9)	C27	-H28	1.0797
C15	-C16	1.368(8)	C28	-H29	1.0798
C17	-C18	1.342(9)	C28	-H30	1.0797
C17	-C22	1.360(8)	C29	-H31	1.0795
C17	-C25	1.519(8)	C29	-H32	1.08
C18	-C19	1.394(9)			
C19	-C20	1.363(9)			
C20	-C21	1.333(10)			
C21	-C22	1.396(9)			
C23	-C24	1.498(8)			
C27	-C28	1.500(9)			
C28	-C29	1.515(8)			

** Note the hydrogen bond lengths are to four decimal places with terminal zero's omitted and have no esd's as the hydrogen positions were not refined. The bond lengths and following derived data were all obtained via the crystallographic program tool PLATON[108].

For ease of description the bond lengths (to 2 decimal places) are shown on a schematic drawing below:-
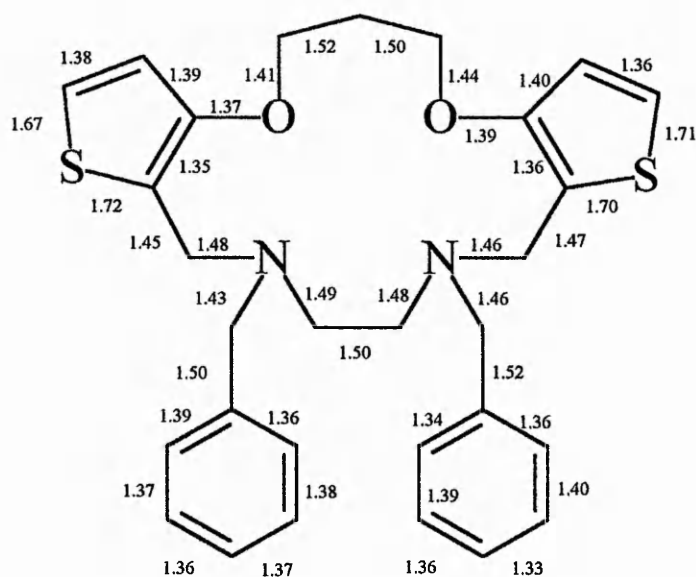
Chemically it would be expected that the two halves of the macrocycle (the compound is chemically mirrored between C23 and C24 and through C28) would have the same bond lengths. This is not the case. In the crystal the macrocycle is not mirrored as depicted above and the two halves of the macrocycle have differing geometries which is reflected in the bond lengths.

Notably the S2 thiophene ring has fairly similar bond lengths either side of the sulfur atom whereas the bond lengths for the S1 thiophene ring are asymmetric either side of the S1 atom (but only by 0.010Å if 3σ is added to the shortest and subtracted from the longest bond). This could indicate that the S2 thiophene ring is more aromatic in character than the S1 thiophene ring.

The bond lengths in the benzene rings vary in the range 1.33-1.40Å. The aromatic C-O bonds are shorter (0.04 and 0.05Å) than the aliphatic C-O bonds as is known for phenolic compounds. The C-N bonds vary from 1.43 to 1.49Å.

The C1-C5 (1.45Å) and C11-C26 (1.47Å) bond lengths are shorter than the expected 1.52Å[109] and may indicate some π delocalisation from the thiophene rings into these bonds.

The esd's for the bond lengths are reasonable.

BOND ANGLES.						
BOND			ANGLE(°)	BOND		ANGLE(°)
C1	-S1	-C4	93.3(3)	C2	-C3	-H1	123.99
C8	-S2	-C11	93.0(3)	C4	-C3	-H1	124.1
C2	-O1	-C29	117.1(5)	S1	-C4	-H2	124.46
C10	-O2	-C27	113.5(5)	C3	-C4	-H2	124.43
C5	-N1	-C6	110.3(4)	N1	-C5	-H3	108.75
C5	-N1	-C23	112.0(4)	N1	-C5	-H4	108.71
C6	-N1	-C23	110.7(4)	C1	-C5	-H3	108.67
C24	-N2	-C25	108.6(4)	C1	-C5	-H4	108.66
C24	-N2	-C26	112.2(4)	H3	-C5	-H4	109.45
C25	-N2	-C26	112.0(4)	N1	-C6	-H5	108.8
S1	-C1	-C2	109.2(4)	N1	-C6	-H6	108.82
S1	-C1	-C5	121.8(4)	C7	-C6	-H5	108.85
C2	-C1	-C5	128.7(5)	C7	-C6	-H6	108.9
O1	-C2	-C1	119.9(5)	H5	-C6	-H6	109.43
O1	-C2	-C3	125.6(5)	S2	-C8	-H7	124.09
C1	-C2	-C3	114.5(5)	C9	-C8	-H7	124.02
C2	-C3	-C4	111.9(6)	C8	-C9	-H8	124.98
S1	-C4	-C3	111.1(5)	C10	-C9	-H8	124.92
N1	-C5	-C1	112.6(5)	C7	-C12	-H9	120.17
N1	-C6	-C7	112.0(4)	C13	-C12	-H9	120.22
C6	-C7	-C12	120.8(5)	C12	-C13	-H10	119.54
C6	-C7	-C16	120.0(5)	C14	-C13	-H10	119.55
C12	-C7	-C16	119.2(5)	C13	-C14	-H11	119.99
S2	-C8	-C9	111.9(5)	C15	-C14	-H11	120.14
C8	-C9	-C10	110.1(6)	C14	-C15	-H12	120.01
O2	-C10	-C9	123.4(6)	C16	-C15	-H12	120.17
O2	-C10	-C11	120.2(5)	C7	-C16	-H13	119.76
C9	-C10	-C11	116.3(6)	C15	-C16	-H13	119.61
S2	-C11	-C10	108.7(4)	C17	-C18	-H14	119.23
S2	-C11	-C26	122.3(4)	C19	-C18	-H14	119.22
C10	-C11	-C26	128.5(5)	C18	-C19	-H15	120.52
C7	-C12	-C13	119.6(5)	C20	-C19	-H15	120.36

C12	-C13	-C14	120.9(6)	C19	-C20	-H16	119.93
C13	-C14	-C15	119.9(5)	C21	-C20	-H16	119.86
C14	-C15	-C16	119.8(6)	C20	-C21	-H17	120.04
C7	-C16	-C15	120.6(6)	C22	-C21	-H17	120.09
C18	-C17	-C22	118.2(5)	C17	-C22	-H18	119.53
C18	-C17	-C25	121.1(5)	C21	-C22	-H18	119.48
C22	-C17	-C25	120.6(5)	N1	-C23	-H19	109.64
C17	-C18	-C19	121.5(6)	N1	-C23	-H20	109.69
C18	-C19	-C20	119.1(6)	C24	-C23	-H19	109.6
C19	-C20	-C21	120.2(6)	C24	-C23	-H20	109.67
C20	-C21	-C22	119.9(6)	H19	-C23	-H20	109.42
C17	-C22	-C21	121.0(6)	N2	-C24	-H21	109.05
N1	-C23	-C24	108.8(4)	N2	-C24	-H22	109
N2	-C24	-C23	111.4(4)	C23	-C24	-H21	109
N2	-C25	-C17	111.1(4)	C23	-C24	-H22	108.94
N2	-C26	-C11	114.0(5)	H21	-C24	-H22	109.46
O2	-C27	-C28	108.3(5)	N2	-C25	-H23	109.05
C27	-C28	-C29	113.8(5)	N2	-C25	-H24	109.1
O1	-C29	-C28	107.5(5)	C17	-C25	-H23	109.01
				C17	-C25	-H24	109.04
				H23	-C25	-H24	109.47
				N2	-C26	-H25	108.39
				N2	-C26	-H26	108.4
				C11	-C26	-H25	108.22
				C11	-C26	-H26	108.29
				H25	-C26	-H26	109.47
				O2	-C27	-H27	109.75
				O2	-C27	-H28	109.74
				C28	-C27	-H27	109.78
				C28	-C27	-H28	109.76
				H27	-C27	-H28	109.52
				C27	-C28	-H29	108.34
				C27	-C28	-H30	108.32
				C29	-C28	-H29	108.42
				C29	-C28	-H30	108.4
				H29	-C28	-H30	109.52
				O1	-C29	-H31	110.01
				O1	-C29	-H32	109.96
				C28	-C29	-H31	109.91
				C28	-C29	-H32	109.93
				H31	-C29	-H32	109.51

** Note the bond angles including hydrogen atoms are to two decimal places with terminal zeros omitted and have no esd's as the hydrogen atom positions were not refined. The esd's are reasonable.

The bond angles for the two thiophene rings are fairly similar with the greatest difference between related angles being C1-C2-C3 = 114.5(5)° and C9-C10-C11 = 116.3(6)° which are within 3σ. The angles within the benzene rings vary between 118.2(5) and 121.5(6)°. The ether bridge has two large angles (> 109.47°) C2-O1-C29 = 117.1(5)° and C27-C28-C29 = 113.8(5)° and may contain two C-H...O hydrogen bonds within the bridge, C29-H32...O2 = 2.5611Å, 95.538° and C27-H28...O1 = 2.5736Å, 94.394°. These close contacts may be simply due to the geometry of the bridge but the symmetry of the bridge viewed down the C27...C29 vector is such that the oxygen and hydrogen atoms in question are rotated so as to be in the same plane. This can be seen by the following torsion angles, O2-C27...C29-H32 = 3.38° and O1-C29...C27-H28 = 3.16°. Typical CH...O hydrogen bond lengths of this kind are in the order of 2.4-2.8Å[110].

3.11.1.7.2. Discussion of structural geometry.

The macrocycle is non-planar with maximum deviations from the least squares plane defined by all the non hydrogen atoms of 3.670(8)Å, C8 and –3.852(7)Å, C4. The two thiophene rings do not lie in the same plane. The bridge containing the two nitrogen atoms provides their greatest separation approximately perpendicular to the plane of the rings, whilst the bridge containing the two oxygen atoms provides their greatest separation approximately in the plane of the thiophene rings. The angle between the

plane of each of the thiophene rings is 49.8(3)°. Probably the most significant factor affecting the non-planarity of the macrocycle is the two benzyl substituents. The geometry between the two benzene rings is similar to the 'zig zag' of aliphatic hydrocarbons. The geometry of the rest of the macrocyclic ring has two approximately planar regions joined by the ether bridge so that the greatest area of the macrocyclic cavity is viewed looking approximately in the plane of the thiophene rings. Deviations from the least squares planes of these regions are given below:-

Atoms describing least squares plane = S1, O1, C1, C2, C3 and C4.

Deviations from the plane (Å) = S1 0.004(2), O1 –0.003(4), C1 –0.005(5), C2 0.009(5), C3 0.000(6), C4 –0.004(7), C5 –0.133(6), N1 –1.475(4), C28 –0.171(6), C29 –0.176(6).

Atoms describing least squares plane = S2, O2, C8, C9, C10 and C11.

Deviations from the plane (Å) = S(2) –0.010(2), O2 –0.013(4), C8 0.001(8), C9 0.000(7), C10 0.014(6), C11 0.008(6), C26 –0.155(6), N2 0.512(4), C27 1.095(6), C28 1.186(6).

As can be seen above the oxygen atoms are in the plane of the thiophene rings. For the plane including the S1 thiophene ring the three methylene carbons C5, C28 and C29 are almost in the plane (deviation ≈ 0.1-0.2Å) with the nitrogen (N1) considerably out of the plane (deviation ≈ 1.5Å). The distance between S1 and N1 = 3.336(5)Å (Sum of van der Waals radii = 3.45Å[45]). The plane containing the S2 thiophene ring has only the C26 methylene carbon (between the thiophene ring and N2) nearly planar and the N2 atom is much closer to the plane (0.512(4)Å cf. –1.475(4)Å) than N1 is to the previous plane. The distance between S2 and N2 = 3.113(4)Å (+ [3 × 0.004] = 3.125Å). This is significantly lower than the sum of their van der Waals radii 3.45Å (contact radii =

3.35Å[45]). This suggests a non-bonded interaction. This short S...N contact is a common feature in appropriately 2-substituted thiophenes[111]. In 12 examples the bond distances vary between 2.927Å and 3.094Å with torsion angles from 0.3 to 10.8°. Note that many of these examples have sp^2 rather than sp^3 hybridised nitrogen atoms and thus have shorter C...N distances. Support for this view is provided by the much smaller S2-C11-C26 angle of 122.3(4)° compared to the C10-C11-C26 angle of 128.5(5)°. The torsion angle S2-C11-C26-N2 in this case is –38.34° (cf. S1-C1-C5-N1 = -69.17°). This angle is much greater than 10.8° but in this case there are extreme steric restrictions due to the thiophene ring and nitrogen atom being part of a ring. Therefore that the interaction occurs at all is quite remarkable and must be considered as a contributor in determining the compound's geometry.

The structure contains four aromatic rings and the packing of these is probably another contributor to the macrocycle's geometry. The geometry of the rings within the assymetric unit and in the overall crystal packing will be discussed. The angles between the planes of the rings are given below.

S1 thiophene – S2 thiophene = 49.8(3)°

S1 thiophene – C7 benzene = 131.9(3)°

S1 thiophene – C17 benzene = 73.4(3)°

S2 thiophene – C17 benzene = 101.2(3)°

S2 thiophene – C7 benzene = 86.7(3)°

C7 benzene – C17 benzene = 79.0(3)°

The angles between each thiophene ring and the two benzene rings consist of one acute and one obtuse angle as in the stacking for naphthalene[112] however in the present

compound the planes of the benzene rings are twisted relative to the 'middle' thiophene ring. The larger angle between the S1 thiophene ring and the C7 benzene ring may be a consequence of an intermolecular C-H...O hydrogen bond; C13-H10(x,y,z)...O1(1-x,1-y,1-z) = 2.501(4)Å. The angle C-H...O = 172.0(3)°. This is shown in figure 43.

Figure 43.
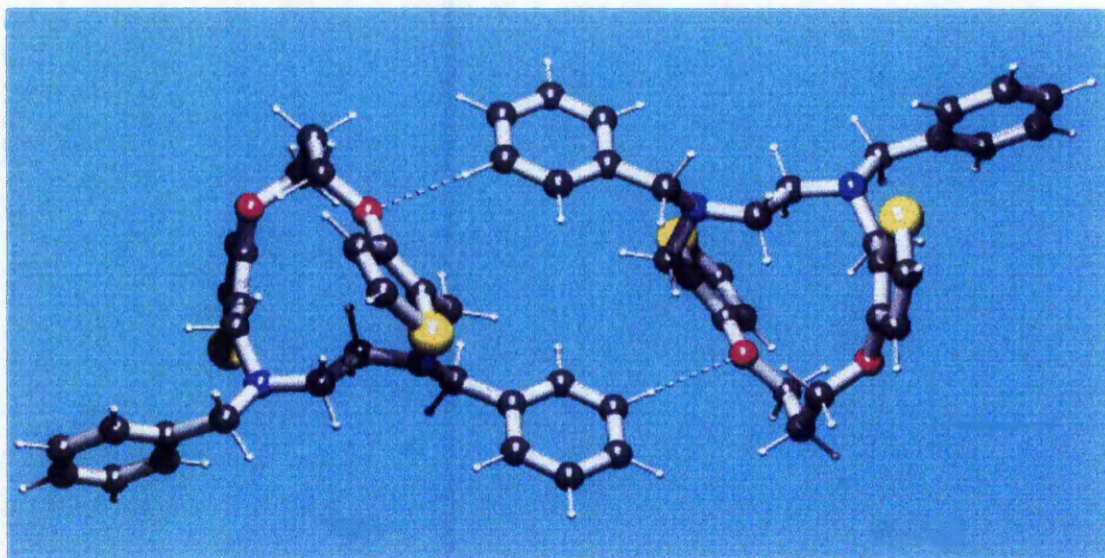
The literature[45] contact distance for the H and O atoms is 2.72Å. It should be noted that the hydrogen atoms were placed in calculated positions with C-H distances of 1.08Å. The formation of C-H...O hydrogen bonds is now an accepted interaction[110]. The ability of a C-H group to act as a proton donor depends on the carbon hybridisation $C(sp)$-H > $C(sp^2)$-H > $C(sp^3)$-H. The near linear angle, the bond length[110] and the fact that the hydrogen atom appears to be directed towards where one would expect to find one of the oxygen lone pairs make this very likely to be a genuine C-H...O hydrogen bond. There may be another although weaker hydrogen bond between a hydrogen attached to a carbon of the same benzene ring and O2 of a different symmetry related macrocycle; C15-H12(x.1/2-y,1/2+z)...O2(x,y,z) = 2.6773Å (128.21°). The influence of these interactions is almost certainly a factor in determining the packing arrangement within

the crystal. Also of interest is another possible hydrogen bond to the O1 atom, this time intramolecular; C5-H4...O1 = 2.537(4)Å. The angle C-H...O = 101.2(3)°. The geometry of this interaction could be a consequence of the strained nature of the macrocyclic ring rather than the hydrogen atom being genuinely directed towards one of the oxygen lone pairs. However a similar interaction occurs on the other side of the ring C26-H25...O2 = 2.6369Å, 97.376° and also as will be discussed later, in the structure M2.

The arrangement of the aromatic rings within the crystal is shown in the CHEM-X drawing shown in figure 44. All other (non-aromatic) atoms have been deleted. The view consists of packing from –0.5 to 2.5 along the a axis and –0.5 to 1.5 along the b and c axes.

Figure 44.
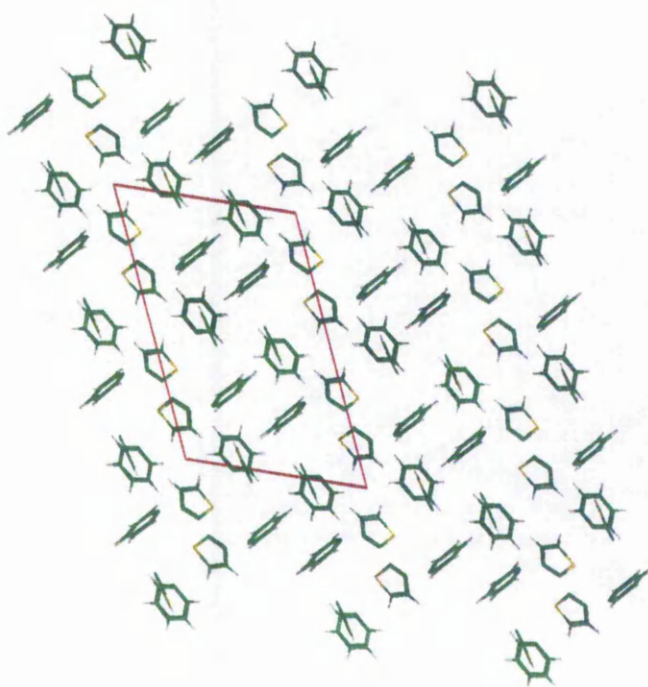
In figure 44 the view is down the b-axis and the pattern is repeated perpendicular to the plane of the paper i.e. behind each ring lies another and another etc. From this picture it can be seen that the aromatic rings make a recognisable repeating pattern. It can be seen from figure 44 that two benzene and two thiophene rings appear to be stacked (parallel to the a-axis) with inclination to this axis (like the stacking in naphthalene[112]). However when this stacking is viewed down the a-axis (as in figure 45) it can be seen that the two benzene rings are displaced along the b-axis, so that their π clouds are not optimally stacked as figure 44 (first) implies. The same is the case for the two thiophene rings, however their displacement is much less. The benzene and thiophene ring stacks are also displaced with regard to each other along the b-axis. Figures 45 and 46 show the pattern down the a and c axes respectively and it can be seen from these that the rings appear to be packed to optimise repulsive forces (interatomic contacts) rather than dispersion forces (π stacking). The two sets of shortest ring interactions with small dihedral angles between the ring planes suggest possible π stacking (which optimises dispersion forces):-

S1 thiophene – S1thiophene [1-x, -y, 1-x]

Distance between ring centroids = 4.960Å

Dihedral angle between planes = 0.00°

S2 thiophene – C7 benzene [-x, 1/2+y, 1/2-z]

Distance between ring centroids = 4.512Å

Dihedral angle between planes = 6.38°

Figure 45.
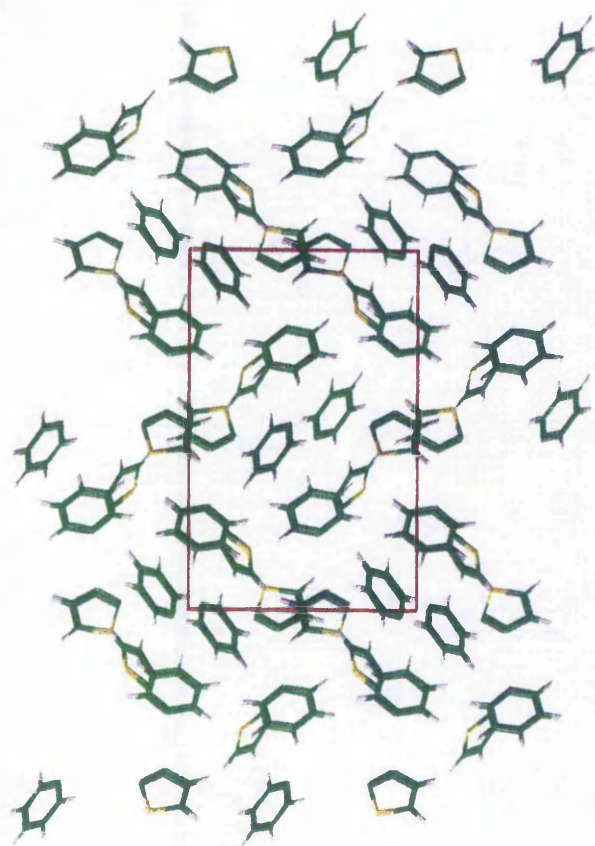
Figure 46.
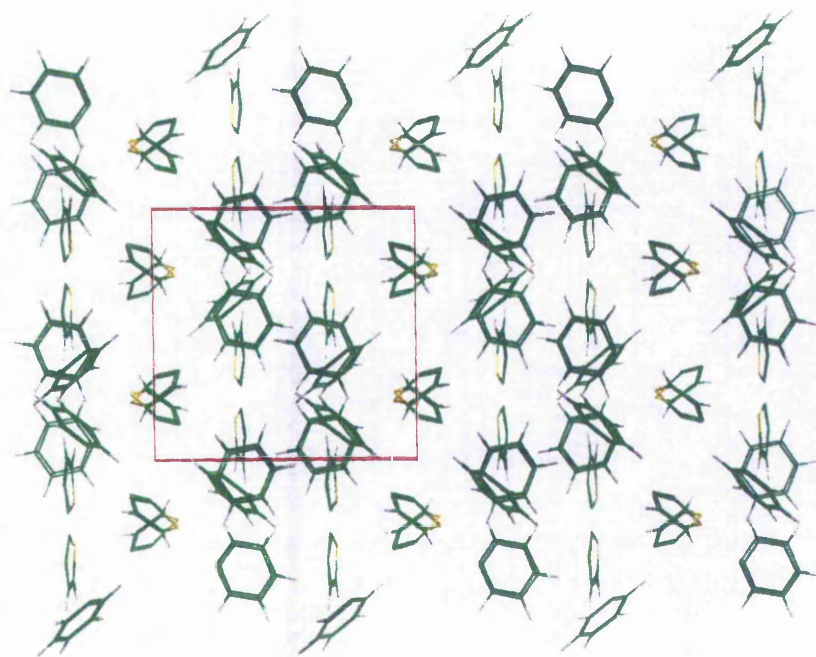
The structure contains six potential donor atoms (2S, 2N and 2O) and the orientation of their lone pairs of electrons is important not only for donation in possible metal complexes but also for possible hydrogen bonds, dipole interactions etc which influence the observed geometry. The lone pair on each nitrogen atom is directed away from the macrocyclic cavity and can be described as sitting at the bottom of a cup whose sides are described by the adjacent thiophene and benzene rings as shown in figure 47.

Figure 47.
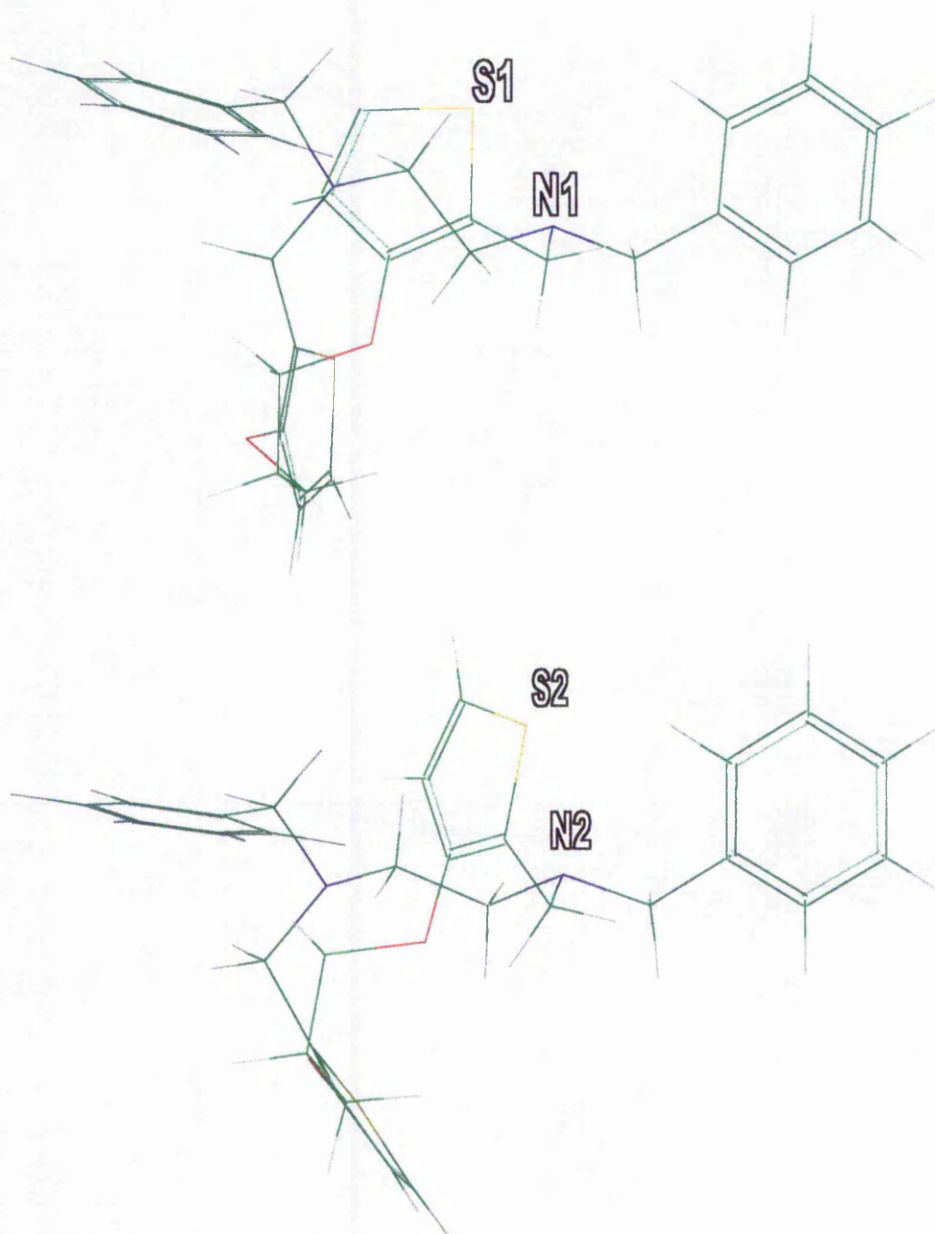
In the previous diagram the arrangement of the bonds in the aromatic rings should be ignored as they are chemically non-sensible due to CHEM-X designating bond types to bonds of certain lengths from a (rather narrow range) internal parameter file.

There are no significant contacts for either nitrogen atom apart from the N...S interaction discussed previously. The lone pairs on the oxygen atoms are also directed away from the macrocyclic cavity and the CH...O hydrogen bond to O1 has been discussed. The lone pair of each sulfur atom is directed towards the adjacent nitrogen atom however the interaction is much more directed for the S2 and N2 atoms as previously discussed.

The structure contains various other contacts less than the sum of the van der Waals radii for each atom. Most of these are C...H or H...H contacts and occur mainly around the congested nitrogen atoms. Only one of these is less than the sum of the van der Waals radii (−0.25Å) and is H6...H19 = 2.0743Å (hydrogens attached to methylene carbons C6 and C23 either side of N1). Further evidence of the congested nature of the nitrogen containing bridge between the thiophene rings are two C...C distances less than their contact distance of 3.40Å; C1...C24 = 3.291(8)Å, C11...C23 = 3.153(8)Å.

The shortest intermolecular contacts besides the CH...O hydrogen bond are listed below:-

S1...H8 [x,1/2-y,1/2+z] = 2.9390Å. Sum Rad. = 3.00Å.

S2...H6 [-x,-1/2+y,1/2-z] = 2.9458Å.

O2...H12 [x,1/2-y,-1/2+z] = 2.6773Å. Sum Rad. = 2.72Å.

C11...H6 [-x,-1/2+y,1/2-z] = 2.6413Å. Sum Rad. = 2.90Å.

C22...H11 [-x,1-y,1-z] = 2.6789Å.

H15...H28 [-x,-1/2+y,1/2-z] = 2.3344Å. Sum Rad. = 2.40Å.

H19...H26 [-x,1/2+y,1/2-z] = 2.3723Å.

Having discussed the macrocycle's intramolecular and intermolecular geometry a view of the packing within the unit cell is shown in figure 48, viewed down the b-axis with the packing range 0-1, 0-1, –0.5-1.5 for the three axes.

Figure 48.
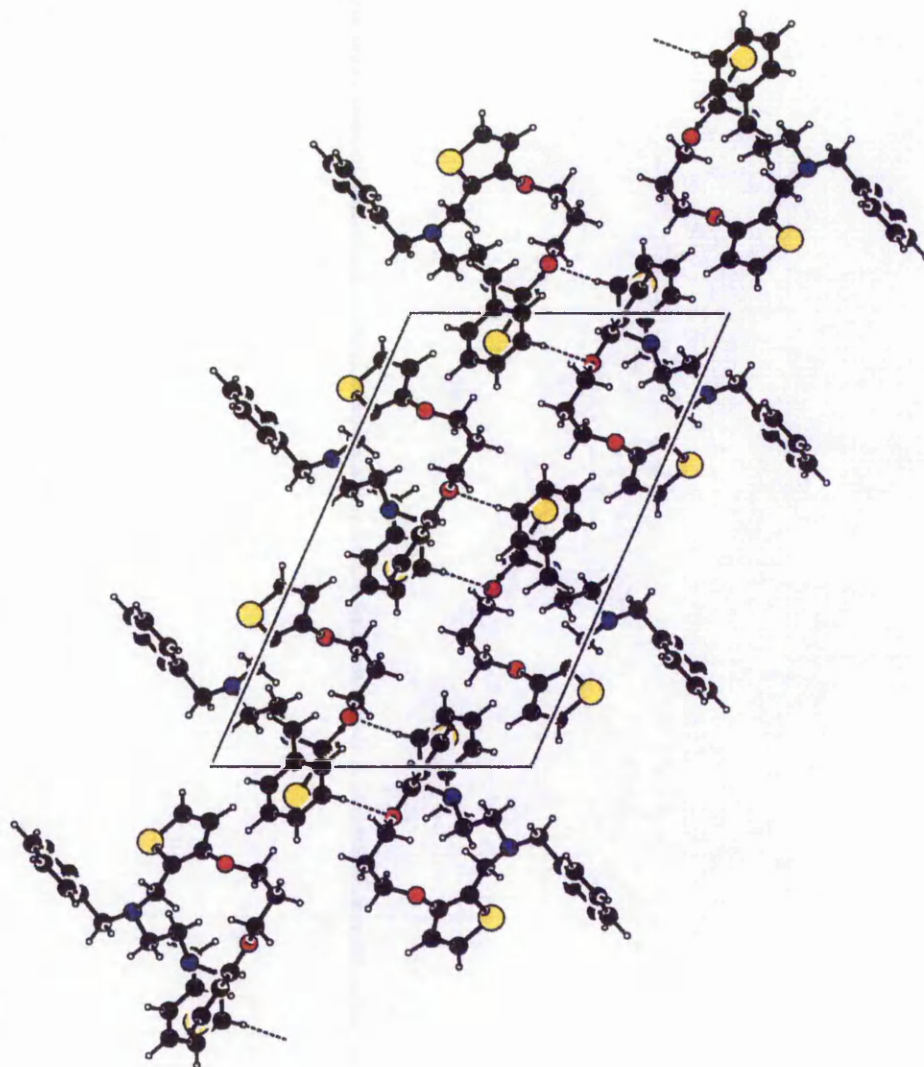
As can be seen in the diagram each macrocycle is bound to another in the successive layer of macrocycles along the b-axis by two hydrogen bonds.

3.11.1.7.3. Implications for metal ion complexation.

As mentioned in the discussion of the macrocycle's geometry (section 3.11.1.7.2) the lone pairs on both the oxygen and nitrogen atoms are directed away from the macrocyclic cavity. This would require the macrocycle to undergo conformational change in order to coordinate a metal ion effectively with all four donor atoms. Analogous macrocycles[113,114] of this type i.e with two oxygen and two nitrogen atoms, form complexes with (square) planar arrangements of the donor atoms with Ni^{2+} and Cu^{2+} ions. This planar arrangement of donor atoms would be unfavourable for the present macrocycle due to the bulky benzyl substituents. However as can be seen from figure 49 the macrocycle need undergo only relatively minor rearrangement to form a 'tetrahedral' complex with Ni^{2+}.

Figure 49.
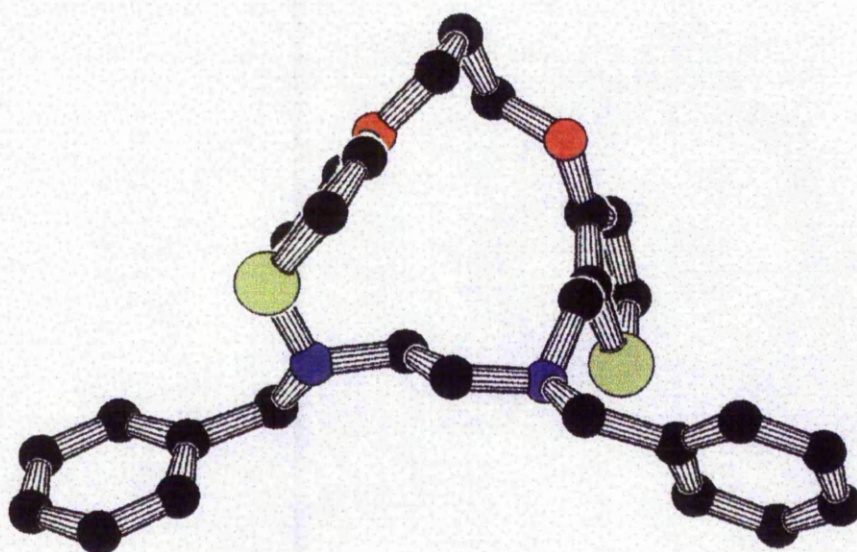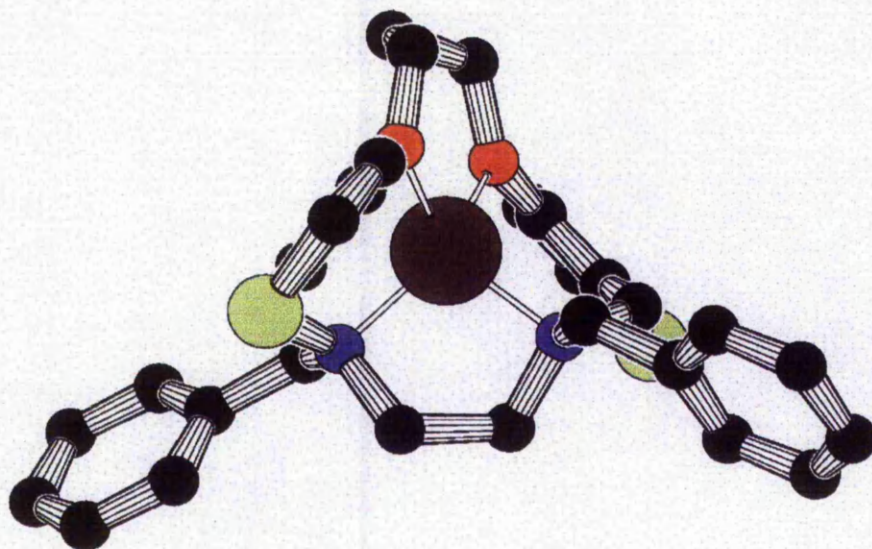
Figure 49 shows the PLUTON[108] drawings (hydrogens excluded) of the free macrocycle (co-ordinates from SHELX76) and the Ni^{2+} complex which was obtained in the following manner:-

The macrocycle data was loaded into CHEM-X and the 3D sketch mode entered. The Ni atom was placed approximately in the centre of the cavity. Bonds were then made between the donor and Ni atoms. The bond length parameters for the Ni-O and Ni-N bonds were then set at 2.23Å and 2.05Å respectively. These values were taken from analogous 2O,2N planar macrocyclic complexes[113]. These bond lengths were the only restraints imposed during refinement using the program's Energy Molecular Mechanics Optimise XYZ routine. During this routine the program optimises the energy of the molecule via bond rotation using set parameterised bond lengths etc. For a full description see reference 100.

As can be seen from the diagram above the most major rearrangement required to complex the Ni^{2+} ion occurs for the N-C-C-N bridge. In order that the lone pairs on the

nitrogen atoms are directed towards the metal ion the bridging carbons C23 and C24 must adopt a 'chelate ring' type geometry rather than the 'zig zag' geometry in the uncomplexed macrocycle. The torsion angle N1-C23-C24-N2 is 170.01° in the free macrocycle and 54.11° in the postulated complex. For the oxygen atoms to interact with the Ni^{2+} ion they are brought into the same plane as the Ni atom which necessitates the conformational change of the ether bridge. In the free macrocycle the three carbon atoms C27, C28 and C29 are approximately in the same plane with the oxygen atoms displaced similarly either side of this plane; O2-C27-C28-C29 = -58.49°, O1-C29-C28-C27 = -58.24°. In the postulated complex the carbon atoms C27 and C29 are approximately in the same plane as the two oxygen and Ni atoms with the C28 atom moved out to one side of the plane altering the torsion angles above to 67.31° and -80.85° respectively.

In another attempt to assess the macrocycle's suitability to form the postulated 'tetrahedral' complex the angular relationships of the donor atoms about the Ni atom were examined. For the postulated complex these were simply derived from CHEM-X;

O1-Ni-O2 = 100.87°   O1-Ni-N1 = 103.80°   O1-Ni-N2 = 122.96°

O2-Ni-N1 = 129.91°   O2-Ni-N2 = 103.11°   N1-Ni-N2 = 98.86°

For the free macrocycle the centre of the donor atoms was assessed by deleting all but the oxygen and nitrogen atoms and using CHEM-X, creating a mass centre. This was judged to be a reasonable approximation of the centre of the atoms due to their similar masses. The angular relationships about the mass centre could then be compared with those about the Ni atom for the postulated complex thus indicating how predisposed for complexation (ignoring lone pair directions) the donor atoms are.

In the list below M = mass centre.

$$O1-M-O2 = 78.12° \quad O1-M-N1 = 120.39° \quad O1-M-N2 = 135.50°$$

$$O2-M-N1 = 159.68° \quad O2-M-N2 = 87.04° \quad N1-M-N2 = 84.43°$$

As can be seen from the angular relationships the postulated complex has angles closer to the ideal tetrahedral angle of 109.47° with the free macrocycle having significant deviations from this. The molecular mechanics program CHEM-X when given the Ni-donor bond length restraints described minimises the energy of the complex which results in a 'tetrahedral' geometry about the Ni atom. However there are many other influences on the geometry unaccounted for, such as anions. Therefore attempts to obtain a tetrahedral complex of this type would require the use of non-coordinating anions.

As well as macrocyclic octahedral complexes containing a planar set of donor atoms there are N2O2 and N4 donor octahedral macrocyclic complexes[16,20,21] which have a β-cis configuration (see section 1.2.3) where the macrocycle is folded in the metal complex. One particular example of this is the complex Co(O-en-N-tn)(NCS)$_2$[20] whose geometry is shown below:-
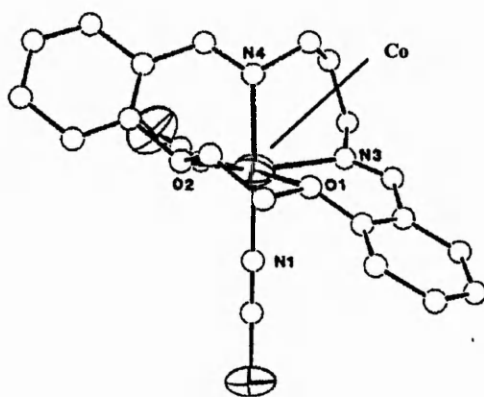
The angles between the macrocyclic donor atoms and the cobalt ion are given below of which four are comparable with the mass centre-donor angles for the free macrocycle in the present work:-

O1-Co-O2 = 75.5°   O1-Co-N3 = 80.7°   O1-Co-N4 = 95.5°

O2-Co-N3 = 150.9°   O2-Co-N4 = 81.0°   N3-Co-N4 = 85.0°

As can be seen from the edited free macrocycle diagram below the ring shape as well as the bond angles are similar to the cobalt complex above. There are obviously differences but it should be noted that the cobalt complex has three carbons between its nitrogen donors and two between its oxygen atoms whereas the reverse is the case for the free macrocycle.
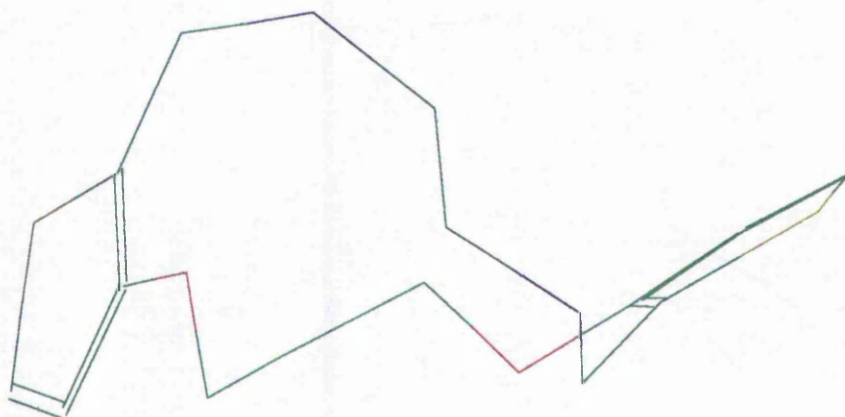
Therefore although the donor atoms of the free macrocycle are not directed towards the cavity there may be only relatively minor conformational changes required to complex metal ions in either a 'tetrahedral' or folded β-cis fashion.

3.11.2. 12,15-dibenzyl-2,5-dioxa-9,18-dithia-12,15-diazatricyclo[15.3.0^{6,10}]heneicosa-1^{17},19,6^{10},7-tetraene. (M2).

3.11.2.1. Crystal morphology.

The compound was obtained as a golden yellow powder after reaction work up. In order to obtain crystals the compound was redissolved in 1:1 methanol / DCM. The crystals obtained had similar morphology to the macrocycle M1. The tabular needles were obtained in inseparable stacks and no single crystals could be isolated for photographic examination. On dissolution in 1:1 ethanol / DCM single isolated crystals were obtained. The process of elucidating the space group of the crystals via X-ray photographs and the examination of the crystal's morphology were done concurrently due to the polymorphic nature of the crystals. To try and elucidate the crystal's point group many drawings of the crystal's morphology were made. The complicated morphology meant that examination of the crystal's extinctions under the polarising microscope was extremely difficult due to not knowing where one crystal face being examined was in relation to another. It was hoped that the morphology drawings would help with this. After much examination it was found that the major polymorph had the appearance described in the computer generated[107] drawings below (figure 50). It must be stressed that the representation is not an accurate depiction of one crystal but the general morphology of the major polymorph and some individual crystals varied in minor details from this. The face labels are speculative after X-ray photographs (Pca2$_1$ axes).

Figure 50.
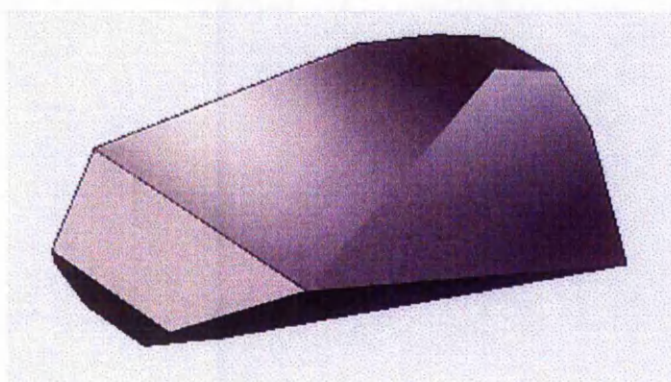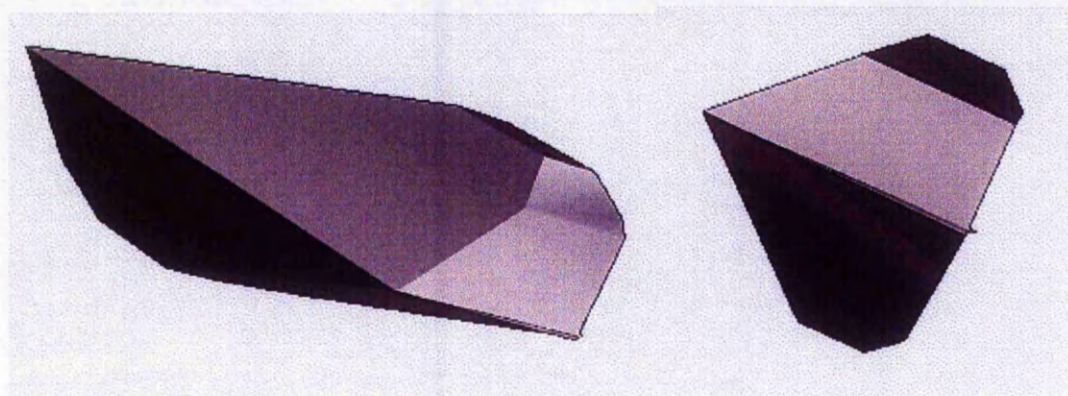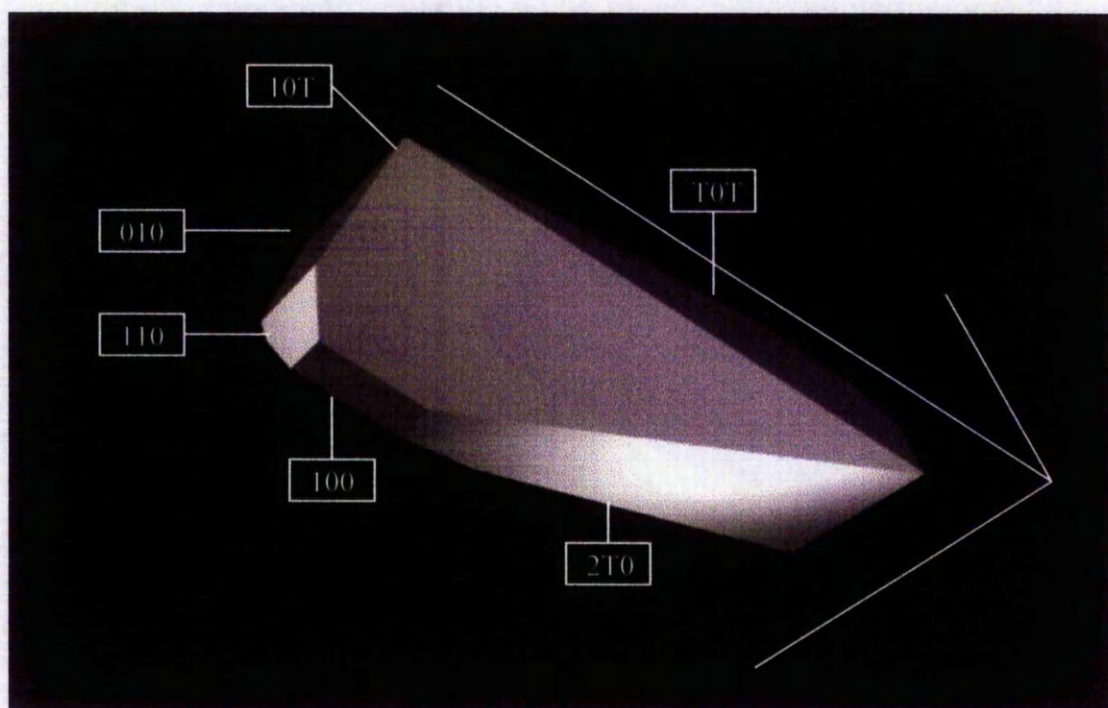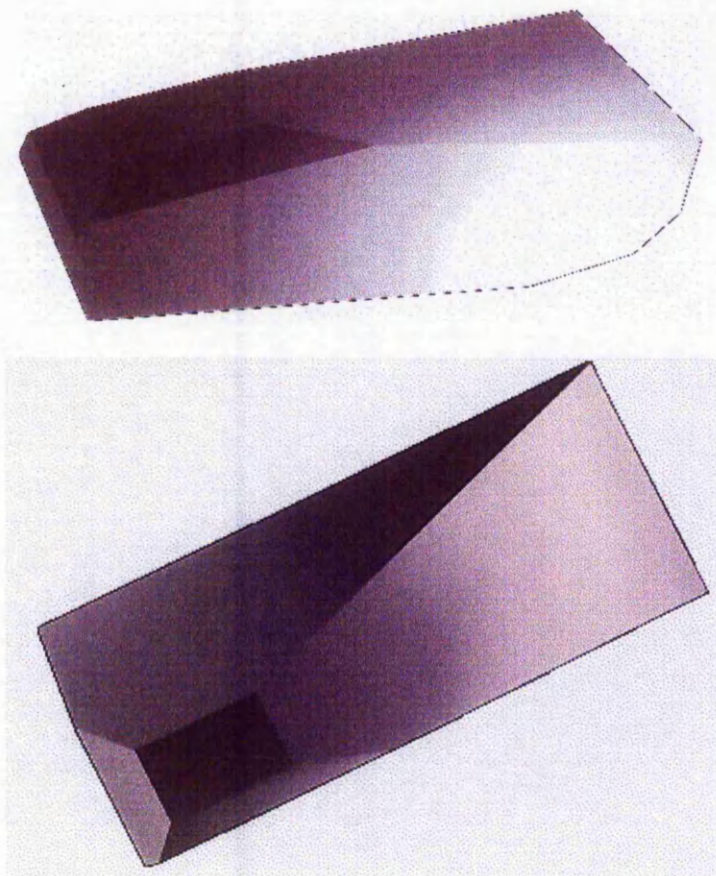
The morphology shown above did not seem to fit any one point group. There were however crystals with approximately the same population as those drawn above where the 100 face was centred along the b-axis with symmetrical faces either side of it (i.e. 110 and 1T0 or 210 and 2T0) which suggests the point group mm2. The one consistency for all of the polymorphs is the 001 face ($Pca2_1$ axes) which has extinctions every 90° occurring parallel to the 100 and 010 faces.

3.11.2.2. X-ray photographs.

The first indication of the more complicated nature of these crystals was some unusual streaking shown on the first set of Weissenberg photographs obtained when the crystal was set parallel to the longest crystal edge on the 001 face ($Pca2_1$ b-axis). Streaking on X-ray photographs is not uncommon (due to white radiation, especially when

photographs are over exposed) however the streaking shown (see figure 51) is of a different nature. Unlike that due to white radiation which tends to give streaks parallel (or nearly parallel) to the axes on the Weissenberg photographs, this streaking occurred between the spots on the festoons between the axes.

Figure 51.
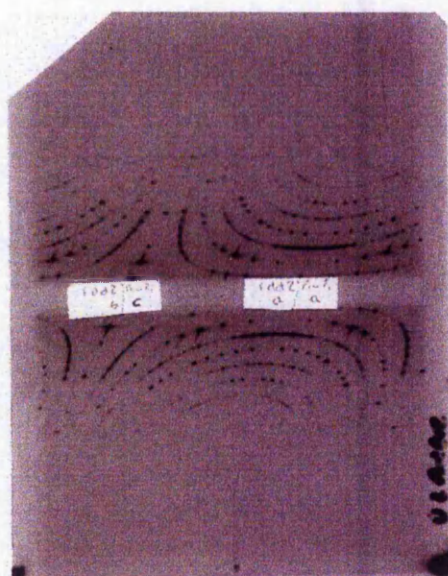
Zero Layer.   First Layer.
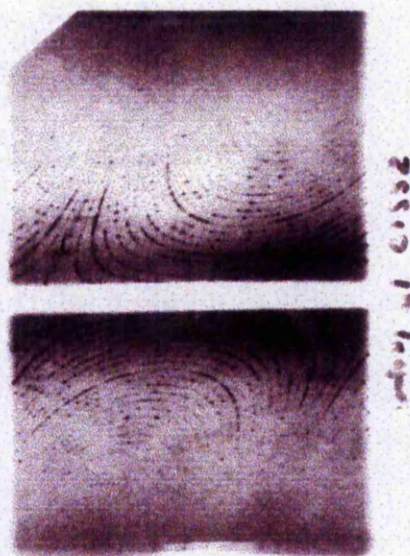
This streaking is indicative of disorder within the crystal. The disorder could be due to a stacking disorder where in travelling through the crystal in a certain direction there is a slight shift in the alignment of the unit cells which gives rise to the streaking seen. One possible reason for this might be the incorporation of solvent molecules during the crystallisation process which do not fit the symmetry of the unit cell developed or, the solvent molecules are unevenly distributed. Alternatively some other structural effect may give rise to the disorder. This is discussed further in section 3.11.2.7.2.

In order to determine whether or not solvent was incorporated within the crystals and if so which one (EtOH or DCM or both) and how much, the NMR and microanalysis

results were re-examined. Only the NMR prior to crystallisation (i.e. powder form compound) had been obtained, which showed no solvent peaks so the NMR of the compound after crystallisation was now examined. This NMR showed a singlet at 1.6 ppm (integral = 1 proton) which disappeared upon deuteration (and a small triplet whose integral was only a tenth of this). Assuming this to be the hydroxyl proton of ethanol substantiated solvent inclusion however the lack of evidence of the carbon chain made this only an assumption. The microanalysis results (obtained with and without drying) allowed for the inclusion of up to 1/2 EtOH per macrocycle however the results agreed much better with the inclusion of 1/4 EtOH per macrocycle (but see density measurement, section 3.11.2.3).

Apart from the streaking shown on one set of the photographs obtained, the sets of photographs obtained contradicted each other in terms of axis lengths and systematic absences in some cases and this pointed to more than one crystal type being present. This led to the adoption of more than one space group to explain the photographic evidence as this was obtained over a period of time. The task of resolving the differing polymorphs of these crystals could not be completed within the time available.

Overall it was decided that the space group of the most common polymorph was probably $Pca2_1$.

$Pca2_1$ conditions observed.	Conditions required.
(2) 0kl:- l = 2n (0k0:- k = 2n)*	l = 2n
(1) h0l:- h = 2n (h00:- h = 2n , 00l:- l = 2n)	h = 2n
(3) hk0:- (0k0:- k = 2n)*	No conditions.
	Plus :- h00:- h = 2n , 0k0:- No cond's, 00l:- l = 2n

*For this space group to be the correct choice requires the 0k0 condition to be spurious, later during intensity data collection some very weak intensity was found for some reflections with k odd.

The conditions for this space group are also satisfied by the centrosymmetric space group Pcam (non-standard setting of Pbcm) however the morphology of the crystals suggested the point group mm2 and therefore the noncentrosymmetric space group. The final choice of space group (Pca2$_1$) was made after some preliminary intensity data collection as not only were the X-ray photographs from different crystals contradictory but due to the polymorphic nature of the crystals the space group of the crystal chosen for data collection could not be assumed.

Approximate cell dimensions were obtained from the photographs but were obtained accurately on the diffractometer for the crystal used for intensity data collection.

3.11.2.3. Density measurement.

The density of the crystals was measured by flotation (section 2.11.1) at 1.33(2) g/cm^3. From the axis lengths obtained on the diffractometer the density calculated for 8 macrocycles per unit cell gives poor agreement (1.25 g/cm^3) with the measured density. When EtOH is included in the calculation at 3/4 of a molecule per macrocycle the density agrees with that measured. This is just outside the limits allowed from the microanalyses. The inclusion of 1/4 EtOH per macrocycle which gives the best fit for the microanalyses (if any solvent is included) gives a calculated density of 1.28 g/cm^3 whereas for 1/2 EtOH per macrocycle (still within microanalysis the results) gives a calculated density of 1.31 g/cm^3. The strong suggestion of solvent inclusion from the

185

density calculations may help to explain the disorder shown on the X-ray photographs. If the solvent molecule cannot fit the symmetry of the apparent space group in its position or if its positions are unevenly distributed throughout the crystal this could give rise to the disorder shown. It should also be noted that for the space group $Pca2_1$ the inclusion of eight macrocycles (plus possible EtOH) in the unit cell would require each asymmetric unit to consist of two macrocycles (plus possible EtOH).

3.11.2.4. Intensity data collection.

A good quality crystal having the morphology of similar crystals whose photographs gave the conditions for the space group $Pca2_1$ was chosen and mounted on a set of arcs about its a-axis. This axis was chosen as the most marked disorder occurred in the ac plane with little in the bc plane. The crystal was approximately set via an oscillation photograph and then transferred to the 2-circle diffractometer. The crystal was then centred and set using the diffractometer. The cell dimensions were refined by obtaining the centring, i.e. maximum intensity of about 20 chosen reflections and the cell dimensions used for data collection were :-

$a = 22.733$Å, $b = 11.397$Å, $c = 20.115$Å, α, β, $\gamma = 90°$.

Before the data collection proceeded some preliminary intensity measurements were undertaken to check the correct unit cell dimensions and space group symmetry had been chosen. Intensity data were collected up to and including the 19th layer, $\mu = 17.277$. It was noted that the intensity data after the 9th layer were extremely weak as can be observed on the X-ray photographs.

3.11.2.5. Data manipulation.

The data were manipulated in the same manner as section 3.11.1.5. Lorentz, polarisation and absorption corrections (crystal size = $1.00 \times 0.52 \times 0.52$ mm) were applied.

3.11.2.6. Structure solution.

After the success of the direct methods program MULTAN87 in providing a structure fragment which led to structure solution for M1 the same method was utilised for the X-ray data from M2. The program was run using the space group Pca2$_1$ but failed to give any recognisable fragments.

Interpretation of the Patterson map from SHELX76 was also tried without success. It should be noted that the Patterson map was very weak and when any atom coordinates from either the direct methods or the Patterson results were entered into SHELX76 for least squares refinement the resulting difference maps had peak heights corresponding to no more than 2.4 electrons. The structure was eventually solved using the PC versions of SHELXS97 and SHELXL97[115] programs.

SHELXS97 failed to provide any recognisable fragments using the default settings for the direct methods command TREF. When the number of direct methods attempts was increased from the default 100 to 5000 and the minimum and maximum E-values were set at 0.9 (default 1.2) and 6.0 (default 5.0) respectively the program gave a solution with CFOM (combined figure of merit) = 15.1 which contained two fragments recognisable as thiophene rings. The program ORTEX[116] was used to view the output files from both SHELXS97 and SHELXL97. The coordinates of the thiophene rings

were input into the structure refinement program SHELXL97 for four cycles of least squares and a difference map produced. The coordinates of the 20 new peaks determined from this were added to those already found and visualised using ORTEX. The peaks which could be recognised as part of the macrocycle(s) were kept and refined via SHELXL97, the rest were discarded. Repeating this cycle of adding recognisable peaks from successive difference maps was continued until all the atoms of the structure had been found (after 15 difference maps). As expected from the density measurement, the asymmetric unit consisted of two macrocycles. At this stage the atom coordinates were transferred to the SHELX76 input file. SHELX76 was used to refine the structure as for the previous structure, M1.

3.11.2.6.1 Structure refinement.

The reflection data file was checked for beam stop affected reflections i.e low angle reflections with F_o much less than F_c and eight reflections were removed.

The structure was refined in much the same way as for M1. Overall and interlayer scale factors were introduced and refined from 1.0. The four benzene rings (the asymmetric unit consists of two macrocycles) were constrained into regular hexagons using AFIX 66 with C17, C24, C17A and C24A as the pivot atoms. The positional parameters were refined with fixed isotropic temperature factors of 0.05 in two blocks, one for each macrocycle due to the large number of parameters. The isotropic temperature factors were refined. Anisotropic temperature factors were not introduced as the intensity data was much weaker than in the previous structure and the ratio of data to parameters would have been extremely small. The hydrogen atoms were introduced riding on their

respective carbon atoms with fixed isotropic temperature factors of 0.06. Overall and interlayer scale factors were refined separately. In the last refinement run the positional and non hydrogen isotropic temperature factors were refined to give R = 0.1347 using OMIT 6. A difference map for the last run had a maximum peak corresponding to 0.54 e$Å^{-3}$. In total 242 parameters were refined using 1245 reflections giving a reflection to parameter ratio of 5.1 : 1.

3.11.2.7. Discussion of the structure.

Given below is a summary of the crystal, data collection and refinement data.

Empirical Formula	C28 H30 N2 O2 S2
Formula Weight	490.69
Crystal System	Orthorhombic
Space group	Pca2$_1$ (No. 29)
a, b, c [Å]	22.733 11.397 20.115
α, β, γ	90° 90° 90°
V [Å^3]	5211.56
Z	8
D(obs), D(calc) [g/cm^3]	1.33, 1.251
F(000) [Electrons]	2080
μ (MoKα) [/cm]	1.90
Crystal Size [mm]	1.00 x 0.52 x 0.52
Temperature [°C]	35-40
Radiation [Å]	MoKα 0.7107
Theta Min-Max	3.0°, 60.0°

189

Scan Type	variable ω scan
Hor. and vert. aperture [mm]	1.00 1.00
Standard	measured every 10 reflections
	(different for each layer line)
Dataset ± h : ± k : ± l	0:19 ; 0:16 ; 0:20
Tot., Uniq. Data, R(int)	5499, 5275, 0.000
Min./Max. Transmission factors	0.82, 0.91
Observed data [I > 6.0 sigma(I)]	1245
(Observed data [I > 4.0 sigma(I)])	1737
Nref, Npar	1245, 242
R, S	0.1347, 2.48

3.11.2.7.1. Derived structural data.

Estimated standard deviations are given in brackets.

FRACTIONAL COORDINATES AND ISOTROPIC TEMPERATURE FACTORS.				
ATOM	X	Y	Z	U(ISO)
MOLECULE 1				
S1	0.0953(8)	0.0468(14)	0.4869(9)	0.107(5)
S2	0.1807(6)	-0.0137(14)	0.8271(7)	0.083(4)
O1	0.2332(12)	-0.140(2)	0.5203(15)	0.064(9)
O2	0.2453(12)	-0.037(2)	0.6528(13)	0.049(8)
N1	0.072(2)	-0.198(4)	0.579(2)	0.100(15)
N2	0.0777(17)	-0.053(3)	0.7168(19)	0.072(12)
C1	0.1497(15)	-0.078(3)	0.5046(18)	0.028(10)
C2	0.1985(12)	-0.042(2)	0.5062(13)	0.000(7)
C3	0.2046(13)	0.069(3)	0.4921(15)	0.013(8)
C4	0.1660(19)	0.129(4)	0.479(2)	0.052(12)
C5	0.1083(18)	-0.188(3)	0.514(2)	0.052(13)
C6	0.1180(17)	-0.207(4)	0.6393(18)	0.044(12)
C7	0.087(2)	-0.185(4)	0.705(3)	0.082(17)
C8	0.128(2)	0.029(4)	0.702(3)	0.083(17)
C9	0.183(3)	-0.004(5)	0.741(3)	0.098(19)
C10	0.235(2)	-0.034(4)	0.721(2)	0.056(13)

C11	0.282(3)	-0.058(5)	0.770(3)	0.12(2)
C12	0.259(2)	-0.052(4)	0.823(3)	0.068(15)
C13	0.282(2)	-0.121(4)	0.627(2)	0.077(16)
C14	0.2917	-0.1069	0.5495	0.067(15)
C15	0.0277(15)	-0.285(3)	0.5803(18)	0.025(9)
C16	-0.0232	-0.2612	0.5263	0.000(6)
C17	-0.0498(11)	-0.1517(17)	0.5190(12)	0.054(13)
C18	-0.093	-0.135	0.4706	0.057(13)
C19	-0.1095	-0.2279	0.4295	0.053(13)
C20	-0.0829	-0.3374	0.4368	0.075(15)
C21	-0.0398	-0.3541	0.4852	0.079(16)
C22	0.025(3)	-0.005(5)	0.694(3)	0.11(2)
C23	-0.0062	0.0816	0.7321	0.072(16)
C24	-0.0489(16)	0.153(3)	0.7026(13)	0.10(2)
C25	-0.0797	0.234	0.7409	0.089(18)
C26	-0.0678	0.2446	0.8087	0.060(14)
C27	-0.0251	0.1737	0.8381	0.057(13)
C28	0.0057	0.0922	0.7998	0.077(16)
H1	0.3278	-0.0788	0.7591	0.06
H2	0.2843	-0.0654	0.8673	0.06
H3	0.3242	-0.1158	0.6512	0.06
H4	0.2628	-0.2063	0.6358	0.06
H5	0.3265	-0.1637	0.5319	0.06
H6	0.3023	-0.017	0.5376	0.06
H7	0.0475	-0.3696	0.5708	0.06
H8	0.0079	-0.2853	0.6292	0.06
H9	-0.037	-0.0798	0.5508	0.06
H10	-0.1139	-0.0504	0.4653	0.06
H11	-0.1433	-0.2152	0.3924	0.06
H12	-0.0959	-0.4094	0.4051	0.06
H13	-0.019	-0.4388	0.4906	0.06
H14	0.0341	0.0327	0.6456	0.06
H15	-0.0047	-0.078	0.6884	0.06
H16	-0.0583	0.145	0.6501	0.06
H17	-0.1123	0.2894	0.7189	0.06
H18	-0.0908	0.3065	0.8391	0.06
H19	-0.0153	0.1793	0.8906	0.06
H20	0.0388	0.035	0.8219	0.06
H21	0.2483	0.1059	0.4916	0.06
H22	0.1699	0.2201	0.4645	0.06
H23	0.1362	-0.2649	0.5119	0.06
H24	0.0775	-0.1898	0.4735	0.06
H25	0.1524	-0.143	0.6318	0.06
H26	0.1369	-0.2939	0.6402	0.06
H27	0.1141	-0.218	0.7443	0.06
H28	0.0449	-0.2293	0.7053	0.06

H29	0.1371	0.0265	0.6489	0.06
H30	0.1148	0.1161	0.7158	0.06
MOLECULE 2				
S1A	0.2764(5)	-0.4467(10)	0.7728(6)	0.053(3)
S2A	0.1905(8)	-0.5000(16)	0.4462(9)	0.105(5)
O1A	0.1450(14)	-0.651(3)	0.7602(17)	0.079(10)
O2A	0.1234(17)	-0.544(3)	0.621(2)	0.110(13)
N1A	0.3037(10)	-0.6886(18)	0.6856(12)	0.003(6)
N2A	0.2974(14)	-0.540(3)	0.5517(15)	0.041(9)
C1A	0.2458(13)	-0.584(2)	0.7570(13)	0.000(6)
C2A	0.185(2)	-0.563(5)	0.762(3)	0.078(16)
C3A	0.166(2)	-0.437(5)	0.770(3)	0.089(16)
C4A	0.2198(19)	-0.365(4)	0.776(2)	0.061(13)
C5A	0.2722(19)	-0.695(4)	0.747(2)	0.060(14)
C6A	0.2687(17)	-0.717(3)	0.6337(18)	0.042(12)
C7A	0.2895(16)	-0.672(3)	0.5621(17)	0.031(10)
C8A	0.246(2)	-0.471(4)	0.567(2)	0.071(15)
C9A	0.1906(18)	-0.500(3)	0.5318(17)	0.030(10)
C10A	0.1427(15)	-0.541(3)	0.5573(18)	0.020(9)
C11A	0.1018(17)	-0.569(3)	0.5076(19)	0.042(11)
C12A	0.127(3)	-0.547(5)	0.445(3)	0.10(2)
C13A	0.089(2)	-0.639(4)	0.651(2)	0.079(16)
C14A	0.0984	-0.6443	0.7237	0.061(14)
C15A	0.3576(17)	-0.767(4)	0.692(2)	0.056(13)
C16A	0.4032	-0.729	0.7369	0.081(16)
C17A	0.4231(13)	-0.812(2)	0.7830(17)	0.065(14)
C18A	0.467	-0.7814	0.8283	0.061(14)
C19A	0.491	-0.6688	0.8276	0.061(14)
C20A	0.4711	-0.5863	0.7816	0.11(2)
C21A	0.4272	-0.6164	0.7363	0.080(16)
C22A	0.3525(12)	-0.493(2)	0.5782(13)	0.000(7)
C23A	0.3777	-0.3965	0.5331	0.052(13)
C24A	0.4249(11)	-0.332(2)	0.5581(11)	0.013(8)
C25A	0.4484	-0.2396	0.5211	0.082(16)
C26A	0.4246	-0.2117	0.4591	0.067(15)
C27A	0.3774	-0.2762	0.4342	0.075(16)
C28A	0.3539	-0.3686	0.4711	0.048(12)
H1A	0.058	-0.6027	0.5154	0.06
H2A	0.1035	-0.5608	0.3988	0.06
H3A	0.0433	-0.6258	0.6405	0.06
H4A	0.1036	-0.721	0.6293	0.06
H5A	0.0728	-0.7195	0.7388	0.06
H6A	0.0775	-0.5651	0.7413	0.06
H7A	0.3769	-0.7728	0.6425	0.06
H8A	0.3429	-0.8525	0.7071	0.06
H9A	0.4046	-0.8988	0.784	0.06

H10A	0.4822	-0.8435	0.8644	0.06
H11A	0.5246	-0.6436	0.8621	0.06
H12A	0.4895	-0.4989	0.7794	0.06
H13A	0.4119	-0.5542	0.699	0.06
H14A	0.3443	-0.4558	0.6268	0.06
H15A	0.3839	-0.5634	0.5825	0.06
H16A	0.4432	-0.3537	0.6061	0.06
H17A	0.4849	-0.1895	0.5408	0.06
H18A	0.443	-0.1398	0.4308	0.06
H19A	0.3594	-0.2543	0.386	0.06
H20A	0.3177	-0.4186	0.4513	0.06
H21A	0.1217	-0.4043	0.771	0.06
H22A	0.2206	-0.2707	0.7817	0.06
H23A	0.3016	-0.7156	0.787	0.06
H24A	0.2387	-0.7619	0.743	0.06
H25A	0.2663	-0.8115	0.6312	0.06
H26A	0.2254	-0.6817	0.6429	0.06
H27A	0.2575	-0.7023	0.5263	0.06
H28A	0.3316	-0.7117	0.5519	0.06
H29A	0.2377	-0.4803	0.6199	0.06
H30A	0.256	-0.3799	0.5565	0.06

** Note the positions are to four decimal places with terminal zeros omitted.

The coordinates with no esd's were not refined.

The estimated standard deviations for the atomic positions are up to ten times those in the M1 structure indicating the lower precision of the data and the lower degree of certainty that can be placed on the atomic positions. The isotropic temperature factors are also in some cases obviously not representative of the thermal motion but are rather soaking up inadequacies in the model. The high R factor also indicates that the model doesn't fit the intensity data as well as would be desired. The reasons that the model should be generally accepted and the quality of the intensity data questioned are outlined below:

The choice of the space group Pca2$_1$ is correct as judged by the fact that no additional symmetry is evident from the use of the MISSYM[117] algorithm in PLATON97 and that the structure could not be solved and failed to refine in any of the other possible space groups. The orientation of the two molecules which make up the asymmetric unit make sense chemically with no intermolecular non-hydrogen atom contacts less than 3.5Å. Although some of the bond lengths and angles (see later discussion) are unusual this is a consequence of the lack of precision with which the atoms can be placed. The fact that the final Fourier difference map shows no significant electron density indicates that there is no solvent included within the unit cell as confirmed by PLATON which calculates only 29Å^3 of potential solvent area out of the unit cell volume of 5212Å^3. The absence of solvent within the crystal means that there is a discrepancy of approximately 0.08g/cm^3 in the calculated and measured densities. These two facts along with the esd's for the Y co-ordinates being approximately twice those of the X and Z co-ordinates may indicate errors in the size of the unit cell especially the b-axis length (the larger esd's for the b-axis coordinates could also be due to absorption as this is the longest crystal dimension). Other indications of the poorer quality of the X-ray data is its weak nature and the unresolved disorder demonstrated on the X-ray photographs. The absorption correction applied by SHELX76 is also of greater inadequacy for this crystal compared to that applied to the data from M1 as the crystal was approximated to a box (symmetry = mmm) whereas the crystal habit is much more complex (with mm2 symmetry).

The minimum overlap view of the asymmetric unit comprised of two molecules of the macrocycle is shown in figure 52 with hydrogen atoms omitted for clarity.

Figure 52.

The atomic radii are drawn at half the covalent radii*
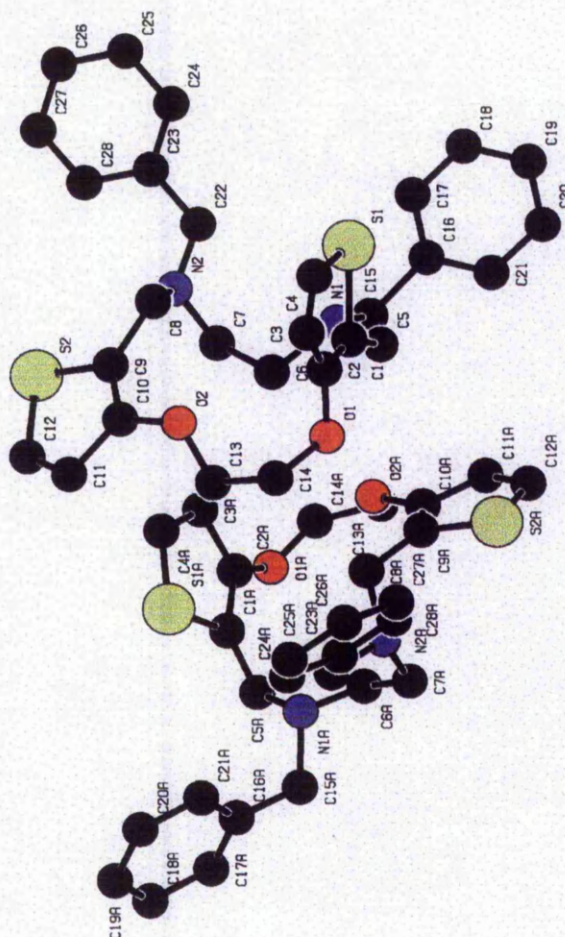
* S = 1.02Å, O = 0.68Å, N = 0.68Å, C = 0.68Å[11]

The two molecules which make up the asymmetric unit have very similar geometries and are shown individually in figure 53. Both molecules are drawn as projected down the b-axis with Molecule 1 having been rotated 180° in the plane of the projection, please note due to this the labels are upside down.

Figure 53.

Molecule 1.
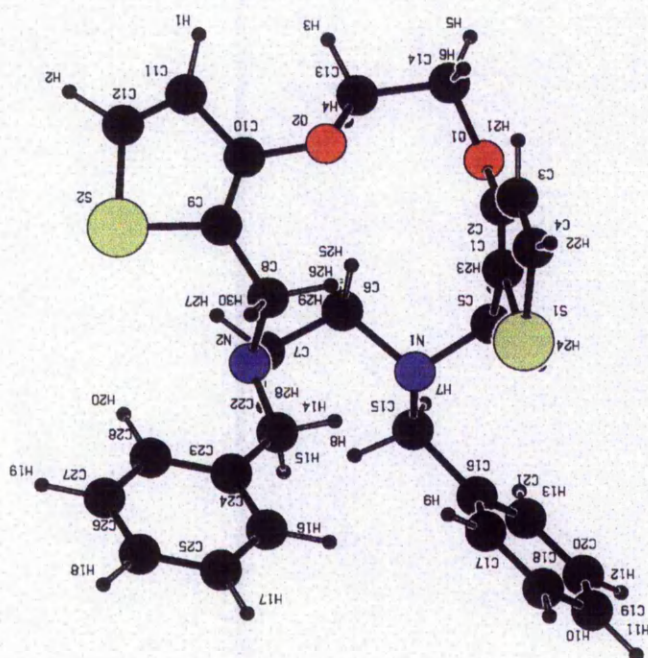
Molecule 2.
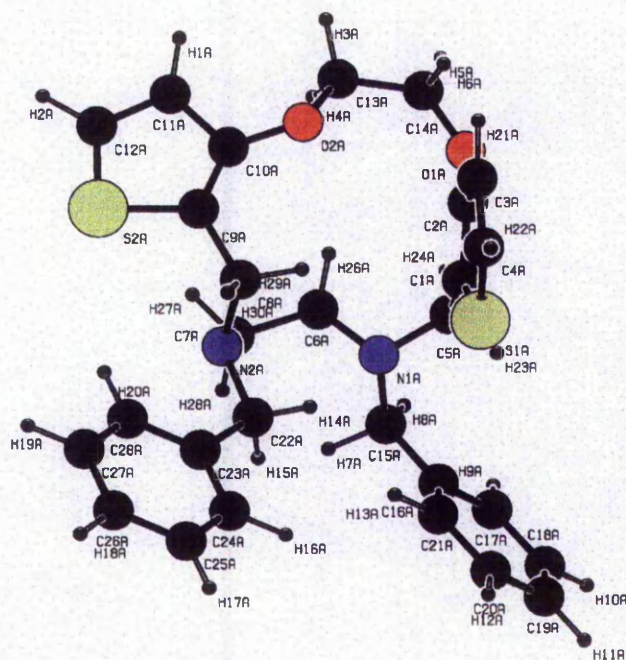
The structural geometry and relationships of the two macrocycles are discussed in section 3.11.2.7.2.

BOND LENGTHS				
BOND	LENGTH(Å)	BOND		LENGTH(Å)
MOLECULE 1				
S1 -C1	1.92(4)	C24	-C25	1.39(3)
S1 -C4	1.87(5)	C25	-C26	1.40
S2 -C9	1.74(6)	C26	-C27	1.39
S2 -C12	1.83(5)	C27	-C28	1.40
O1 -C2	1.40(3)	C3	-H21	1.08
O1 -C14	1.50(3)	C4	-H22	1.08
O2 -C10	1.39(5)	C5	-H23	1.08
O2 -C13	1.37(5)	C5	-H24	1.07
N1 -C5	1.55(6)	C6	-H25	1.08
N1 -C6	1.60(6)	C6	-H26	1.08
N1 -C15	1.41(6)	C7	-H27	1.07
N2 -C7	1.54(6)	C7	-H28	1.08
N2 -C8	1.51(6)	C8	-H29	1.09
N2 -C22	1.39(8)	C8	-H30	1.07
C1 -C2	1.18(4)	C11	-H1	1.09
C1 -C5	1.58(5)	C12	-H2	1.07
C2 -C3	1.30(4)	C13	-H3	1.08
C3 -C4	1.14(5)	C13	-H4	1.08
C6 -C7	1.52(7)	C14	-H5	1.08
C8 -C9	1.52(8)	C14	-H6	1.08
C9 -C10	1.29(8)	C15	-H7	1.08
C10 -C11	1.48(8)	C15	-H8	1.08
C11 -C12	1.19(8)	C17	-H9	1.08
C13 -C14	1.58(4)	C18	-H10	1.08
C15 -C16	1.61(4)	C19	-H11	1.08
C16 -C17	1.39(2)	C20	-H12	1.08
C16 -C21	1.40	C21	-H13	1.08
C17 -C18	1.40(2)	C22	-H14	1.08
C18 -C19	1.40	C22	-H15	1.08
C19 -C20	1.39	C24	-H16	1.08
C20 -C21	1.39	C25	-H17	1.07
C22 -C23	1.44(6)	C26	-H18	1.07
C23 -C24	1.40(3)	C27	-H19	1.08
C23 -C28	1.39	C28	-H20	1.09
MOLECULE 2				
S1A -C1A	1.74(3)	C24A	-C25A	1.40(2)
S1A -C4A	1.59(5)	C25A	-C26A	1.40
S2A -C9A	1.72(4)	C26A	-C27A	1.39
S2A -C12A	1.54(7)	C27A	-C28A	1.39

197

O1A -C2A	1.35(6)	C3A -H21A	1.07
O1A -C14A	1.29(3)	C4A -H22A	1.08
O2A -C10A	1.35(5)	C5A -H23A	1.07
O2A -C13A	1.47(6)	C5A -H24A	1.08
N1A -C5A	1.43(5)	C6A -H25A	1.08
N1A -C6A	1.35(4)	C6A -H26A	1.08
N1A -C15A	1.52(5)	C7A -H27A	1.08
N2A -C7A	1.53(5)	C7A -H28A	1.08
N2A -C8A	1.44(6)	C8A -H29A	1.09
N2A -C22A	1.46(4)	C8A -H30A	1.08
C1A -C2A	1.41(5)	C11A -H1A	1.08
C1A -C5A	1.41(5)	C12A -H2A	1.08
C2A -C3A	1.51(8)	C13A -H3A	1.07
C3A -C4A	1.48(7)	C13A -H4A	1.08
C6A -C7A	1.60(5)	C14A -H5A	1.08
C8A -C9A	1.48(6)	C14A -H6A	1.08
C9A -C10A	1.29(5)	C15A -H7A	1.09
C10A -C11A	1.40(5)	C15A -H8A	1.07
C11A -C12A	1.41(7)	C17A -H9A	1.08
C13A -C14A	1.48(4)	C18A -H10A	1.07
C15A -C16A	1.44(4)	C19A -H11A	1.07
C16A -C17A	1.40(3)	C20A -H12A	1.08
C16A -C21A	1.39	C21A -H13A	1.09
C17A -C18A	1.40(3)	C22A -H14A	1.08
C18A -C19A	1.39	C22A -H15A	1.08
C19A -C20A	1.39	C24A -H16A	1.08
C20A -C21A	1.39	C25A -H17A	1.08
C22A -C23A	1.54(2)	C26A -H18A	1.08
C23A -C24A	1.39(2)	C27A -H19A	1.08
C23A -C28A	1.40	C28A -H20A	1.08

The bond lengths and following derived data were all obtained via the crystallographic program tool PLATON[108].

Only limited discussion of the bond lengths can be made due to their lack of precision. The S1-C1 bond length minus 3σ is still 1.80Å, which is 0.061Å greater than the longest S-C bond (+ 3σ) from M1. The C3-C4 bond length + 3σ = 1.29Å which is

0.038Å shorter than the shortest corresponding bond (-3σ) in M1. All other bond lengths are within 3σ of chemically accepted values[109].

BOND ANGLES				
BOND		ANGLE(°)	BOND		ANGLE(°)
MOLECULE 1				
C1	-S1	-C4	80.4(19)	N1	-C6	-H25	108.85
C9	-S2	-C12	87(3)	N1	-C6	-H26	109.31
C2	-O1	-C14	112.3(19)	C7	-C6	-H25	110.25
C10	-O2	-C13	119(3)	C7	-C6	-H26	108.76
C5	-N1	-C6	107(3)	H25	-C6	-H26	109.49
C5	-N1	-C15	117(3)	N2	-C7	-H27	107.99
C6	-N1	-C15	114(3)	N2	-C7	-H28	109.51
C7	-N2	-C8	118(4)	C6	-C7	-H27	108.52
C7	-N2	-C22	117(4)	C6	-C7	-H28	109.77
C8	-N2	-C22	110(4)	H27	-C7	-H28	109.94
S1	-C1	-C2	111(3)	N2	-C8	-H29	108.78
S1	-C1	-C5	103(2)	N2	-C8	-H30	108.08
C2	-C1	-C5	146(3)	C9	-C8	-H29	110.06
O1	-C2	-C1	105(3)	C9	-C8	-H30	108.94
O1	-C2	-C3	139(3)	H29	-C8	-H30	109.34
C1	-C2	-C3	115(3)	C10	-C11	-H1	126.59
C2	-C3	-C4	123(4)	C12	-C11	-H1	127.78
S1	-C4	-C3	110(3)	S2	-C12	-H2	121.15
N1	-C5	-C1	118(3)	C11	-C12	-H2	120.08
N1	-C6	-C7	110(3)	O2	-C13	-H3	109.4
N2	-C7	-C6	111(4)	O2	-C13	-H4	108.68
N2	-C8	-C9	112(4)	C14	-C13	-H3	108.38
S2	-C9	-C8	120(5)	C14	-C13	-H4	108
S2	-C9	-C10	109(4)	H3	-C13	-H4	109.59
C8	-C9	-C10	131(5)	O1	-C14	-H5	111.67
O2	-C10	-C9	118(4)	O1	-C14	-H6	110.45
O2	-C10	-C11	122(4)	C13	-C14	-H5	111.31
C9	-C10	-C11	120(5)	C13	-C14	-H6	110.24
C10	-C11	-C12	106(6)	H5	-C14	-H6	109.4
S2	-C12	-C11	119(5)	N1	-C15	-H7	109.01
O2	-C13	-C14	113(3)	N1	-C15	-H8	108.39
O1	-C14	-C13	104(2)	C16	-C15	-H7	109.28
N1	-C15	-C16	112(3)	C16	-C15	-H8	108.36
C15	-C16	-C17	122.2(16)	H7	-C15	-H8	109.34
C15	-C16	-C21	117.8(12)	C16	-C17	-H9	120
C17	-C16	-C21	120.0(10)	C18	-C17	-H9	119.96
C16	-C17	-C18	120.0(15)	C17	-C18	-H10	120
C17	-C18	-C19	119.9(8)	C19	-C18	-H10	120.06
C18	-C19	-C20	120.02	C18	-C19	-H11	119.92

C19	-C20	-C21	120.03	C20	-C19	-H11	120.05
C16	-C21	-C20	120.01	C19	-C20	-H12	119.93
N2	-C22	-C23	121(5)	C21	-C20	-H12	120.04
C22	-C23	-C24	121(3)	C16	-C21	-H13	120
C22	-C23	-C28	119(2)	C20	-C21	-H13	119.98
C24	-C23	-C28	119.9(12)	N2	-C22	-H14	106.67
C23	-C24	-C25	120.0(19)	N2	-C22	-H15	105.65
C24	-C25	-C26	120.1(12)	C23	-C22	-H14	107.51
C25	-C26	-C27	119.94	C23	-C22	-H15	106.07
C26	-C27	-C28	120.06	H14	-C22	-H15	109.38
C23	-C28	-C27	119.99	C23	-C24	-H16	120.16
C2	-C3	-H21	118.57	C25	-C24	-H16	119.82
C4	-C3	-H21	118.13	C24	-C25	-H17	120.75
S1	-C4	-H22	125.09	C26	-C25	-H17	119.18
C3	-C4	-H22	124.97	C25	-C26	-H18	121.39
N1	-C5	-H23	106.57	C27	-C26	-H18	118.67
N1	-C5	-H24	106.93	C26	-C27	-H19	121.56
C1	-C5	-H23	106.79	C28	-C27	-H19	118.38
C1	-C5	-H24	108.23	C23	-C28	-H20	118.72
H23	-C5	-H24	109.68	C27	-C28	-H20	121.28
MOLECULE 2							
C1A	-S1A	-C4A	102(2)	N1A	-C6A	-H25A	107.73
C9A	-S2A	-C12A	91(3)	N1A	-C6A	-H26A	108.37
C2A	-O1A	-C14A	121(3)	C7A	-C6A	-H25A	107.02
C10A	-O2A	-C13A	126(3)	C7A	-C6A	-H26A	107.72
C5A	-N1A	-C6A	111(3)	H25A	-C6A	-H26A	109.5
C5A	-N1A	-C15A	107(3)	N2A	-C7A	-H27A	107.6
C6A	-N1A	-C15A	113(3)	N2A	-C7A	-H28A	106.41
C7A	-N2A	-C8A	114(3)	C6A	-C7A	-H27A	107.37
C7A	-N2A	-C22A	114(3)	C6A	-C7A	-H28A	107.4
C8A	-N2A	-C22A	115(3)	H27A	-C7A	-H28A	109.68
S1A	-C1A	-C2A	103(3)	N2A	-C8A	-H29A	107.26
S1A	-C1A	-C5A	131(3)	N2A	-C8A	-H30A	108.12
C2A	-C1A	-C5A	125(3)	C9A	-C8A	-H29A	107.38
O1A	-C2A	-C1A	122(4)	C9A	-C8A	-H30A	107.39
O1A	-C2A	-C3A	121(4)	H29A	-C8A	-H30A	108.72
C1A	-C2A	-C3A	117(4)	C10A	-C11A	-H1A	126.12
C2A	-C3A	-C4A	107(4)	C12A	-C11A	-H1A	124.74
S1A	-C4A	-C3A	110(4)	S2A	-C12A	-H2A	121.75
N1A	-C5A	-C1A	107(3)	C11A	-C12A	-H2A	122.78
N1A	-C6A	-C7A	116(3)	O2A	-C13A	-H3A	109.43
N2A	-C7A	-C6A	118(3)	O2A	-C13A	-H4A	107.93
N2A	-C8A	-C9A	118(3)	C14A	-C13A	-H3A	109.93
S2A	-C9A	-C8A	119(3)	C14A	-C13A	-H4A	108.59
S2A	-C9A	-C10A	113(3)	H3A	-C13A	-H4A	109.81
C8A	-C9A	-C10A	127(3)	O1A	-C14A	-H5A	103.61

O2A	-C10A	-C9A	131(4)	O1A	-C14A -H6A	102.95
O2A	-C10A	-C11A	117(3)	C13A	-C14A -H5A	103.46
C9A	-C10A	-C11A	111(3)	C13A	-C14A -H6A	103.09
C10A	-C11A	-C12A	109(4)	H5A	-C14A -H6A	109.52
S2A	-C12A	-C11A	115(4)	N1A	-C15A -H7A	106.4
O2A	-C13A	-C14A	111(3)	N1A	-C15A -H8A	107.82
O1A	-C14A	-C13A	133(2)	C16A	-C15A -H7A	107.52
N1A	-C15A	-C16A	117(3)	C16A	-C15A -H8A	108.61
C15A	-C16A	-C17A	116(2)	H7A	-C15A -H8A	109.18
C15A	-C16A	-C21A	123.5(18)	C16A	-C17A -H9A	120.52
C17A	-C16A	-C21A	120.1(11)	C18A	-C17A -H9A	119.83
C16A	-C17A	-C18A	119.7(17)	C17A	-C18A -H10A	120.54
C17A	-C18A	-C19A	120.2(10)	C19A	-C18A -H10A	119.25
C18A	-C19A	-C20A	120.01	C18A	-C19A -H11A	121.28
C19A	-C20A	-C21A	119.99	C20A	-C19A -H11A	118.71
C16A	-C21A	-C20A	120.05	C19A	-C20A -H12A	121.52
N2A	-C22A	-C23A	111(2)	C21A	-C20A -H12A	118.48
C22A	-C23A	-C24A	116.8(13)	C16A	-C21A -H13A	118.68
C22A	-C23A	-C28A	123.1(10)	C20A	-C21A -H13A	121.24
C24A	-C23A	-C28A	120.0(9)	N2A	-C22A -H14A	108.98
C23A	-C24A	-C25A	120.0(16)	N2A	-C22A -H15A	108.9
C24A	-C25A	-C26A	120.0(10)	C23A	-C22A -H14A	108.50
C25A	-C26A	-C27A	119.95	C23A	-C22A -H15A	109.48
C26A	-C27A	-C28A	120.12	H14A	-C22A -H15A	109.48
C23A	-C28A	-C27A	119.93	C23A	-C24A -H16A	119.87
C2A	-C3A	-H21A	126.94	C25A	-C24A -H16A	120.13
C4A	-C3A	-H21A	125.58	C24A	-C25A -H17A	119.75
S1A	-C4A	-H22A	124.96	C26A	-C25A -H17A	120.26
C3A	-C4A	-H22A	125.08	C25A	-C26A -H18A	119.52
N1A	-C5A	-H23A	110.32	C27A	-C26A -H18A	120.53
N1A	-C5A	-H24A	108.95	C26A	-C27A -H19A	119.45
C1A	-C5A	-H23A	110.71	C28A	-C27A -H19A	120.42
C1A	-C5A	-H24A	110.03	C23A	-C28A -H20A	120.38
H23A	-C5A	-H24A	109.92	C27A	-C28A -H20A	119.69

Again only limited inferences can be made from the bond angles due to their imprecise nature. The angle C1-S1-C5 = 80.4(19)° +3σ = 86.1° which is 6° less than the smallest corresponding angle (-3σ) in M1. The angle O1A-C14A-C13A = 133(2)° -3σ = 127° which is 17.2° greater than the largest corresponding angle (+3σ) in M1. Other notably

large angles are: C2-C1-C5, O1-C2-C3, C8-C9-C10, S1A-C1A-C5A, O2A-C10A-C9A, C8A-C9A-C10A.

3.11.2.7.2. Discussion of structural geometry.

The asymmetric unit consists of two isolated macrocycles. The two macrocycles are not related by crystallographic (space group) symmetry* but may be approximately related to one another by rotation[108] through 179.67° via the direct lattice vector [-0.020 1.000 0.011] and an associated shift of –5.718Å. The RMS fit (hydrogens excluded) between the two macrocycles is then 0.258Å calculated using PLATON. The similarity between the two macrocycles (which results in this fairly good fit) can be seen in figure 53 where molecule 1 has been rotated 180° in the plane of the paper with regard to molecule 2. The most significant differences between the two macrocycles occur between O2 and N1 incorporating the S1 thiophene ring. The bridge containing the two oxygen atoms have slightly different geometries and the S1A thiophene ring plane is at a slightly acuter angle to the plane of the S2A thiophene ring compared with that between the S1 and S2 ring planes. There are also differences in comparable bond lengths and angles but overall the two macrocycles have similar geometries.

* All attempts at relating one of the molecules of the asymmetric unit to the other via space group symmetry, i.e. which would reduce the asymmetric unit to just one molecule, failed. The shift of approximately half (5.718Å) the b-axis can be mimicked by introducing four further equivalent positions as for Pca2$_1$ and adding 1/2 to the y component but in no way can the rotation be introduced via crystallographic symmetry. The symmetry relationship between the two molecules approximates to a 2$_1$ screw axis

parallel to b but this is not at 1/4 of the unit cell. This psuedo 2_1 axis may account for the near extinction of the odd 0k0 reflections. The only higher symmetry space group which is non-centrosymmetric and contains suitable positions is Fdd2 which has 16 equivalent positions. To match this space group the macrocycle would have to have internal two fold symmetry which it definitely has not. It also is possible that the observed pseudosymmetry is due to twinning of the crystal which is possible in the orthorhombic system[82], however this could not be fully investigated in the time available.

The macrocycles are non planar with maximum deviations from the least squares plane with all non hydrogen atoms defining the plane of 3.37(4)Å, C4 and –2.00(5)Å, C7 for molecule 1 and 3.32(4)Å, C4A and –2.01(3)Å, C7A for molecule 2. The angle between the planes of the two thiophene rings (denoted by the sulfur atom label) are in both cases much larger than for M1 [49.8(3)°]: S1-S2 = 76(2)°, S1A-S2A = 84(2)°. The geometry of the two molecules differ appreciably from that of M1. When the molecules are viewed down the S2-C9 bond (see figure 54) the plane of the S1 thiophene ring is almost in the plane of the paper. The two bridges attaching the thiophene rings are not almost perpendicular to one another as in M1, but are almost parallel with the nitrogen atom containing bridge displaced to one side of the thiophene rings via the C1-C5 bond on one side and the C8-N2, N2-C7 bonds on the other side. The oxygen containing bridge runs not far from the plane of the S2 ring with the methylene carbons C13 and C14 the uppermost atoms in this view, O2A-C13A-C14A-O1A = -53(5)°, O2-C13-C14-O1 = -70(3)°.

Figure 54.
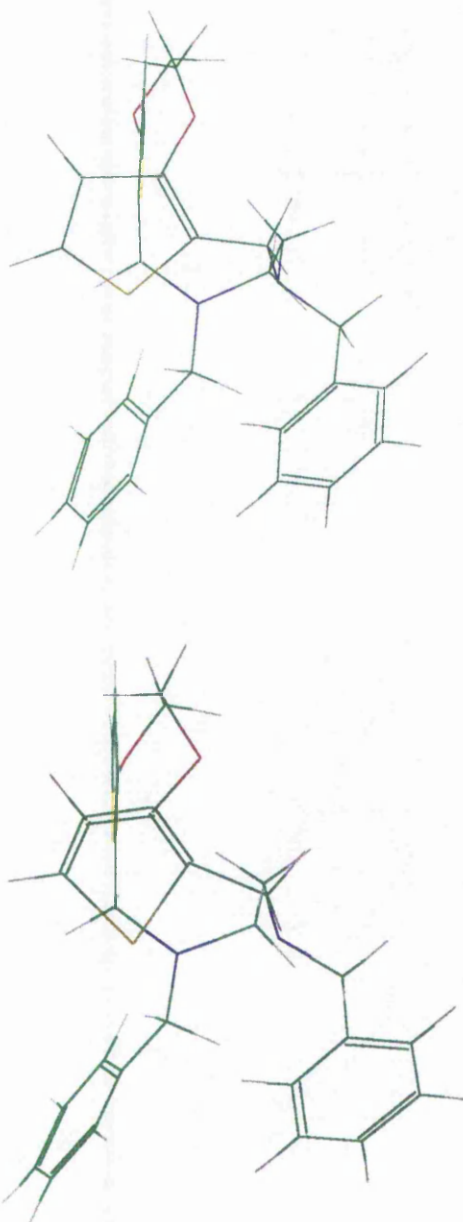
The carbon atoms C6 and C7 between the two nitrogen atoms are orientated up towards the oxygen containing bridge reducing the size of the macrocyclic cavity, N1A-C6A-C7A-N2A = -59(4)°, N1-C6-C7-N2 = -80(4)°. In molecule 1 this orientation results in a cross ring intramolecular CH...O hydrogen bond: C6-H25...O2 = 2.47(3)Å. The CH...O angle = 158(2)°. A cross ring hydrogen bond of this type occurs in

18-crown-6[119]. Also the possible intramolecular hydrogen bonds between the two bridges mentioned in the discussion of M1:- C5-H4...O1 = 2.537(4)Å, 101.2(3)° and C26-H25...O2 = 2.6369Å, 97.376° occur in molecule 1:- C5-H23...O1 = 2.6277Å, 93.052° and C8-H29...O2 = 2.5639Å, 99.591° and in molecule 2:- C5A-H24A...O1A = 2.50(3)Å, 103(2)° and C8A-H29A...O2A = 2.6966Å, 101.504° making these much more likely to be genuine interactions.

The two benzyl groups of each molecule are orientated differently from those in M1, with the planes of both benzene rings lying very approximately in the plane of the nitrogen containing bridge. This results in the angle between the planes of the two rings in each molecule being far smaller than in M1. In M1 the angle between the two rings C7 benzene – C17 benzene = 79.0(3)°. For this structure C16 benzene – C23 benzene = 36.6(6)° and C16A benzene – C23A benzene = 22.8(5)°.

The four thiophene rings are planar with the greatest deviations (in Å) from the least square planes (ring atoms determine the planes) given below:

S1 ring: C1 –0.03(4), C4 –0.03(4)

S1A ring: C1A –0.04(3), C2A 0.04(6)

S2 ring: C9 0.03(6), C10 –0.03(5)

S2A ring: C9A 0.02(4), C10A –0.02(3)

The planarity extends beyond the rings themselves as in M1 and the deviations of local atoms are given below:

S1 ring: O1 –0.01(3), C5 –0.06(4), [N1 1.24(4)]

S1A ring: O1A 0.16(3), C5A –0.07(4), [N1A –1.31(2)]

S2 ring: O2 –0.07(2), C8 0.05(5), [N2 –1.13(3)]

S2A ring: O2A 0.13(3), C8A –0.11(5), [N2A –1.27(3)]

The deviations from the ring planes of the nitrogen atoms are in the order of that for the S1 ring and N1 atom in M1 where no S…N interaction occurs. The distances between the S2 and N2 atoms in both molecules, 3.26(4)Å and 3.26(4)Å are smaller than the sum of the contact radii, 3.35Å but are not significant by the 3σ criteria. A reason for the absence of this non-bonded interaction may be the competition for the N2 lone pair by the H20 atom. These possible C-H…N hydrogen bonds are C28-H20…N2 = 2.5015Å, 98.0357° and C28A-H20…N2A = 2.4912Å, 97.7906°. The contact radii for the two atoms is 2.75Å. These hydrogen positions were not refined and therefore the bonds have no esd's but if the likely esd's are taken as being similar to those for the C-H…O hydrogen bonds then they are likely to be significant. Hydrogen bonds of this type do not occur in the M1 structure and it seems likely that one stabilising attraction (N…S) has been replaced by another (N…H) in this structure.

The packing of the aromatic rings as in M1 is biased towards the optimisation of repulsive rather than dispersion forces. However there exists a H-π ring interaction between molecule 1 and molecule 2: C14-H5…C23A benzene ring = 2.441Å, 175.71°. When the interaction is visualised via CHEM-X looking down the C-H bond the hydrogen atom is directed towards the centre of the ring.

The geometry of the macrocyclic ring in molecules 1 and 2 is shown in figure 55 along with that of M1 for comparison.

Figure 55.

M1.
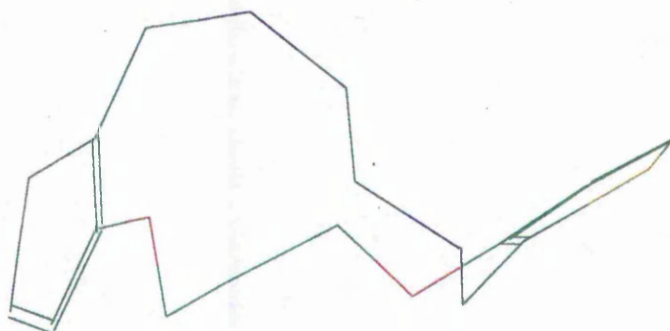
M2 Molecule 1.
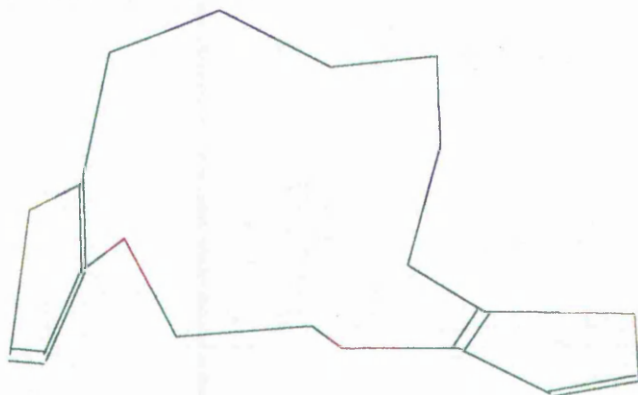
M2 Molecule 2.
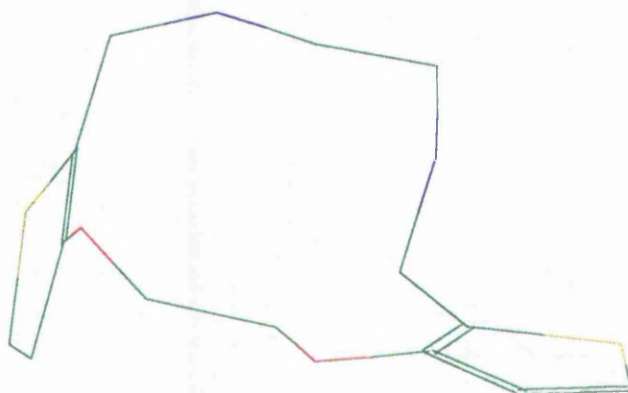
The major difference between the M1 ring geometry and that of molecules 1 and 2 in M2 is that in M1 one of the nitrogen atoms lies approximately in the same plane as the two oxygen atoms, whereas in molecules 1 and 2 the aforementioned nitrogen atom lies more in the plane of the other nitrogen atom. The result being that the nitrogen to

nitrogen bridge lies approximately parallel to that of the oxygen to oxygen bridge as previously discussed. As in M1 the lone pairs of the donor atoms in M2 are not directed towards the macrocyclic cavities but some are involved in hydrogen bonding as discussed. Therefore rearrangement of the macrocyclic ring would be required if coordination to a metal ion was to take place.

The structure contains various intramolecular contacts less than the sum of the van der Waals radii for each atom. Most of these are C...H or H...H contacts and occur mainly around the congested nitrogen atoms. Four of these are less than the sum of the van der Waals radii (–0.25Å) and are H6...H21 = 2.0797Å, H8...H28 = 1.8596Å, H15...H28 = 2.0882Å and H25...H29 = 1.9928Å.

The shortest intermolecular contacts besides the H-π ring interaction are listed below:-

H10A...H18A [1-x,-1-y,1/2+z] = 2.1706Å Sum Rad. = 2.40Å

H19...H24 [-x,-y,1/2+z] = 2.1896Å

H27...H21A [x,y,z] = 2.1969Å

H30...H5A [x,1+y,z] = 2.1532Å

Having discussed the structure's intramolecular and intermolecular geometry a view of the packing within the unit cell is shown in figure 56, viewed down the b-axis with the packing range (only whole asymmetric units) 0-1, 0-1, 0-1 for the three axes. Hydrogen atoms have been omitted for clarity.

Figure 56.
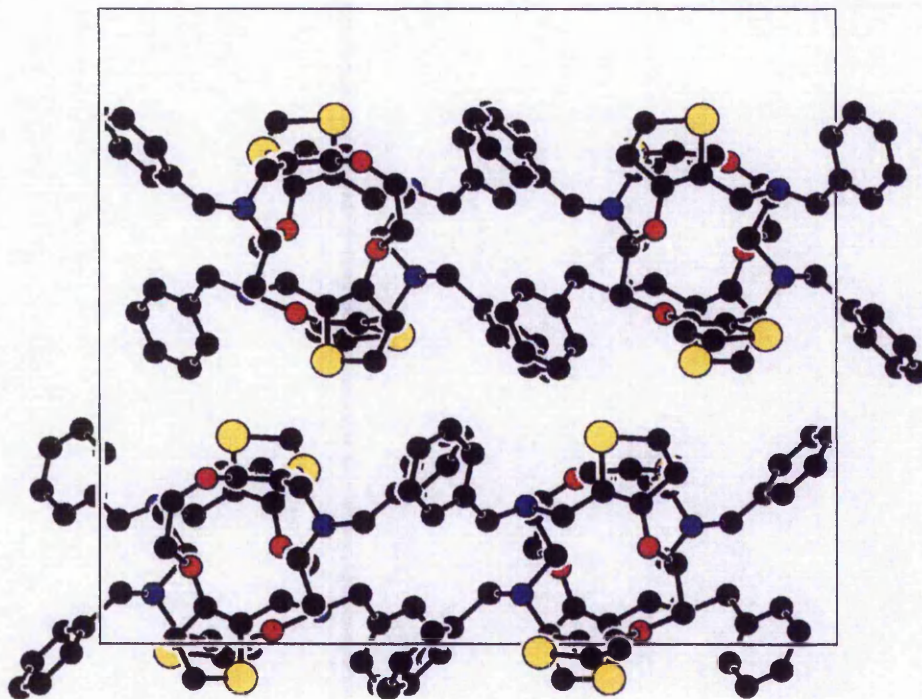
To conclude, due to time restraints this structure has not been resolved as fully as desired. At this stage the high R value and esd's indicate that there may be room for improvement in the structural model as it stands at present. However all the resources available within the time allowed have been used to ensure the model is as correct as possible. The psuedo-symmetry present has not been found to fit any crystallographic symmetry and has therefore not induced a change of space group. The presence of this psuedo-symmetry may explain the disorder shown on the X-ray photographs. This disorder is about the b-axis which fits with the psuedo 2_1 screw axis found parallel to the b axis. The possibility of twinning to some extent cannot be ruled out as this can sometimes lead to psuedo-symmetry however this was not investigated due to time constraints. The high temperature in the X-ray laboratory during data collection may be a factor contributing to the high R value.

3.11.3. *N,N'*-ethylenebis(3-methoxythiophene-2-aldimine).
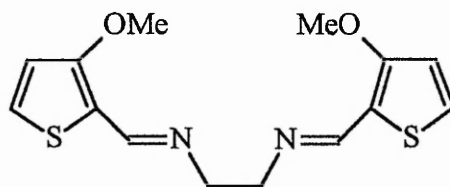
3.11.3.1. Crystal morphology.

Good quality crystals were obtained from methanol with short needle type habit.

3.11.3.2. X-ray photographs.

After the problems of polymorphism encountered with M2 the X-ray photographs (rotation and Weissenberg) about the three axes were obtained from one crystal by the careful removal and regluing of the fibre after each set of photographs had been obtained.

After measurements taken from the X-ray photographs the following unit cell dimensions (axes labelled after space group determination) were obtained (corroborated by each set of photographs):-

$$a = 7.690\text{Å} \quad b = 9.135\text{Å} \quad c = 11.076\text{Å} \quad \alpha = \beta = \gamma = 90°$$

The diffraction patterns showed the following conditions:-

hkl:- none   0kl:- none   h0l:- l+h = 2n   hk0:- none

h00:- h = 2n   0k0:- none   00l:- l = 2n

The axis labels above are for the chosen space group $Pmn2_1$. The conditions (differently labelled) also satisfy the centrosymmetric space group, Pmmn. This was not chosen however as the X-ray photographs imply mm2 rather than mmm symmetry. The space

group Pmn2$_1$ has a setting with two equivalent positions; 0,y,z and 0.5,-y,0.5+z. The density of the crystals was measured by flotation at 1.32g/cm^3. The calculated density with 2 molecules per unit cell equals 1.31g/cm^3. Therefore the choice of Pmn2$_1$ with four equivalent positions implies that the molecule has crystallographic 2-fold symmetry.

3.11.4. 1,5-bis(2-formyl-3-oxythienyl)-3-oxypentane.
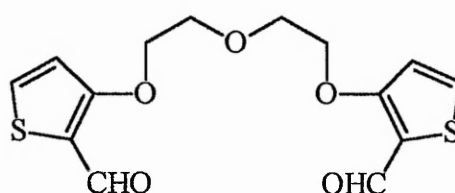
3.11.4.1 Crystal morphology.

The crystals were obtained with needle type habit after recrystallisation from ethanol.

3.11.4.2. X-ray photographs.

Rotation photographs were obtained about all three axes and Weissenberg photographs about two of the axes. After measurements taken from the X-ray photographs the following unit cell dimensions (axes labelled after space group determination) were obtained (corroborated by each set of photographs):-

$$a = 16.102\text{Å} \quad b = 9.573\text{Å} \quad c = 10.137\text{Å} \quad \alpha = \gamma = 90° \quad \beta = 93°$$

The diffraction patterns showed the following conditions:-

hkl:- h+k = 2n   h0l:- l = 2n (h = 2n)   0k0:- k = 2n

The observed conditions satisfy the space groups Cc and C2/c. There is no way of determining which of these is the true space group at this stage. The density of the

crystals was measured by flotation at $1.40g/cm^3$ and with four molecules per unit cell was calculated at $1.387g/cm^3$.

4. CONCLUSIONS.

4.1. Synthetic work.

The *N,N'*-dibenzylalkyldiamines synthesised as starting materials for a new series of macrocycles produced via the Mannich reaction were obtained in satisfactory yields. These proved to be appropriate compounds for coupling in the Mannich reaction. Another compound synthesised as a starting material, which due to time constraints was not fully utilised, was 3-hydroxythiophene-2-carbaldehyde. This compound is an analogue of salicylaldehyde, which has been used widely as a starting material for benzene based macrocycles. If this compound can be made on a satisfactory scale it may prove possible to synthesise a wide variety of analogous thiophene based macrocycles.

The synthetic work had the aim of investigating existing and new routes to thiophene based macrocycles / macrocyclic complexes which could be obtained preferably in crystalline form (for further study) in good yields without the need for elaborate purification, and produced the three main series of compounds outlined below.
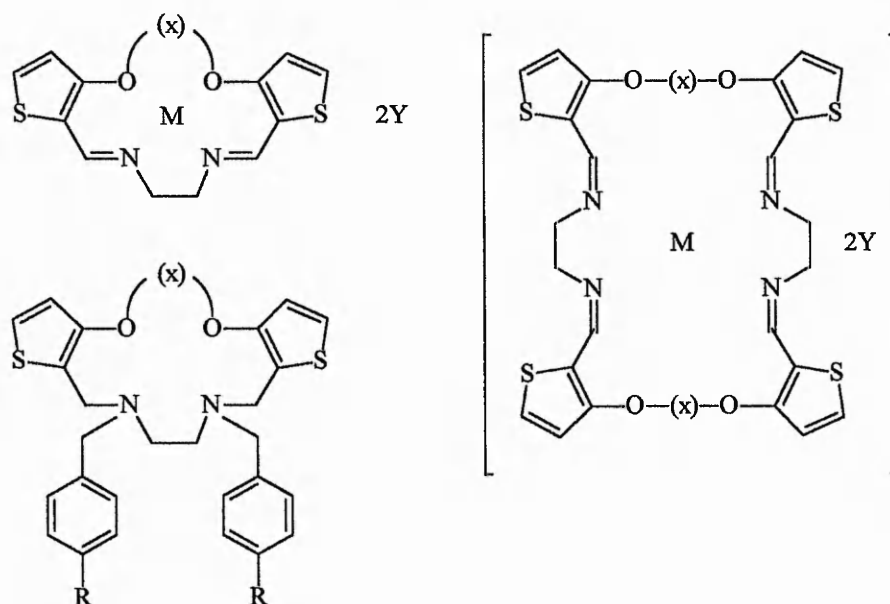
Attempts to produce the [1+1] diimine macrocycles using in-situ metal ion templates failed. The series of complexes were produced successfully by adding the metal salt to the dialdehyde and diamine mixture after heating. This suggests that the metal ion is sequestering a pre-condensed macrocycle rather than organising the reaction sites and is therefore acting as a thermodynamic template.

The series of [2+2] macrocyclic complexes formed via templated Schiff base condensations were difficult to characterise (therefore bracketed, as they could not be fully characterised, see discussion) and tended to hydrolyse in solution. There was evidence of incomplete cyclisation in two complexes and the third whose spectra indicated complete cyclisation gave unsatisfactory microanalysis reults. As for the [1+1] complexes the possibility of and evidence for contamination has been discussed. The characterisation was therefore via derivatisation whereby the complexes were reduced and the free ligand characterised. These problems meant the complexes were not investigated any further.

The route involving the reaction of 3- and 3,4-di- methoxythiophene-2-carbaldehydes with ethylenediamine failed to give macrocyclic products due to the instability of the demethylated 3-hydroxy compounds. However the potentially tetradentate acyclic ligands *N,N'*-ethylenebis(3,4-methoxythiophene-2-aldimine) and *N,N'*-ethylenebis(3-methoxythiophene-2-aldimine) were produced in high yields. The latter compound was examined via X-ray diffraction and the unit cell dimensions and space group were determined.

Further approaches to macrocyclic compounds avoiding the saponification and decarboxylation of methyl 3-hydroxythiophene-2-carboxylate did not result in any macrocyclic compounds due to the low reactivity of the ester group towards amide formation. Even when methyl 3-hydroxythiophene-2-carboxylate was complexed with Ni^{2+} which would increase the positive polarisation of the carbonyl carbon and increase the likelihood of nucleophilic attack, the amide formed by reaction with ethanolamine was produced in only 5% yield. This route was therefore abandoned.

Using the Mannich reaction utilising new benzylic diamines produced crystalline macrocycles in good yields which were obtained pure or via simple recrystallisation. Two of these compounds were obtained as powders and required redissolving in suitable solvents to induce crystallisation. The compounds were readily soluble in DCM but only sparingly soluble in polar solvents such as methanol and ethanol. The crystals were obtained via dissolution in a mixture of DCM and ethanol, however as has been discussed, the crystals of M2 were polymorphic in nature. Therefore introducing a heterogeneous background produced non-homogeneous crystals. The sparing solubility of the compounds in polar solvents also presented problems in obtaining metal complexes of these macrocycles. This work has not been presented in the main body of this thesis due its incomplete and ongoing nature but attempts were made to obtain crystalline metal salt complexes of these macrocycles. Those attempts involving the mixing (with and without heating) of appropriate amounts of macrocycle and metal salt in various solvents resulted in complex formation in solution, indicated by colour changes and polarographic work by Coomber[120], however on precipitation the macrocycle and metal salt separated out as crystals and powder respectively. This is indicative of the stability of the uncomplexed form of these crystals and the sparing

solubility of the compounds in the polar solvents required to dissolve the metal salts thus far attempted. As discussed it is important to choose a metal ion whose size and coordination preferences suit the stable free form of the macrocycle so that little rearrangement of the ligand is required. It also seems from these experiments that an appropriate anion with good solubility in less polar solvents should be chosen in order to prevent the early precipitation of the free ligand and crystallise the complex from solution intact.

Two of the compounds produced via the Mannich reaction were examined via X-ray crystallography in order to gain information on the structural geometry and the macrocyclic cavity.

4.2. X-ray crystallography.

The crystal structures of the two compounds, M1 and M2 were obtained. The compounds M1 and M2 differ from each other chemically by only one CH_2 group in the ether bridge. The crystal structures however have only limited similarities. The crystals of M1 belong to the monoclinic space group $P2_1/c$ whereas the crystals of M2 belong to the orthorhombic space group $Pca2_1$. The compound M1 crystallises in a centrosymmetric space group whereas M2 crystallises in a non-centrosymmetric space group. The dimensions of the unit cell differ for the two compounds. The unit cell for M2 is approximately twice as large as that for M1. This is due to the fact that M2 crystallises with eight macrocycles per unit cell whereas M1 crystallises with four. The b-axis lengths are similar: M1 = 11.2994Å, M2 = 11.397Å. Although this distance is perpendicular to the 'plane' of the macrocyclic ring in both structures the macrocycle in M1 and the two in M2 have very different dimensions across the molecule in the

direction of the b-axis (M1: C19-C13 = 12.76Å, M2: C20-C26 = 10.00Å and C26A-C17A = 9.44Å). The packing of the individual macrocycles in M1 is influenced by intermolecular CH...O hydrogen bonds as discussed. The packing of the macrocycles in M2 is influenced by intermolecular attractions between the two molecules which make up the asymmetric unit. Only one of these interactions has been discussed (H-π C14-H5...C23A) but there are also another possible three intermolecular interactions, another H-π interaction (H-thiophene) and two CH...O interactions with donor-acceptor distances 2.81-2.87Å. However due to the imprecise nature of the model these are tenuous.

The macrocycles in both structures have a non-planar geometry. This is to be expected with such bulky benzyl substituents on the nitrogen atoms. Although the geometry of the macrocycles in the structures M1 and M2 varies considerably the geometry of the macrocyclic rings is comparable as has been discussed.

The structure M2 has two macrocycles within the asymmetric unit, each with very similar molecular geometries. These do however deviate from one another and no crystallographic symmetry has been found to relate the two independent molecules of the asymmetric unit. The pseudo 2_1 screw axis found does not fit any space group symmetry and even if this were crystallographic further symmetry would be required to fit another of the 230 space groups or a non-standard setting thereof. There are other factors still not fully investigated due to time constraints such as the possibility of twinning to some extent and whilst the R value remains high the possibility for improvement in the present model remains open.

Both structures contain various CH...O (and in M2 CH...N) hydrogen bonds. The number of these found in both structures indicates the importance these have in stabilising the structures in the absence of stronger H-bonds. The fact that solvent was not found to be included in M2 although EtOH was present in the crystallisation process may indicate that the formation of many weaker CH...O or CH...N hydrogen bonds outweighs the gain in forming stronger O or N hydrogen bonds with EtOH and the disruptive influence solvent may introduce in the crystal packing. The initial assumption that the disorder shown in the photographs of M2 was caused by solvent inclusion has been dispelled and replaced by the assumption that the disorder arises from the psuedo symmetry found.

In the structure M1 there is a S...N non-bonded intramolecular attraction and although this has been documented for other thiophene compounds with appropriate nitrogen containing 2-position substituents[111] the fact that it occurs in a ring compound with such conformational constraints is quite remarkable.

As for other macrocycles such as 18-crown-6[119], in the free uncomplexed state, the lone pairs of some of the ring donor atoms in both structures are directed away from the macrocyclic cavity. Therefore in order to coordinate to any potential metal ions some conformational change within the ligands would be necessary. The Ni^{2+} complex of M1 was modelled via CHEM-X and the macrocycle M1 was shown to coordinate the metal ion in a tetrahedral manner with only minor changes in the macrocycle's geometry.

Overall during this work a series of thiophene based macrocycles were produced with the properties desired. This allowed the structural investigation of the compounds

which in turn revealed many stabilising interactions within the structures and the type of coordination to which the macrocycles are predisposed.

4.3. Further work.

This work produced a series of stable crystalline macrocycles which are easy to handle and therefore suitable for investigation of their coordination to metal ions. The X-ray diffraction studies revealed that the donor atoms of the macrocycle M1 are predisposed in a tetrahedral fashion. Therefore metal ions should be chosen which allow this mode of coordination e.g. Ni^{2+}, Cu^{2+}. Due to the neutral charge of the macrocycles, metal salts with non-coordinating anions should be chosen so that no competition for the metal ion's coordination sites occurs. The comparison of the distances and angles between the donor atoms of M1 with complexes of similar macrocycles showed that the ligand may also coordinate octahedral metal ions in a β-cis fashion. In order to induce this geometry within the complex one bidentate ligand or anion per metal ion should introduced which would occupy two of the basal octahedral sites thus forcing the macrocycle to adopt the desired geometry. If such complexes could be obtained for example using ethylenediamine or oxalate ions then these could then be investigated via X-ray crystallography to confirm / investigate the coordination modes of the macrocycles.

This work produced macrocycles with substituents on the benzene rings, e.g. Cl. If macrocycles with more reactive substituents could be produced then these would provide a way of bonding the macrocycles to a polymer resin. If the macrocycles are shown to exhibit any selectivity then these would make very good chromatographic separation materials.

The avenues of investigation proposed above are only two of many areas of further research the study of these macrocyclic compounds has to offer.

5. REFERENCES.

1. Barker, J.M., Chaffin, J.D.E., Halfpenny, J., Huddleston, P.R. and Tseki, P.F., J. Chem. Soc. Chem. Commun., (1993), 1733 and Chaffin, J.D.E., Ph.D Thesis 1996, The Nottingham Trent University.

2. Lehn, J.M., Struct. Bonding (Berlin), (1973), 16, 1 and Chock, P.B., Eggers, F., Eigen, M., Winkler, R., Biophys. Chem., (1977), 6, 239.

3. Pedersen, C.J., J. Am. Chem. Soc., (1967), 89, 2495 and 7017.

4. Pedersen, C.J., J. Am. Chem. Soc., (1970), 92, 386.

5. Cram, D.J., J. Am. Chem. Soc., (1975), 97, 1257.

6. Nelson, S.M., Inorg. Synth., (1985), 23, 173.

7. Mackay, K.M. and Mackay, R.A., Introduction to Modern Inorganic Chemistry, Blackie, 4th Edition, (1989), page 20.

8. Van Veggel, F.C.J.M., Bos, M., Harkema, S., Van de Bovenkamp, H., Verboom, W., Reedijk, J. and Reinhondt, D.N., J. Org. Chem., (1991), 56, 225.

9. Lindoy, L.F., The Chemistry of Macrocyclic Complexes, Cambridge University Press, (1989), page 176.

10. Lindoy, L.F. and Smith, R.J., J. Am. Chem. Soc., (1979), 101:14, 4014.

11. Constable, E.C., Metals and Ligand Reactivity, Ellis Horwood, 1990 and Melson, G.A.(Ed), Coordination Chemistry of Macrocyclic Compounds, Plenum, (1979).

12. Lindoy, L.F., The Chemistry of Macrocyclic Complexes, Cambridge University Press, (1989).

13. Izatt, R.M. and Christensen, J.J., Synthesis of Macrocycles. Progress in Macrocyclic Chemistry, Vol. 3, Wiley, (1987), page 54.

14. Armstrong, L.G. and Lindoy, L.F., Inorg. Chem., (1975), 14:6, 1322.

15. Izatt, R.M. and Christensen, J.J., Synthesis of Macrocycles. Progress in Macrocyclic Chemistry, Vol. 3, Wiley, (1987), pages 3-9.

16. Curtis, N.F., Coord. Chem. Rev., (1968), 3, 3.

17. Lindoy, L.F. and Busch, D.H., Inorg. Nucl. Chem. Lett., (1969), 5, 525.

18. Armstrong, L.G. and Lindoy, L.F., Inorg. Nucl. Chem. Lett., (1974), 10, 349.

19. Lindoy, L.F., Lip, H.C., Power, L.F. and Rea, J.H., Inorg. Chem., (1976), 15:7, 1724.

20. Armstrong, L.G., Lindoy, L.F., McPartlin, M., Mockler, G.M. and Tasker, P.A., Inorg. Chem., (1977), 16:7, 1665.

21. Curtis, N.F., J. Chem. Soc. A, (1971), 1771.

22. Drew, M.G.B., Rodgers, A., McCann, M. and Nelson, S.M., J. Chem. Soc. Chem. Commun., (1978), 415.

23. Cook, D.H., Fenton, D.E., Drew, M.G.B., Rodgers, A., McCann, M. and Nelson, S.M., J. Chem. Soc. Dalton, (1979), 414.

24. Cairns, C., McFall, S.G., Nelson, S.M. and Drew, M.G.B., J. Chem. Soc. Dalton, (1979), 446.

25. Nelson, S.M., McCann, M., Stevenson, C. and Drew, M.G.B., J. Chem. Soc. Dalton, (1979), 1477.

26. Nelson, S.M., Knox, C.V., McCann, M. and Drew, M.G.B., J. Chem. Soc. Dalton, (1981), 1669.

27. Bailey, N.A., Eddy, M.M., Fenton, D.E, Moss, S., Mukhopadhyay, A. and Jones, G., J. Chem. Soc. Dalton, (1984), 2281.

28. Frommel, T., Angew. Chem. Int. Ed. Engl., (1992), 31, 612.

29. Holm, R.H., J. Am. Chem. Soc., (1961), 83, 4683.

30. Sone, T., Sato, K. and Ohba, Y., Bull. Chem. Soc. Jpn., (1989), 62, 838.

31. Sanchez-Delgado, R.A., Marquez-Silva, R.L., Puga, J., Tiripicchio, A. and Camellini, M.T., J. Organomet. Chem., (1986), 316, C35.

32. Lockemeyer, J.R., Rauchfuss, T.B, Rheingold, A.L. and Wilson, S.R, J. Am. Chem. Soc., (1989), 111, 8828.

33. Luo, S., Rauchfuss, T.B. and Wilson, S.R., Organometallics, (1992), 11, 3497.

34. Polam, J.R. and Porter, L.C., Organometallics, (1993), 12, 3504.

35. Choi, M-G. and Angelici, R.J., J. Am. Chem. Soc., (1989), 111, 8753.

36. Angelici, R.J. and Chen, J., Organometallics, (1990), 9, 879.

37. Cordone, R., Harman, W.D. and Taube, H., J. Am. Chem. Soc., (1989), 111, 5969.

38. Sanchez-Delgado, R.A., Herrera, V., Bianchini, C., Masi, D. and Mealli, C., Inorg. Chem., (1993), 32, 3766.

39. Cooney, J.M., Gommans, L.H.P, Main, L. and Nicholson, B.K., J. Organomet. Chem., (1988), 349, 197.

40. Mizuno, H., Kita, M., Fujita, J. and Nonoyama, M., Inorg. Chim. Acta., (1992), 202, 183.

41. Lucas, C.R., Liu, S., Newlands, M.J. and Gabe, E.J., Can. J. Chem., (1990), 68, 1357.

42. Amari, C., Ianelli, S., Pelizzi, C., Pelizzi, G. and Predieri, G., Inorg. Chim. Acta., (1993), 211, 89.

43. Van Stein, G.C., Inorg. Chim. Acta., (1983), 78, L61.

44. Van Stein, G.C., Inorg. Chim. Acta., (1985), 98, 107.

45. Bondi, A., J. Phys. Chem., (1964), 68, 441.

46. Drew, M.G.B., Harding, C.J., Howarth, O.W., Lu, Q., Marrs, D.J., Morgan, G.G., McKee, V. and Nelson, J., J. Chem. Soc. Dalton, (1996), 3021.

47. Modder, J.F., Leijen, R.J., Vrieze, K., Smeets, W.J.J., Spek, A.L. and Koten, G.V., J. Chem. Soc. Dalton, (1995), 4021.

48. Das, A., Polyhedron, (1995), 14, 495.

49. Christidis, P.C. and Triantafyllon, S.T., Z. Kristallogr., (1994), 209, 502.

50. Pillai, M.R.A., Barnes, C.L., John, C.S., Troutner, D.E. and Schlemper, E.O., J. Cryst. Spec. Res., (1993), 23, 949.

51. Amer, S.A., Trans. Met. Chem., (1991), 16, 152.

52. Lavery, A., Nelson, S.M. and Drew, M.G.B., J. Chem. Soc. Dalton, (1987), 2975.

53. Hartough, H.D., J. Am. Chem. Soc., (1949), 71, 3922.

54. Barker, J.M., Huddleston, P.R. and Wood, M.L., Synth. Commun., (1975), 5(1), 59.

55. Lukyanenko, N.G., Pastushok, V.N. and Bordunov, A.V., Synthesis, (1991), 241.

56. Lukyanenko, N.G., Pastushok, V.N., Bordunov, A.V., Vetrogon, V.I., Vetrogon, N.I. and Bradshaw, J.S., J. Chem. Soc. Perkin Trans., (1994), 1489.

57. Bordunov, A.V., Lukyanenko, N.G., Pastushok, V.N., Krakowiak, K.G., Bradshaw, J.S., Dalley, N.K., Kou, X., J. Org. Chem., (1995), 60, 4912.

58. Bordunov, A.V., Hellier, P.C., Bradshaw, J.S., Dalley, N.K., Kou, X., Zhang, X.X. and Izatt, R.M., J. Org. Chem., (1995), 60, 6097.

59. Pastushok, V.N., Bradshaw, J.S., Bordunov, A.V. and Izatt, R.M., J. Org. Chem., (1996), 61, 6888.

60. Meth-Cohn, O., Quart. Reports on Sulphur Chem., (1970), 5(2), 129.

61. Newkome, G.R., Chem. Rev., (1977), 77(4), 513.

62. Ladd, M.F.C and Palmer, R.A., Structure Determination by X-ray Crystallography, Plenum, New York, 2nd Ed., (1985), page 423.

63. Ladd, M.F.C and Palmer, R.A., Structure Determination by X-ray Crystallography, Plenum, New York, 2nd Ed., (1985), page 424.

64. Ladd, M.F.C and Palmer, R.A., Structure Determination by X-ray Crystallography, Plenum, New York, 2nd Ed., (1985), page 425.

65. Von Laue, M., Sitz. math. phys. Klasse Bayer, Akad. Wiss., (1912), 303.

66. Stout, G.H. and Jensen, L.H., X-ray Structure Determination. A Practical Guide, Wiley, 2nd Ed., (1989), page 50.

67. Miller, W.H., Treatise on Crystallography, (1839).

68. Bragg, W.L., Proc. Camb. Phil. Soc., (1913), 17, 43.

69. Woolfson, M.M., An Introduction to X-ray Crystallography, Cambridge Univ. Press, (1970), page 76.

70. Theory and method described in: Buerger, M.J., X-ray Crystallography, Wiley, (1942), Ch.12 and Stout, G.H. and Jensen, L.H., X-ray Structure Determination. A Practical Guide, Wiley, 2nd Ed., (1989), pages 118-119.

71. Nuffield, E.W., X-ray Diffraction Methods, Wiley, (1966), page 247.

72. Ladd, M.F.C and Palmer, R.A., Structure Determination by X-ray Crystallography, Plenum, New York, 2nd Ed., (1985), page 134.

73. Weissenberg, K., Z. Physik, (1924), 23, 229.

74. Ibers, J.A. and Hamilton, W.C. (Ed's), International Tables for X-ray Crystallography Vol IV, Kynoch Press, Birmingham, England, (1974), pages 71-147.

75. Mellor, J.W., Higher Mathematics for Students of Chemistry and Physics, Dover, New York, (1955), pages 280-286.

76. Busing, W.R. and Levy, H.A., Acta Cryst., (1957), 10, 180.

77. Sheldrick, G.M., SHELX76 Program for Crystal Structure Determination, University of Cambridge, England, (1976).

78. Wilson, A.J.C., Acta Cryst., (1950), $\underline{3}$, 397.

79. Patterson, A.L., Phys. Rev., (1934), $\underline{36}$, 372 and Zeit. f. Kristallog., (1935), $\underline{90}$, 517.

80. Harker, D. and Kasper, J.S., Acta Cryst., (1948), $\underline{1}$, 70.

81. Karle, J. and Karle, I.L., Acta Cryst., (1966), $\underline{21}$, 849.

82. Kasper, J.S. and Lonsdale, K. (Ed's), International Tables for X-ray Crystallography Vol II, Kynoch Press, Birmingham, England, (1959), pages 355-366.

83. Stout, G.H. and Jensen, L.H., X-ray Structure Determination. A Practical Guide, Wiley, 2nd Ed., (1989), page 358.

84. Aldrich Chemical Co., Catalogue Handbook of Fine Chemicals, 33902-4.

85. Korvenranta, J., Suomen Kemistilehti B, (1969), $\underline{42}$, 274.

86. Nasanen, R., Lemmetti, L., Lamminsivu, U. and Abdalla, H.,Suomen Kemistilehti B, (1968), $\underline{48}$, 1.

87. Rochow, E.G., Inorganic Syntheses, McGraw-Hill, (1960), Vol. 6, page 198.

88. Rochow, E.G., Inorganic Syntheses, McGraw-Hill, (1960), Vol. 6, page 200.

89. Moeller, T., Inorganic Syntheses, McGraw-Hill, (1957), Vol. 5, page 17.

90. Huddleston, P.R., Unpublished Work, The Nottingham Trent University.

91. Adam, K.R., Anderegg, G., Lindoy, L.F., Lip, H.C., McPartlin, M., Rea, J.H., Smith, R.J. and Tasker, P.A., Inorg. Chem., (1980), $\underline{19}$, 2956.

92. Hartshorne, N.H. and Stuart, A., Crystals and the Polarising Microscope, Arnold, 4th Ed., (1970), Ch. 4.

93. Nuffield, E.W., X-ray Diffraction Methods, Wiley, (1966), page 210.

94. Nuffield, E.W., X-ray Diffraction Methods, Wiley, (1966), page 285.

95. Nuffield, E.W., X-ray Diffraction Methods, Wiley, (1966), page 302.

96. BBC Utilities Program, Watford Electronics.

97. BEEBDOS, BBC and IBM File Interchange, Microboss Ltd.

98. Small, R.W.H., DATR (1977), Program for Reducing Raw Stadi-2 Data to Intensities, University of Lancaster.

99. Debaerdemaeker, T., MULTAN87, Computer Programs for the Automatic Solution of Crystal Structures from X-ray Diffraction Data.

100. CHEM-X, Chemical Design Ltd, Chipping Norton, UK.

101. Black, D.St.C and McLean, I.A., Inorg. Nucl. Chem. Lett., (1970), 6, 675.

102. Huddleston, P.R., Personal Communication.

103. Hathaway, B.J., J. Chem. Soc., (1961), 3091.

104. Wilkinson, Gillard and McCleverty (Ed's), Comprehensive Coordination Chemistry, Pergamon Press, Vol 6, pages 155-203.

105. Adam, K.R., Anderegg, G., Henrick, K., Leong, A.J., Lindoy, L.F., Lip, H.C., McPartlin, M., Smith, R.J. and Tasker, P.A., Inorg. Chem., (1981), 20, 4048.

106. Huddleston, P.R., Personal Communication.

107. Autodesk 3D Studio.

108. Spek, A.L., PLATON97, Acta Cryst., (1990), A46, C-34.

109. Ladd, M.F.C and Palmer, R.A., Structure Determination by X-ray Crystallography, Plenum, New York, 2nd Ed., (1985), page 359.

110. Steiner, T., Cryst. Rev., (1996), 6, 1.

111. Koziol, A.E., Palenik, R.C. and Palenik, G.J., J. Chem. Soc. Chem. Commun., (1988), 226.

112. Abrahams, S.C., Robertson, J.M. and White, J.G., Acta Cryst., (1949), 2, 233 and Cruickshank, D.W.J., Acta Cryst., (1957), 10, 504.

113. Goodwin, H.J., Henrick, K., Lindoy, L.F., McPartlin, M. and Tasker, P.A., Inorg. Chem., (1982), 21, 3261.

114. Drummond, L.A., Henrick, K., Kanagasundaram, M.J.L., Lindoy, L.F., McPartlin, M. and Tasker, P.A., Inorg. Chem., (1982), 21, 3923.

115. Sheldrick, G.M., SHELXS-97 and SHELXL-97, University of Gottingen.

116. McArdle, P., ORTEX for WINDOWS v.6f, UCG Crystallography Centre, Chemistry Department, University College, Galway, Ireland.

117. Le Page, Y., J. Appl. Cryst., (1987), 20, 264 and J. Appl. Cryst., (1988), 21, 983.

118. Cambridge Crystallographic Database Manual, Administrative Secretary, 12 Union Road, Cambridge, CB2 1EZ.

119. Goldberg, I., Complexes of Crown Ethers with Molecular Guests, In *Inclusion Compounds*, Atwood, J.L., Davies, J.E. and MacNicol, D.D. (Ed's), London Academic Press, Vol 2, pages 261-335.

120. Coomber, D, Personal Communication.